TECHNICAL REPORT STANDARD TITLE PAGE

1. Report No.	2. Government Accession No.	3. Recipient's Catalog No.
FHWA/TX-79/10+209-1F		

4. Title and Subtitle

FATIGUE LOADING OF CANTILEVER SIGN STRUCTURES FROM TRUCK WIND GUSTS

5. Report Date

April 1979

6. Performing Organization Code

7. Author(s)

Bruce M. Creamer, Karl H. Frank, and Richard E. Klingner

8. Performing Organization Report No.

Research Report 209-1F

9. Performing Organization Name and Address

Center for Highway Research
The University of Texas at Austin
Austin, Texas 78712

10. Work Unit No.

11. Contract or Grant No.

Research Study 3-5-77-209

12. Sponsoring Agency Name and Address

Texas State Department of Highways and Public Transportation; Transportation Planning Division
P. O. Box 5051
Austin, Texas 78763

13. Type of Report and Period Covered

Interim

14. Sponsoring Agency Code

15. Supplementary Notes

Study conducted in cooperation with the U. S. Department of Transportation, Federal Highway Administration
Research Study Title: "Fatigue Loading in Sign Structures"

16. Abstract

This is the final report of an experimental and analytical study to determine the fatigue loading on cantilever highway signs from gusts produced by trucks passing under the sign. Three sign structures were instrumented in the field to determine their response from truck gusts. These signs were then analyzed using a three-dimensional dynamic analysis computer program. A loading was developed from the computer analysis which produced a response which simulated the response measured in the field study. A matrix of standard Texas State Department of Highways and Public Transportation standard sign structures was analyzed using the same computer program and the simulated loading. The result of this analysis was the development of dynamic load factors for these signs.

A simple method of estimating the three primary modal frequencies of typical signs was developed using single degree of freedom models. Means of correcting the results of these simple models to agree with the computer analysis was developed. The resulting frequencies allow the dynamic load factor to be calculated without the use of the complex three-dimensional computer analysis.

A method of analyzing the anchor bolts of the signs for fatigue is presented. The analysis uses the loading developed in this study amplified using the dynamic loading factors calculated from the modal frequencies estimated from the single degree of freedom models. The low measured stresses in the superstructure did not indicate any potential fatigue problems. The anchor bolt fatigue stresses are primarily caused by bending of the bolt between the base plate and the foundation.

17. Key Words	18. Distribution Statement
fatigue loading, cantilever highway signs, wind gusts, trucks, computer program, simulated loading, dynamic load factors	No restrictions. This document is available to the public through the National Technical Information Service, Springfield, Virginia 22161

19. Security Classif. (of this report)	20. Security Classif. (of this page)	21. No. of Pages	22. Price
Unclassified	Unclassified	114	

Form DOT F 1700.7 (8-69)

FATIGUE LOADING OF CANTILEVER SIGN STRUCTURES FROM TRUCK WIND GUSTS

by

Bruce M. Creamer
Karl H. Frank
and
Richard E. Klingner

Research Report No. 209-1F

Research Report No. 3-5-77-209

"Fatigue Loading in Sign Structures"

Conducted for

Texas
State Department of Highways and Public Transportation

In Cooperation with

U. S. Department of Transportation
Federal Highway Administration

by the

CENTER FOR HIGHWAY RESEARCH
THE UNIVERSITY OF TEXAS AT AUSTIN

April 1979

S U M M A R Y

This is the final report of an experimental and analytical study sponsored by the Texas State Department of Highways and Public Transportation to determine the fatigue loading on cantilever highway signs from gusts produced by trucks passing under the sign. Three sign structures were instrumented in the field to determine their response from truck gusts. These signs were then analyzed using a three-dimensional dynamic analysis computer program. A loading was developed from the computer analysis which produced a response which simulated the response measured in the field study.

A matrix of standard Texas State Department of Highways and Public Transportation standard sign structures was analyzed using the same computer program and the simulated loading. The result of this analysis was the development of dynamic load factors for these signs.

A simple method of estimating the three primary modal frequencies of typical signs was developed using single degree of freedom models. Means of correcting the results of these simple models to agree with the computer analysis was developed. The resulting frequencies allow the dynamic load factor to be calculated without the use of the complex three-dimensional computer analysis.

A method of analyzing the anchor bolts of the signs for fatigue is presented. The analysis uses the loading developed in this study amplified using the dynamic loading factors calculated from the modal frequencies estimated from the single degree of freedom models. The low measured stresses in the superstructure did not indicate any potential fatigue problems. The anchor bolt fatigue stresses are primarily caused by bending of the bolt between the base plate and the foundation.

IMPLEMENTATION

This report develops a method for checking the fatigue of cantilever highway sign structures for truck-induced gust loading. The anchor bolts are the critical elements governed by this loading. The low damping of the structures results in many stress cycles from a single loading event. The numerous cycles produced require that the stress ranges in the bolts be less than the threshold stress range of 10 ksi.

The design method presented makes use of a linear varying pressure distribution and a dynamic load factor estimated from the sign's modal frequencies. A simpler and conservative method using the triangular loading of 1.25 psf at the bottom of the sign and zero at the top in conjunction with dynamic load factors of 2.1 for shear and 1.6 for base torque is recommended for most designs. A more rigorous design using the actual dynamic load factors can be performed using the methods presented in the report for situations which warrant a more accurate result.

CONTENTS

Chapter		Page
1	INTRODUCTION	1
	1.1 Purpose	1
	1.2 Objectives	2
	1.3 Dynamic Response Theory	7
	1.3.1 General Equation of Motion	7
	1.3.2 Damping	9
	1.3.3 Structural Idealization	12
	1.4 Experimental Procedure	14
	1.5 Analytical Procedure	16
2	EXPERIMENTAL AND ANALYTICAL RESPONSE	21
	2.1 Experimental Results	21
	2.1.1 Experimental Determination of Frequency, Period, and Damping . . .	21
	2.1.2 Forces in Truss Members	24
	2.1.3 Maximum Sign Responses	26
	2.2 Loading Function	28
	2.3 Correlation of Experimental and Analytical Results	32
	2.3.1 Nodal Load Application	32
	2.3.2 Relative Member Responses	32
3	THE PARAMETRIC STUDY	36
	3.1 Introduction	36
	3.2 SAP4 Natural Frequencies	37
	3.3 The Dynamic Load Factor	47
	3.3.1 The Dynamic Load Factor for Base Shear	47
	3.3.2 Torsional Dynamic Load Factor	51
	3.3.3 Dynamic Load Factor Design Curves . . .	54
	3.4 Estimating the Natural Frequency	55
	3.4.1 Torsional Natural Frequency Estimate .	55
	3.4.2 Flexural Natural Frequency Estimate . .	58
	3.4.3 Rocking Natural Frequency Estimate . .	64
	3.5 Sign Geometries at Mode Shifting	71

Chapter Page

4 DESIGN OF ANCHOR BOLTS FOR FATIGUE 74

4.1 Static Design Load 74
4.2 Fatigue Stress Cycles for Design 76
4.3 Allowable Flexural Bending Stress 78
4.4 Design Example 78

5 CONCLUSIONS 88

APPENDICES 90

A SIGN GEOMETRIES 91

B DISTRIBUTION OF SIGN PRESSURE TO NODAL POINTS . . . 95

REFERENCES 104

LIST OF TABLES

Table		Page
2.1	Experimental Response Values	23
2.2	Summary of Experimental Damping and Natural Frequency	24
2.3	Experimental Force Ratios for the Double Cantilever (Sign No. 1)	25
2.4	Experimental Force Ratios for Sign No. 3	26
2.5	Maximum Recorded Loading Events for Sign No. 1	27
2.6	Maximum Recorded Loading Events for Sign No. 3	27
2.7	Comparison of Experimental and Analytical Frequencies for Sign No. 1	33
2.8	Comparison of Experimental and Analytical Member Force Ratios for Sign No. 1	33
2.9	Comparison of Experimental and Analytical Member Force Ratios for Sign No. 3	35
3.1	(a) 10 ft Truss Length	38
	(b) 25 ft Truss Length	39
	(c) 40 ft Truss Length	40
3.2	(a) Modal Natural Frequencies	41
	(b) Eigenvectors for 10 ft Truss Sign Structure	42
	(c) Eigenvectors for 25 ft Truss Sign Structure	43
	(d) Eigenvectors for 40 ft Truss Sign Structure	44
3.3	SAP4 Shear DLF	48
3.4	Torsional DLF	52
3.5	Torsional Frequency Prediction Accuracy	59
3.6	Flexural Frequency Correlation	65

Table		Page

3.7	Correlation of the Rocking Model Natural Frequencies	69
3.8	Torsional-Flexural Mode Shift Sign Geometries . . .	73
4.1	Effect of Damping on Free Vibration Response of an Underdamped System	77

LIST OF FIGURES

Figure		Page
1.1	Box-type tractor trailer passing under Tidwell Exit sign (Sign No. 3)	3
1.2	Double cantilever (Sign No. 1)	5
1.3	Single cantilever (Sign No. 2)	5
1.4	Single cantilever (Sign No. 3)	6
1.5	Single degree of freedom system	8
1.6	Response to impulse loads	10
1.7	General response to triangular load	11
1.8	The effect of damping on response	13
1.9	Strain gage locations on single cantilever	15
1.10	Instrumentation van and gasoline generator	17
1.11	Strain traces from a vertical forced vibration test of double cantilever sign	18
2.1	Sanborn strip chart recorder and 10 channel amplifier	22
2.2	Particle flow paths around a truck	29
2.3	Simulated truck-induced loading	31
3.1	Shape definitions	46
3.2	Shear DLF vs SAP4 flexural frequency	49
3.3	Dominant frequency vs shear DLF	50
3.4	Torsional frequency vs torsional DLF	53
3.5	Torsional frequency model	56

Figure		Page

Figure		Page
3.6	Torsional frequency correction curves	60
3.7	Flexural frequency model	61
3.8	Flexural frequency correction factors	66
3.9	Rocking frequency model	67
3.10	Rocking frequency correction factor	70
4.1	Experimental-analytical chord 4 force load frequency histogram	75
4.2	Design example	79
4.3	Applied live load forces on anchor bolt group . . .	85
A.1	Dimensions of double cantilever sign--Sign No. 1 .	92
A.2	Dimensions of single cantilever sign--Sign No. 2 .	93
A.3	Tidwell Exit sign, Sign No. 3, and standard SDHPT design structure	94
B.1	Horizontal distribution of sign force to support brackets	97
B.2	Distribution of pressure on sign and lighting case	98
B.3	Vertical distribution of sign force to truss chords	99
B.4	Distribution of vertical forces to truss	101
B.5	Resultant forces on truss	103

CHAPTER 1

INTRODUCTION

1.1 Purpose

As vehicles pass under an overhead cantilever highway sign they induce a gust load to the sign face. These gust loads, great enough to produce large displacement responses of the sign structure, can also be produced by ambient wind.

The gust force on the face induces a torsional moment in the upright support. The amount of torsion increases with the length of the cantilever arm supporting the sign. This torsional moment, and any flexural moments which are also present, must ultimately be resisted by shear and bending of the anchor bolts. The current AASHTO highway sign design specifications do not consider gust-induced stresses in designing the signs.

The results of a recent study by Cocavessis [2] indicate that the fatigue life of anchor bolts is heavily influenced by the magnitude and frequency of vehicle-induced gust loads. A recent anchor bolt failure in a Houston sign appeared to be the result of this fatigue problem.

This report is a summary of a State Department of Highways and Public Transportation-sponsored research project on the response of cantilever highway signs subjected to gust loads from truck traffic.

Field experience has shown that vehicle-induced gust loads are more important in a fatigue study of highway signs than the naturally occurring wind gust forces. Vehicles which project a large flat area into the wind, such as box type tractor-trailers, produce the greatest sign movements (see Fig. 1.1). Unloaded gravel trucks also produced significant response, possibly owing to wind deflection off the cab and closed tailgate.

The purpose of this study was to develop a suitable method for designing cantilever highway signs under the influence of gust loads. To accomplish this the parameters affecting sign response were identified and modeled.

1.2 Objectives

Response data from representative signs were gathered from three field studies. The field data were then used to analytically model the signs' response to gust load. A parametric analytical study of the model sign structures was used to pinpoint the variables most influential to sign response and finally to develop design methods.

The following is a listing of the major research project objectives:

(1) Carry out field measurements of overall sign response characteristics and member forces from vehicle-induced gust loads.

(2) Use the field data to make a preliminary identification of the major variables affecting dynamic response of highway signs.

(3) Develop a structural model and analysis method to investigate analytically the static and dynamic responses of signs.

(4) Develop a gust-loading function capable of simulating the measured field response in the model.

(5) Use the sign model and gust-loading function to study the dynamic response of a variety of sign configurations.

Fig. 1.1 Box-type tractor trailer passing under Tidwell Exit sign (Sign No. 3)

(6) Use the results of the parametric study in (5) to make design recommendations.

In the field study, strain gages were used to measure member forces. A strip chart recorder was used to record the time dependent member force characteristics. The truss members framing into the vertical upright were gaged, as explained in Chapter 4, to determine the resulting anchor bolt forces.

Many factors affect the response of a structure to an impulse load such as that caused by the gust from a vehicle. One important factor is the amount of damping in the structural system. Damping is a measure of the structure's ability to dissipate the kinetic response energy and return to the initial, at-rest state. A structure with a high amount of damping will rapidly cease motion after the load is no longer applied.

The majority of analytical work reported in Ref. [2] and the analysis presented in this thesis utilized a general purpose structural analysis program SAP4 developed at the University of California at Berkeley [3]. The sign model description and program development are discussed in detail in a later section. The loading function developed to simulate truck gust loading effects is also discussed in a later section.

The field study is based on the instrumentation of three highway signs. The response of two of the signs was reported in Ref. [2]. The first sign is a double-cantilever type located in Austin, Texas, at the junction of U.S. Highways 183 and 290. The second sign is a single-cantilever type on Ben White Boulevard in Austin. The third sign is also a single cantilever, located on U.S. Highway 59 at the Tidwell exit in Houston, Texas. Photographs of each sign are shown in Figs. 1.2, 1.3, and 1.4. The dimensions and member sizes of each sign are given in the Appendix. The signs will be referred to as Numbers 1, 2, and 3, respectively.

Fig. 1.2 Double cantilever (Sign No. 1)

Fig. 1.3 Single cantilever (Sign No. 2)

Fig. 1.4 Single cantilever (Sign No. 3)

The analytical study is based on a parametric study of sign response using SAP4. The objective of the analytical study is to develop recommendations, aids, and procedures for the fatigue design of sign anchor bolts, without the necessity of a detailed, three-dimensional dynamic analysis. The ultimate goal is the development of a simple and convenient design process.

1.3 Dynamic Response Theory

A structure's dynamic response depends on its mass, damping, and stiffness, as well as the characteristics of the applied load.

1.3.1 General Equation of Motion.

Figure 1.5 shows the general model for a single degree of freedom system (SDOF); so called because its displacement is constrained to one direction only. The equation of motion for this system is given as: [1]

$$M\ddot{u} + C\dot{u} + Ku = P(t) \tag{1.1}$$

where M = mass of the system

C = equivalent viscous damping of the system

K = stiffness of the system

$u, \dot{u}, \ddot{u}$ = displacement, velocity, and acceleration, respectively

$P(t)$ = time varying load function

The natural circular frequency of an undamped SDOF system is given by Eq. (1.2) [1]

$$\omega = \sqrt{K/M} \tag{1.2}$$

This is the frequency in radians/second at which the system will vibrate in the absence of external load. After the application of an impulse load, for example, an undamped SDOF system would vibrate with frequency ω.

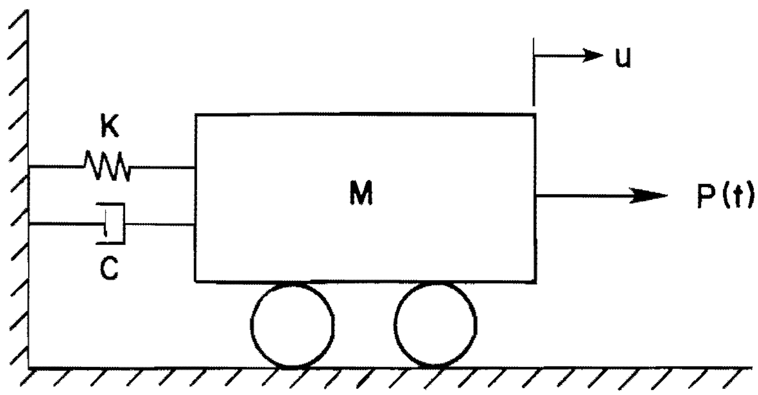

M = MASS
C = DAMPER
K = STIFFNESS
P(t) = LOAD
u = DISPLACEMENT

Fig. 1.5 Single degree of freedom system

The dynamic response of a SDOF system to impulse loads such as truck-induced gusts depends on the magnitude and duration of the load, and also its variation with time. The static response on the other hand, depends only on the maximum magnitude of the load.

The ratio of maximum dynamic to static response is called the "dynamic load factor," or DLF. If the dynamic load factor corresponding to a given combination of loading and structure can be estimated, then the dynamic response can be calculated simply by multiplying the results of a static analysis by that factor.

Figure 1.6 compares the static and dynamic responses of SDOF system to a short impulse load. Note that the static response is constant over time, while the dynamic response oscillates about the static value.

Figure 1.7 shows the general DLF curve of a structure subjected to a triangular impulse load. The period of the structure is defined as T and the duration of the applied load as t_d.

1.3.2 Damping. The amount of damping present is a measure of the sign's ability to dissipate the vibration response energy and return to an at-rest condition. Damping is often modeled analytically as equivalent viscous damping, defined as a percentage of critical damping:

$$\xi = C/2M\omega \times 100 \tag{1.3}$$

where ξ = damping

$\xi_c = 2M\omega$ = critical damping

C = system damping

ω = circular natural frequency

M = system mass

Critical damping is the minimum amount of equivalent viscous damping for which a system will no longer oscillate about its static

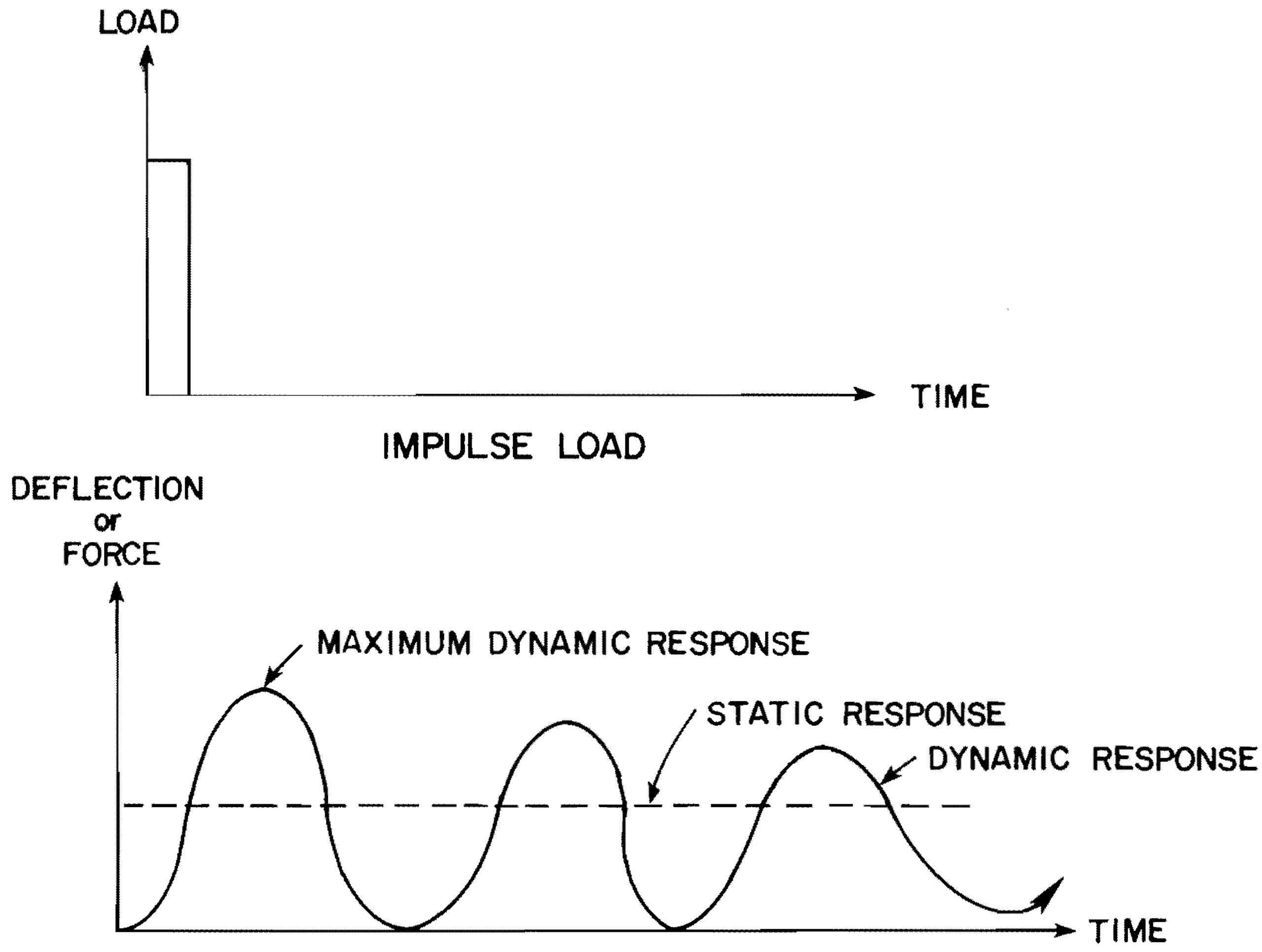

Fig. 1.6 Response to impulse loads

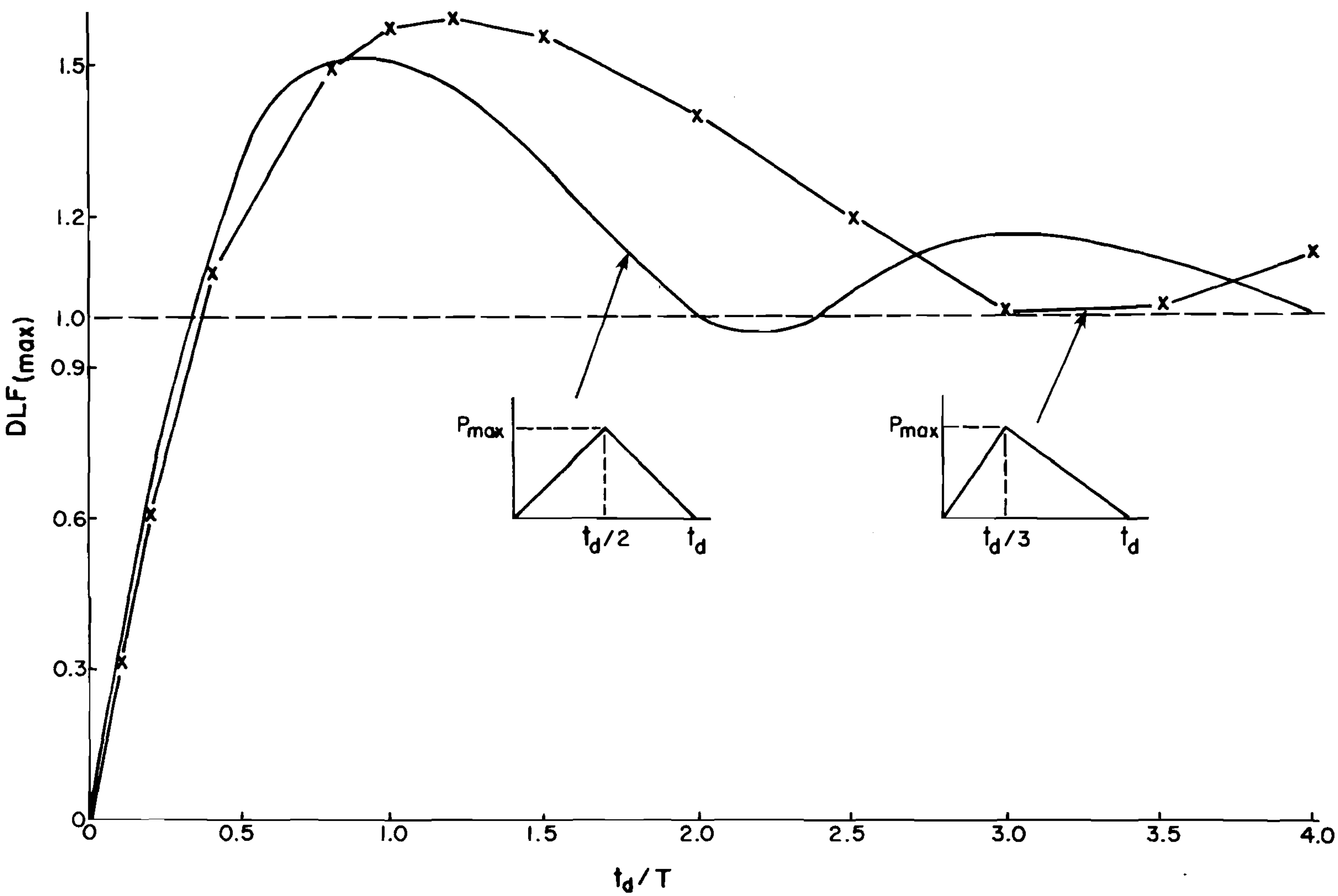

Fig. 1.7 General response to triangular load

equilibrium position. A highly damped structure will quickly expend dynamic energy, with a corresponding rapid decrease in stress magnitude within a small number of oscillations. A low damping ratio results in a low rate of decrease in stress magnitude, over a large number of response cycles. Figure 1.8 shows the effect of damping on response.

As shown by Eq. (1.4), the amount of damping has a direct effect on the fatigue life:

$$N = \frac{A}{S_R^{\,3}} \tag{1.4}$$

where N = number of cycles in fatigue life
A = function of fatigue behavior of detail
S_R = stress range

In a lightly damped structure, a given load produces a large number of stress cycles. This decreases the stress range required to produce a fatigue failure in the structure.

1.3.3 Structural Idealization. A typical cantilever highway sign is composed of a three-dimensional frame supported by a tubular upright. For consistancy with common nomenclature this frame will be referred to as a "truss," even though it is not composed of pin-ended members only. Each joint of the truss is capable of rotational and translational displacements about three axes. The sign must be analyzed as a multiple degree of freedom (MDOF) system

The number of natural vibration frequencies is equal to the number of degrees of freedom. The equations of motion for an N-degree of freedom system are given in Eq. (1.5): [1]

$$[M]\{\ddot{u}\} + [C]\{\dot{u}\} + [K]\{u\} = \{P(t)\} \tag{1.5}$$

where $[M]$ = N x N mass matrix

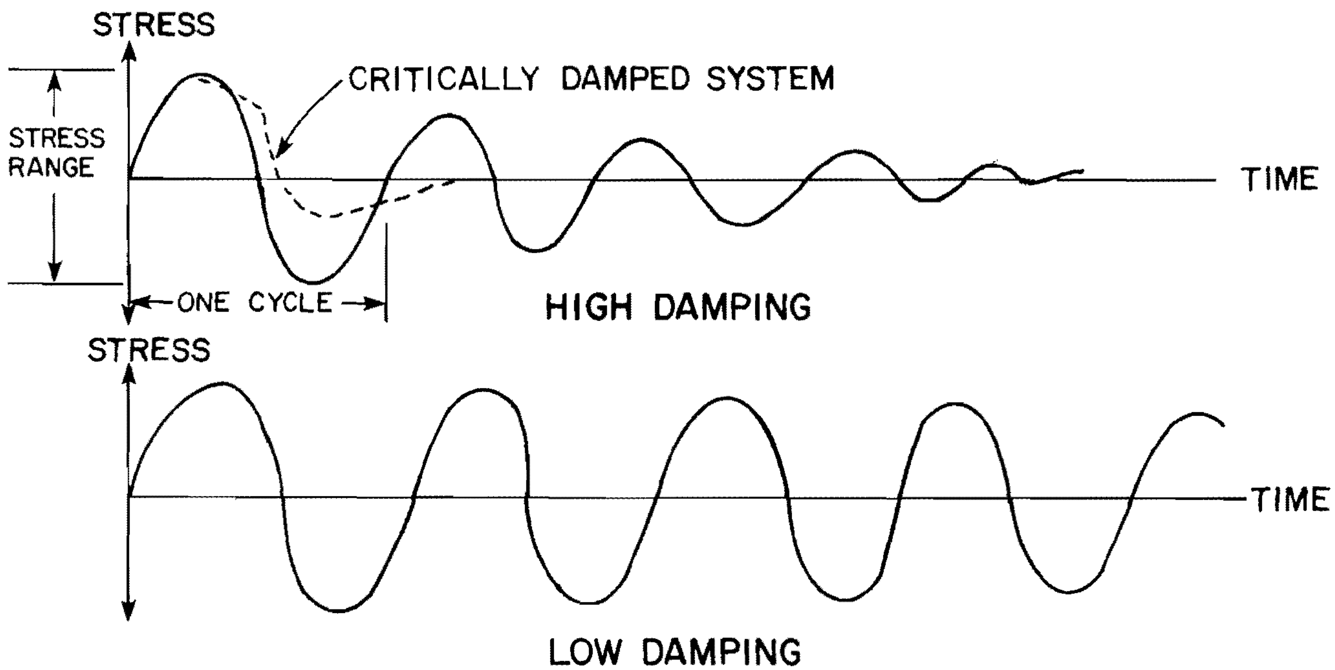

Fig. 1.8 The effect of damping on response

$[C]$ = N x N damping matrix

$[K]$ = N x N stiffness matrix

$\{u, \dot{u}, \ddot{u}\}$ = N x 1 vector of displacements, velocities, and accelerations, respectively

$\{P(t)\}$ = N x 1 vector of applied loading functions

If the loading stops after a short length of time, the vector $\{P(t)\}$ then becomes zero, and the system vibrates at its natural frequencies.

1.4 Experimental Procedure

The three cantilever highway signs described in Sec. 1.2 were instrumented. The anchor bolt reactions induced by gust forces were of interest, but the bolts were not accessible for strain gaging. Consequently, forces in the anchor bolts were determined by measuring the forces carried by the truss members framing into the upright. The forces in the framing members were measured by means of strain gages and the resulting anchor bolt forces calculated.

In all signs the four chord members, the dead load diagonals (on the vertical panels), and one top and one bottom wind load diagonal (on the horizontal panels) were gaged in each arm. Equal and opposite forces were assumed in the two corresponding wind load diagonals not gaged. Figure 1.9 shows the numbering and arrangement of members gaged.

Polyamide-backed SR-4 strain gages of 1/2 in. gage length were used on all signs. The gaging process began with the removal of the galvanized protective coating over a small area at approximately the centroidal axis of the member, so as to minimize the effects of flexural strains on the measured values. The exposed steel was thoroughly cleaned with acetone and a neutralizer. Eastman 910 adhesive was used to fix the gage to the metal. Two coats of Barrier B liquid waterproofing were applied and a Barrier E patch-type

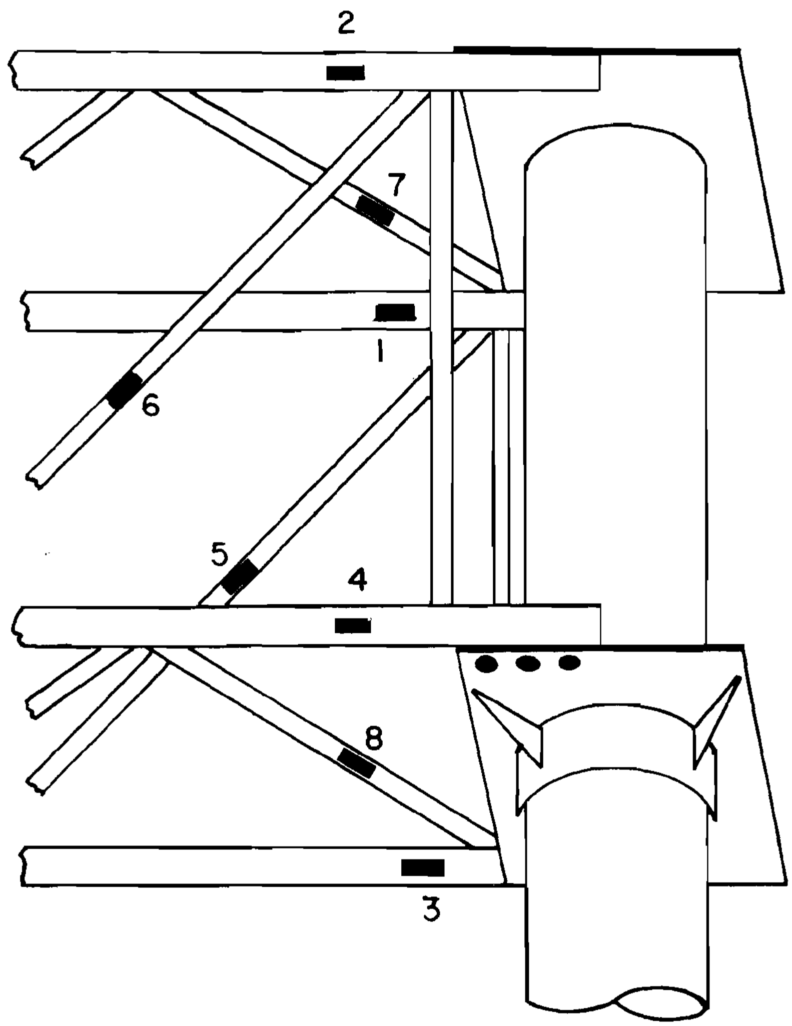

Fig. 1.9 Strain gage locations on single cantilever

waterproofing was applied to protect the strain gage from moisture. Lead wires were soldered to the gages prior to mounting.

The gages were connected through a ten-channel amplifier to an eight-channel Sanborn strip chart analog recorder. A portable, gasoline-powered generator was used to supply power for the recorder and amplifier. All equipment and instruments were transported and housed in the instrumentation van shown in Fig. 1.10.

Measurements taken from the strip chart were converted into stress ranges through the following formula:

$$S_R = N \times \frac{2.00}{G.F.} \times G \times E \tag{1.6}$$

where S_R = stress range

N = number of chart divisions between peaks

$G.F.$ = strain gage factor

G = combined amplifier-recorder system gain

E = steel modulus of elasticity, taken as 29×10^3 ksi

A sample strip chart output for Sign No. 1 is shown in Fig. 1.11.

All signs were excited artificially in order to estimate experimentally the fundamental natural frequency and corresponding modal damping ratio. Excitation was accomplished by standing on the sign truss as close as possible to the upright and shaking the truss horizontally and vertically. In this way the effect of the individual's mass on the sign response was minimized.

1.5 Analytical Procedure

All analyses were carried out using SAP4, a general-purpose structural analysis program for static and dynamic response of linear structures. This program computes and assembles the structure's mass and stiffness matrices using input descriptions of nodal geometry and member properties. All of the cantilever highway sign analyses were based on a three-dimensional model.

Fig. 1.10 Instrumentation van and gasoline generator

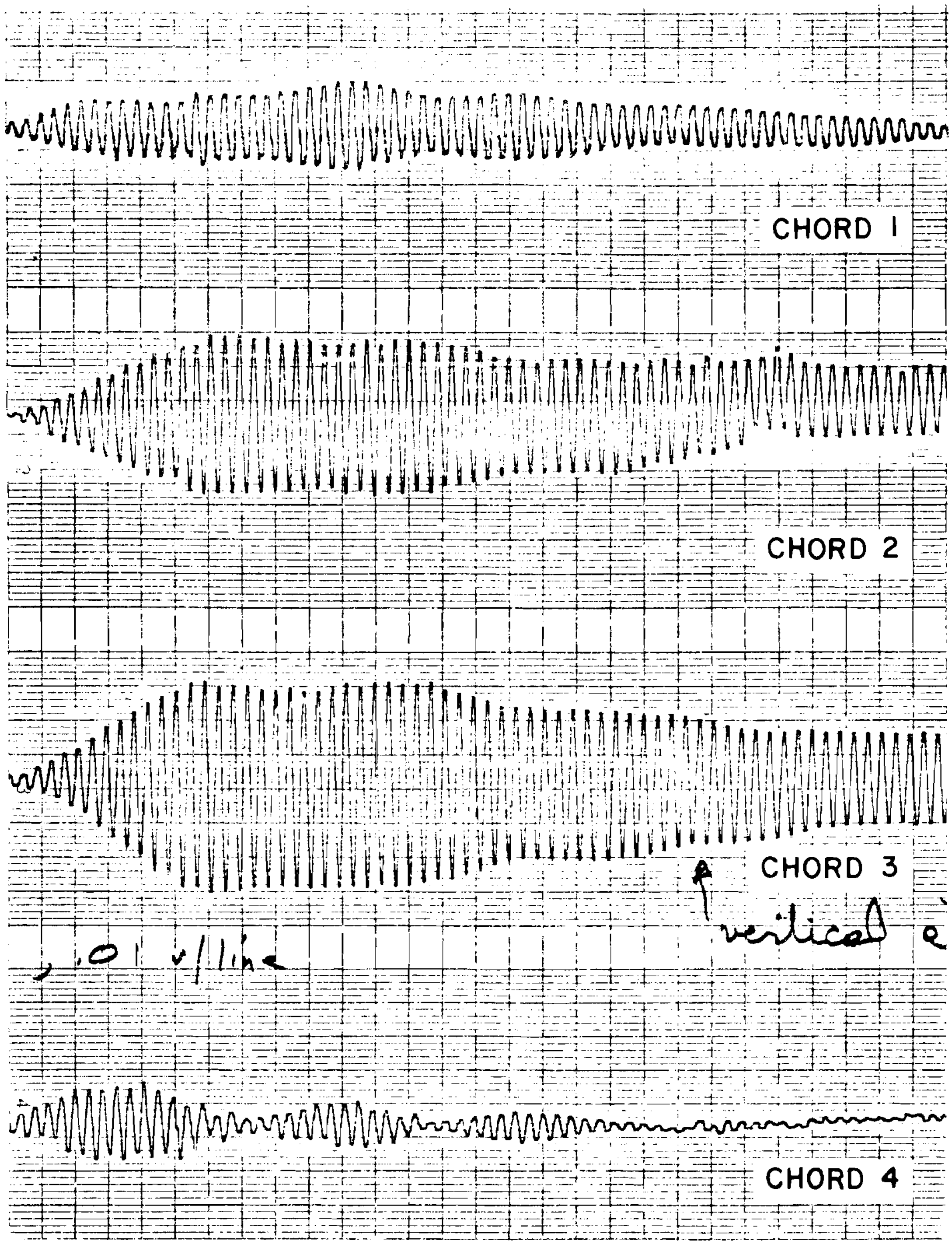

Fig. 1.11 Strain traces from a vertical forced vibration test of double cantilever sign

Preliminary development and refinement of the structural model is described in Ref. 2. Actual member sizes and properties were used for corresponding model elements. The modeling assumptions are presented below:

(1) All chord and support members were modeled as continuous beam elements. In view of their flexible end connections, web diagonals and struts were considered as pin-ended elements.

(2) The base of the support was assumed to be fully fixed. Effects of foundation flexibility were neglected.

(3) All members connecting the truss chords to the tubular upright were modeled using a stiffness equal to that of the upright in order to simulate the high rigidity of the actual plate connection.

(4) The sign, walkway, lights, and lighting ballast box were input as lumped masses at nodal points.

(5) Gust loads were applied only to the sign face, walkway, and lighting case; any effects on member surfaces were neglected. The projected member areas were very small compared to the sign area.

SAP4 assembles a diagonal mass matrix by lumping distributed member masses at connecting nodes. One-half of each member's mass is applied to each of its end nodes.

The loading function, explained in more detail in a later section, was developed to simulate the effect of truck-induced gusts. A time-varying pressure distribution was applied to the major surface areas. The loading duration was related to an assumed vehicle speed.

A parametric study was performed on a variety of different signs. The following major load cases were investigated:

(1) A gravity load analysis resulting from member self-weights.

(2) A static concentrated loading of 20 kips applied horizontally at the free end of the truss.

(3) A static gust loading equal in magnitude to the maximum value of the dynamic gust loading function.

(4) A dynamic analysis based on the gust loading function.

The variables in the study included the truss length, width, and depth, member areas and lengths, upright height, upright stiffness, and member arrangement. Most of the signs analyzed were taken from "Interstate Signing Standards," Texas State Department of Highways and Public Transportation, April 1978 Revision.

The gravity load case was included for completeness and to check the program input. The static and dynamic gust load cases were included to enable the calculation of a dynamic load factor for each sign.

CHAPTER 2

EXPERIMENTAL AND ANALYTICAL RESPONSE

2.1 Experimental Results

The dynamic response of the signs to the passage of a truck was recorded on a strip chart recorder, as shown in Fig. 2.1. The axial force in each strain-gaged member was computed from one-half the stress range using the equation in the previous chapter. Member stresses were assumed to be uniform across the cross section.

2.1.1 Experimental Determination of Frequency, Period, and Damping.

The natural modal frequency, period, and damping as a percent of the critical damping were obtained from strain measurements of the free vibration of the sign after initial excitation. Excitation was generated by standing on the truss near the upright support and shaking the truss in either the horizontal or vertical direction, as desired.

The natural frequency of oscillation was obtained by counting the number of positive or negative peaks occurring in a known time interval. The frequency in cycles per second (cps) is the number of peaks divided by the time interval. The period is the inverse of the natural frequency.

The horizontal or vertical modal damping was estimated using the logarithmic decrement technique in which: [1]

$$\xi = \frac{\ln V_1/V_2}{2\pi} \times 100 \tag{2.1}$$

where ξ = the percent of critical damping

V_1 = a given peak strain amplitude

V_2 = strain amplitude in the next peak

Fig. 2.1 Sanborn strip chart recorder and 10 channel amplifier

This equation assumes that ξ is small, on the order of 10 percent or less. The following table gives the experimental values of natural frequency and damping ratio for Sign No. 1 and Sign No. 2:

TABLE 2.1 EXPERIMENTAL RESPONSE VALUES

Sign Number	Mode	Natural Frequency	Damping Ratio
1	Vertical	1.89-1.90 cps	0.40-0.60 %
1	Horizontal	2.00-2.04 cps	0.61-0.80 %
2	Vertical	1.55-1.56 cps	0.62-0.82 %
2	Horizontal	1.91-1.92 cps	0.64-1.11 %

The damping ratios for both signs are much lower than the 3 percent commonly assumed for steel buildings responding elastically. Consequently, a single impulse load, such as that provided by a truck, produces a large number of cycles.

For Sign No. 3, Eq. 2.1 was modified to allow the use of nonconsecutive peaks [1].

$$\xi = \frac{\ln V_n/V_{n+m}}{2\pi m} \times 100 \tag{2.2}$$

where V_n = the magnitude at peak n

V_{n+m} = the magnitude at peak n+m

m = the number of peaks between points

The two equations differ slightly due to the reading of different points. The percentages of critical damping for Sign No. 3 in the vertical mode ranged from 0.64 to 0.73, with an average value of 0.70. The horizontal mode damping ratios were between 0.53 and 0.61, with the average being 0.57 percent of critical.

The average natural frequencies of vibration for the horizontal and vertical modes of Sign No. 3, as determined from forced vibration data, are shown below. In the vertical mode, the frequency ranged from 1.90-2.00 cps, with an average value of 1.98 cps, resulting in a vertical period of 0.51 seconds. The horizontal mode frequency average was 1.88 cycles per second, the range being 1.80-1.93 cps, resulting in a horizontal period of 0.52 seconds. Table 2.2 summarizes the average experimental natural frequencies and damping ratios for all three signs.

TABLE 2.2 SUMMARY OF EXPERIMENTAL DAMPING AND NATURAL FREQUENCY

Sign No.	Vertical Natural Frequency	Horizontal Natural Frequency	Vertical Damping Ratio	Horizontal Damping Ratio
1	1.90 cps	2.01 cps	0.49 %	0.69 %
2	1.55 cps	1.91 cps	0.73 %	0.77 %
3	1.98 cps	1.88 cps	0.70 %	0.57 %

2.1.2 <u>Forces in Truss Members</u>. Member forces were calculated for each significant truck loading event. The magnitude of the member response varied depending upon the vehicle speed, truck shape, and time interval between trucks. Due to the member force magnitude differences, it was not convenient to compare separate events directly; member force ratios will be examined instead. Force ratios were obtained by dividing the particular member force for an event by the corresponding force in chord member 4. (See Fig. 1.9 for numbering of members.) The strip chart recorder used did not allow the recording of more than eight member strains simultaneously. The sixteen members gaged in the double cantilever could not all be recorded for the same event. Various combinations of strain gages were connected to complete the force ratios for all members. Previously obtained results for Sign No. 1 [2] are presented in Table 2.3. The member numbers with prime marks refer to the exit or generally unloaded side of the double cantilever.

The magnitude of the chord forces varies significantly, the force in chord 3 being approximately 2.5 times the force in the corresponding exist member 3′. The lower chords, members 3 and 4, are seen to carry higher loads than the upper chord members 1 and 2.

TABLE 2.3 EXPERIMENTAL FORCE RATIOS FOR THE DOUBLE CANTILEVER (SIGN NO. 1)

Member	1	2	3	4	1′	2′	3′	4′
Force Ratio From Ref. 2	-0.74	+0.81	-0.83	+1.00	-0.23	+0.21	+0.31	-0.33
Force Ratio From Sanborn Recorder	-0.72	+0.80	-0.95	+1.00	+0.14	-0.09	+0.27	-0.38
Member	**5**	**6**	**7**	**8**	**5′**	**6′**	**7′**	**8′**
Force Ratio From Ref. 2	-0.09	-0.11	+0.17	+0.23	+0.04	+0.10	+0.06	+0.
Force Ratio From Sanborn Recorder	-0.08	-0.07	+0.13	+0.21	+0.05	+0.08	+0.09	+0.1

Table 2.3 also presents additional experimental data taken from the double cantilever using the Sanborn recorder. These values show good agreement with the previous results. The data which differ are thought to be more accurate in the latter case, due to the improved recorder capacity. An additional change was noted in the direction of the force in members 1′ and 2′ on the exit side. This

change is consistent with the anticipated response of the truss. All of the chords now show force direction continuity with their respective members. Due to the lack of significant truck load data, force ratios for Sign No. 2 were not calculated.

This lack of sufficient data for a single cantilever necessitated instrumentation of an additional sign. The Tidwell Exit sign in Houston (Sign No. 3) met the geometric, traffic density, and accessibility requirements. The complete geometric specifications for all three signs are in the Appendix. The experimental results are based on more than 45 significant loading events. Box type and gravel trucks were again found to produce the greatest sign response. Table 2.4 shows the ratios of force values obtained from Sign No. 3 with respect to chord 4.

TABLE 2.4 EXPERIMENTAL FORCE RATIOS FOR SIGN NO. 3

Member	1	2	3	4	5	6	7	8
Force Ratio	-0.59	+0.52	-0.99	+1.00	+0.08	-0.10	+0.20	+0.24

Again, the lower chords were subjected to higher loads than either the top chords or diagonals. The forces carried by chord members 3 and 4 are approximately equal.

2.1.3 Maximum Sign Responses. The two largest sign responses for Sign No. 1 are shown in Table 2.5 [2]. The last two entries are the maximum responses measured using the Sanborn recorder. Extrapolation for the member forces not measured was done using Table 2.3 of the rivised force ratios of Sign No. 1. The experimental data were based on more than 25 hours of recording.

The four largest response events measured for Sign No. 3 are presented in Table 2.6. All of the events from Sign No. 3 were

TABLE 2.5 MAXIMUM RECORDED LOADING EVENTS FOR SIGN NO. 1

Event	Maximum Truss Member Axial Force (lbs)																Support Reactions				
	1	2	3	4	1′	2′	3′	4′	5	6	5′	6′	7	8	7′	8′	Torque (k-in.)	V_y (k)	V_x (k)	M_x (k-in.)	M_y (k-in.)
1	-357	388	-389	466	107	-98	144	-154	-42	-51	19	47	70	107	28	47	41.60	0.181	0.696	25.43	-9.62
2	-262	336	-320	388	89	-81	120	-128	-35	-43	16	30	60	89	23	39	34.22	0.155	0.036	21.74	7.04
3	-209	202	-259	267	37	-24	72	-101	-21	-19	21	22	35	56	31	27	23.68	0.059	0.049	7.80	-16.59
4	-169	207	-222	224	31	-20	60	-85	-18	-16	11	18	23	44	20	34	20.28	0.023	0.004	3.14	-0.21

TABLE 2.6 MAXIMUM RECORDED LOADING EVENTS FOR SIGN NO. 3

Event	Maximum Truss Member Axial Force (lbs)								Support Reactions				
	1	2	3	4	5	6	7	8	Torque (k-in.)	V_y (k)	V_x (k)	M_x (k-in.)	M_y (k-in.)
1	-114	+88	-165	+183	-9	-20	+35	+44	11.24	0.073	0.031	20.88	10.53
2	-107	+84	-160	+181	-8	-17	+33	+45	10.94	0.073	0.022	20.54	7.81
3	-90	+84	-141	+151	-8	-15	+34	+36	9.64	0.065	0.014	18.63	4.93
4	-93	+62	-151	+149	-14	-17	+35	+33	8.45	0.063	0.058	14.15	17.84

measured in the space of three hours and are unlikely to contain the maximum daily loading event.

The values in these two tables indicate that the shear in the direction parallel to the truss length, V_x, is generally much smaller than V_y. Comparing the last two events in Table 2.6, we can see how sensitive M_y is to changes in the forces in members 1, 2, 5, and 6. The torsional moment did not exhibit the same degree of sensitivity to member force changes. Box type trucks were found to produce the largest sign response.

2.2 Loading Function

An analytical study of cantilever highway signs required the development of a loading function. Measurement of the actual gust forces by placing pressure gages on the sign face was not practical, due to the very nature of the highly turbulent flow. The loading function was developed in Ref. [2] by analytically examining member force ratios from various shapes of loading function. The member force ratios were then compared with the experimental data and modifications to the assumed function were made as necessary.

Wind tunnel tests have given the general flow patterns of air particles around vehicle-shaped obstructions [4]. This pattern is shown in Fig. 2.2. As a truck cuts through the surrounding air, momentum is transferred to the air particles. The momentum results from deflection, negative pressure, and drag along the truck surface. At some distance from the truck frictional forces will eventually damp out this imparted motion. Examining the path of an individual particle, we can see that momentum is imparted in both the horizontal and vertical directions. The vertical motion is caused by upward deflection by the cab, and front of the trailer if present. The peak pressure occurs at some point behind the back of the cab. The

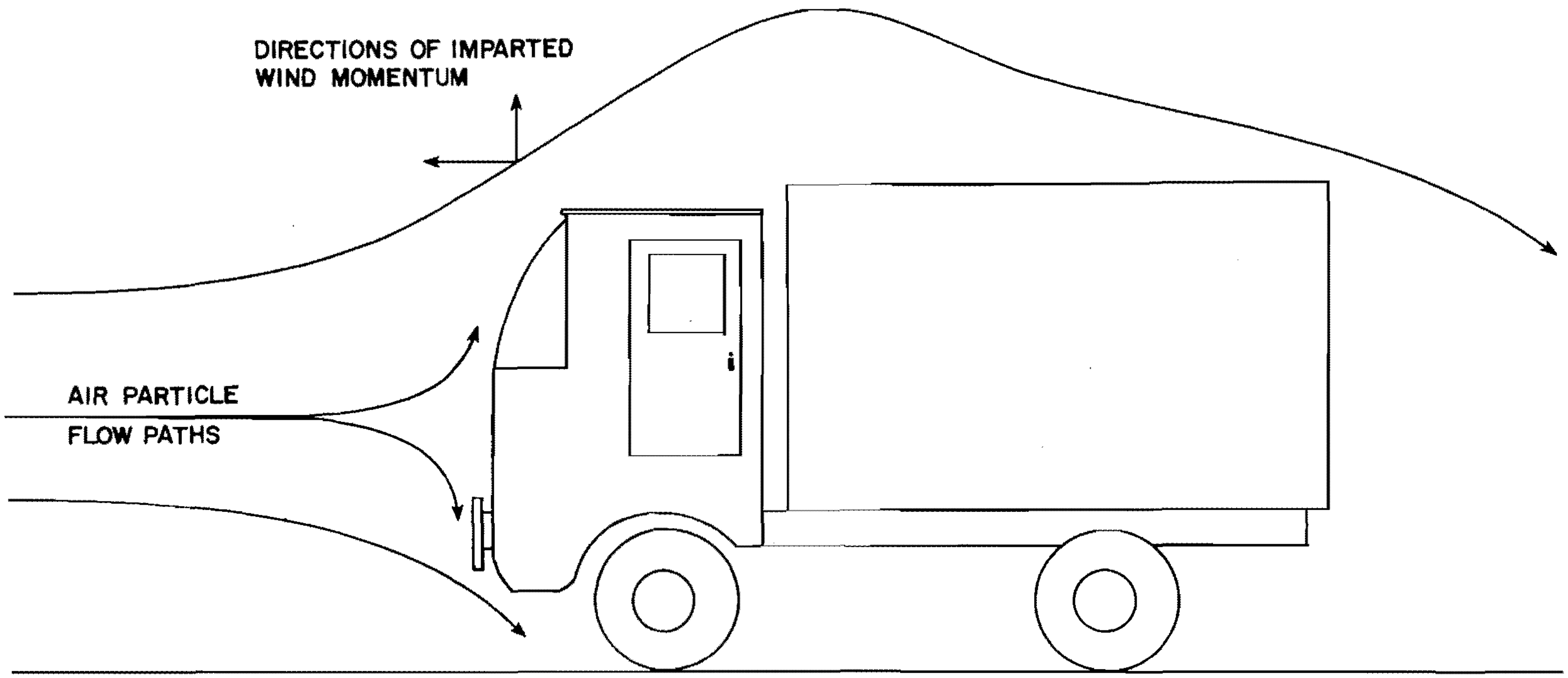

Fig. 2.2 Particle flow paths around a truck

horizontal motion of the particle is the result of negative or suction pressure; through the action of viscous shear forces, the particle is drawn in the direction of vehicle motion. The magnitude of horizontal force is a function of the vehicle's frontal area. The efficiency of horizontal momentum transfer is a function of frictional drag and depends upon truck length, contour, roughness, and velocity. The horizontal velocity of the particle will always be less than the velocity of the vehicle.

The pressure applied to the sign face increases from zero to its maximum value over a certain rise time, and then returns to zero. The rise time is a function of the vehicle speed. The horizontal forces were assumed to vary with time in the same manner as the vertical forces.

The loading function developed is shown in Fig. 2.3. This pressure distribution is not presumed to be the actual gust loading present in the field, but rather one that simulates the member forces measured. The shape of the function and its duration were related to vehicle speed: a truck moving at 55 mph travels approximately 81 ft in one second; maximum truck length limits the gust duration to less than one second. The rise time of one-eighth of a second represents the time taken for the first 10 ft of the truck to pass under the sign face. The total duration of three-eighths of a second corresponds to the time required for the whole vehicle to pass under the sign. By matching the member stresses from the largest recorded loading event on the double cantilever sign to the analytical output for the same sign, the peak pressure was calculated to be 1.23 psf. This pressure corresponds to a wind velocity of 19.2 mph using the standard wind pressure formula:

$$p = 0.00256\ V^2\ C_D \tag{2.3}$$

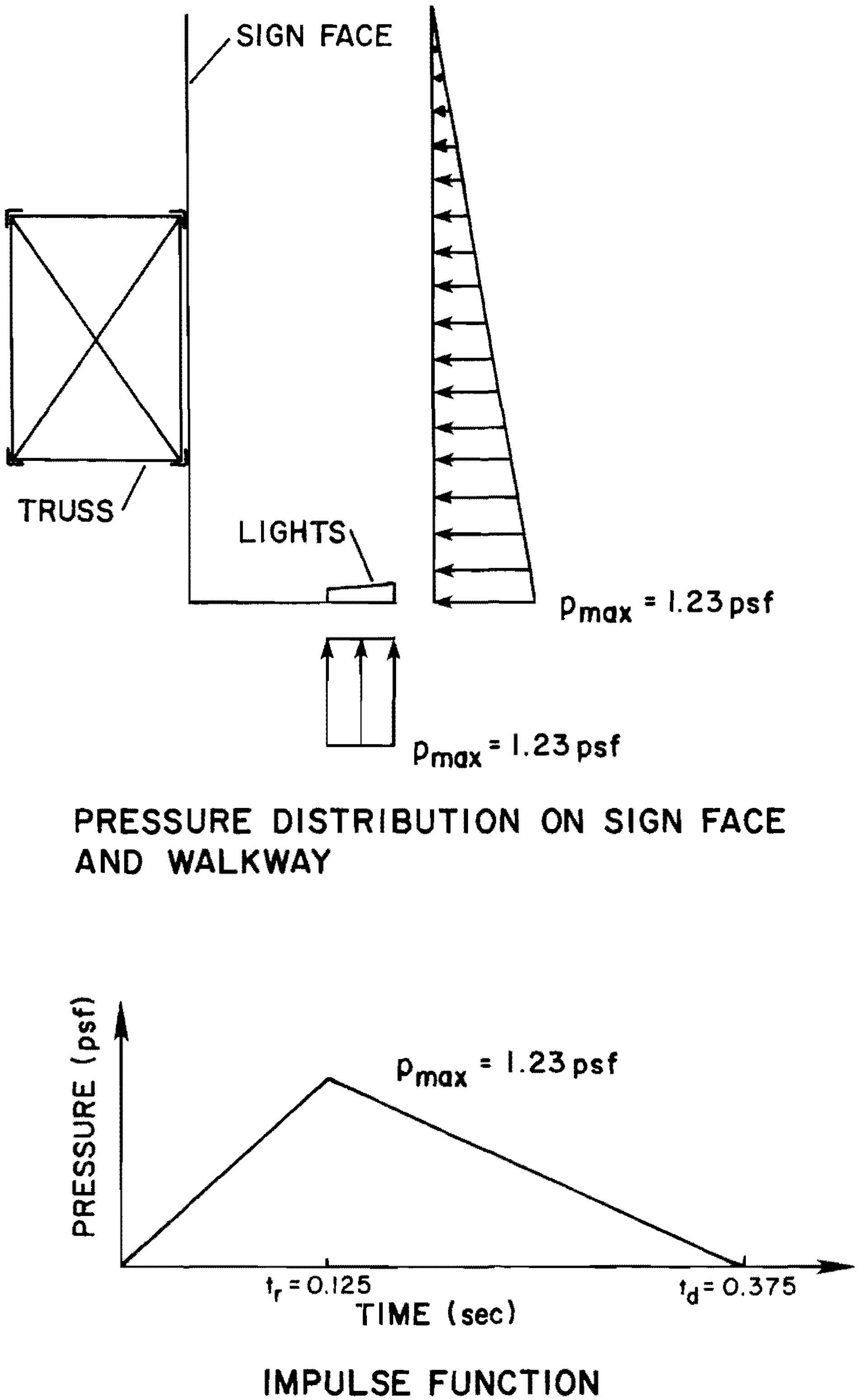

Fig. 2.3 Simulated truck-induced loading

where p = wind pressure in psf

V = wind velocity in mph

C_D = the drag coefficient (1.3 assumed)

The pressure distribution was assumed to vary linearly with elevation, as shown to reflect the decrease in particle motion with distance above the truck. The maximum pressure is applied horizontally to the bottom of the sign face and vertically to the lighting fixtures. The pressure at the top of the sign face was assumed to be zero. Because the greater portion of the horizontal load is below the sign centerline, over the lower truss chords, the increased lower chord forces found experimentally can be simulated analytically.

2.3 Correlation of Experimental and Analytical Results

2.3.1 Nodal Load Application. The loading function outlined in the previous section was applied through the sign to the truss nodes as required by the SAP4 computer program.

In the work done by Cocavessis [2], the loads were applied to the nodes as a function of their tributary areas. This method resulted in the application of approximately 40 percent of the load to the top nodes and 60 percent to the bottom nodes.

For the parametric study of cantilever signs, investigated in detail in the next chapter, a more rational load distribution method was used. Again, approximately 40 percent and 60 percent of the load was applied to the top and bottom modes, respectively; but the load variation along the truss length was slightly altered. A description of the alternate method used is given in the Appendix.

2.3.2 Relative Member Responses. Before a parametric study was begun, the accuracy of the structure model and loading function was checked against the experimental data. In this section the experimental values of modal natural frequencies and member force ratios will be compared to the analytically derived values.

The analytical response of Sign No. 1 and Sign No. 2 were discussed in Ref. 2, and the results are briefly presented below. The error in the analytical estimate of the natural modal frequencies was no more than 5 percent (see Table 2.7). The member force ratios for both the experimental and analytical data along with the percent error are listed in Table 2.8 for the double cantilever.

TABLE 2.7 COMPARISON OF EXPERIMENTAL AND ANALYTICAL FREQUENCIES FOR SIGN NO. 1

Mode	Experimental Frequency (cps)	Analytical Frequency (cps)	% Error
Vertical	1.90	2.00	5
Horizontal	2.01	2.10	4

TABLE 2.8 COMPARISON OF EXPERIMENTAL AND ANALYTICAL MEMBER FORCE RATIOS FOR SIGN NO. 1

Member	1	2	3	4	1′	2′	3′	4′
Experimental Force Ratio	-0.72	+0.80	-0.95	+1.00	+0.14	-0.09	+0.27	-0.38
Analytical Force Ratio	-0.86	+0.75	-0.86	+1.00	+0.03	+0.01	+0.27	-0.31
% Error	+19.4	-6.3	-9.5	0.0	-78.6	88.9	0.0	-18.4
Member	**5**	**6**	**7**	**8**	**5′**	**6′**	**7′**	**8′**
Experimental Force Ratio	-0.08	-0.07	+0.13	+0.21	+0.05	+0.08	+0.09	+0.15
Analytical Force Ratio	-0.01	-0.04	+0.13	+0.15	-0.07	+0.09	-0.01	+0.05
% Error*	-87.5	-42.9	0.0	-28.6	40.0	+12.5	88.9	-66.7

$$*\text{Error} = \frac{\text{ABS(experimental value)} - \text{ABS(analytical value)}}{\text{ABS(experimental value)}} \times 100$$

There is very good agreement for the main side members where the larger strain displacements could be more accurately read. Accuracy is good on those members which are the most influential in transferring force to the anchor bolts, namely the chord members and wind load diagonals. The error was large for those members which were found to carry very low forces.

It was not possible to measure the exact wall thickness of the upright support for Sign No. 3 in the field; all other dimensions of the tubular support were measured. From Texas Department of Highways and Public Transportation standard drawings and the known dimensions, the thickness was estimated to be either 0.25 in. or 0.375 in.

The analytically derived natural frequency values for both thicknesses were compared to the measured results. For the 0.25 in. thickness, the horizontal frequency was 2.00 cps and the vertical frequency was 2.11 cps. The horizontal frequency for the 0.375 in. thickness was 2.34 cps and the vertical frequency was 2.46 cps. The experimental values of 1.88 cps horizontal and 1.98 cps vertical correspond more closely to the 0.25 in. thick upright, and that value was therefore assumed in subsequent analyses.

The analytical and experimental force ratio values are compared in Table 2.9 for Sign No. 3. The force ratios predicted correspond fairly well to the measured ratios. The direction of the forces in the members correspond exactly. The magnitudes differ the most in the diagonal members where the forces are relatively small in the noise range of the recorder system and are very difficult to measure. The analytical results did not duplicate the experimental results in the equality of force carried by chords 3 and 4. The force in the chords is highly dependent on the amount of overturning force applied to the lighting fixture.

TABLE 2.9 COMPARISON OF EXPERIMENTAL AND ANALYTICAL MEMBER FORCE RATIOS FOR SIGN NO. 3

Member	1	2	3	4	5	6	7	8
Experimental Force Ratio	-0.59	+0.52	-0.99	+1.00	-0.08	-0.10	+0.20	+0.24
Analytical Force Ratio	-0.68	+0.62	-0.92	+1.00	-0.06	-0.09	+0.11	+0.17
% Error*	+15.3	+19.2	-7.1	0.0	-25.0	-10.0	-45.0	-29.2

$$*\text{Error} = \frac{\text{ABS(experimental value) - ABS(analytical value)}}{\text{ABS(experimental value)}} \times 100$$

If the vertical pressure were to be neglected, the force in chord 3 would be 11 percent greater than the force in chord 4. A slight change in the vertical pressure would reproduce the experimental data more accurately, but without significantly affecting resulting anchor bolt forces. Without the vertical pressure, the chord force ratios in the analytical study would not be representative of the field data.

The agreement between the analytical and experimental values of both modal frequencies and member force ratios was judged to be sufficiently accurate to allow the use of the assumed loading function as presented.

In the parametric study, the geometric factors which influence cantilever sign response were investigated. Actual Texas Department of Highways and Public Transportation standard cantilever sign specifications were studied. From the information in the analytical parametric study general conclusions about sign response will be made and design guidelines recommended.

CHAPTER 3

THE PARAMETRIC STUDY

3.1 Introduction

In the previous chapter the experimentally measured sign response was compared to the analytical response from SAP4. The natural horizontal and vertical model frequencies and member force ratios were found to correlate well. The assumed loading function adequately simulated the gust-induced sign response that had been measured in the field.

In the design process, the most accurate way to account for the effect of gust loadings would involve the instrumentation of an identical or very similar sign. The experimental procedure outlined in Chapter 1 could be used, but two major problems exist with this design approach. The main drawback would be the high expense in both time and money involved. It would not be economically feasible to do this for each of the many hundreds of signs built in this country each year. The second problem would be in finding a sign similar enough structurally and environmentally to give representative results.

The most economically feasible and convenient approach would be the use of a dynamic response amplification factor to modify assumed static loading. The coefficient would be greater than one to account for increased sign response due to gust loads. This coefficient, or dynamic load factor (DLF) was discussed briefly in the first chapter. It was shown that the DLF depends on the ratio between the frequency of the applied load and the natural frequencies of vibration of the structure. A simple method for estimating the natural frequency of a sign would then be helpful.

Using SAP4, a parametric study was made on actual Texas Department of Highways and Public Transportation cantilever standard sign designs to determine DLF and natural frequency values for a variety of sign geometrics. In Texas, cantilever sign design is based on geographic zones which reflect expected natural loading conditions. Zone one signs are designed for 100 mph winds and no icing, and incorporate the largest truss and upright sections. Zone one signs are the most rigid. In contrast, zone four signs have the smallest section areas and are the most flexible. The zone four design loads are a 70 mph wind with or without ice buildup. Zones one and four constitute upper and lower limits as far as section sizes and sign structure flexibility are concerned.

Within each zone the truss length varies by 5 ft intervals from 10 to 40 ft, inclusive. The support height varies from 14 ft to 32 ft by 1 ft intervals. Tables 3.1(a), (b), and (c) give the geometric properties of the signs used in the parametric study; the signs were chosen to represent a reasonable variety of possible designs [5]. All combinations of 10, 25, and 40 ft truss lengths and 14, 23, and 32 ft support heights were analyzed. Both zone one and zone four signs were investigated for each combination. A representative sign area was used in the study. A sign size of 80 x 120 in. was used for the 10 ft truss and a 120 x 180 in. sign was used for the 25 and 40 ft truss lengths. The larger 12 in. long sign was too large to be used on the 10 ft truss, necessitating the scaled-down version. The general sign structural arrangement is shown in the Appendix.

3.2 SAP4 Natural Frequencies

Table 3.2 shows the three lowest model frequencies of vibration, as well as the corresponding mode shape ordinates at the free end of the truss and at the top of the support.

TABLE 3.1(a) 10 FT TRUSS LENGTH

ZONE 1

TOWER HGT FT.	10' SPAN (TRUSS D.L. DEFLECTION = 0.014")										
	TOWER PIPE			ANCHOR BOLTS			BASE PLATE	DESIGN LOADS			
	DIA IN.	WALL THICK IN	Δ @ ℄ TRUSS	SIZE	NO.	BOLT CIRCLE DIA	SIZE W/OUT STIFF	AXIAL KIPS	SHEAR KIPS	TORSION FT KIPS	MOMENT FT KIPS
14'	16	0.250	0.108	1¼"φ	8	20½"	24x1¼"	2.13	5.61	25.29	77.33
15'			0.124				24x1¼"	2.18	5.64		82.92
16'			0.141				24x1¼"	2.22	5.66		88.55
17'			0.159				24x1¼"	2.26	5.69		94.20
18'			0.178				24x1⅜"	2.30	5.71		99.88
19'			0.198				24x1⅜"	2.35	5.74		105.58
20'			0.220	1¼"φ		20½"	24x1½"	2.39	5.77		111.32
21'		0.250	0.242	1⅜"φ		20¾"	24½x1½"	2.43	5.79		117.09
22'		0.281	0.238				24½x1½"	2.59	5.82		122.88
23'		0.281	0.260				24½x1⅝"	2.64	5.85		128.70
24'		0.281	0.283				24½x1⅝"	2.69	5.87		134.55
25'		0.312	0.279	1⅜"φ		20¾"	24½x1⅝"	2.88	5.90		140.42
26'		0.312	0.302	1½"φ		21"	25x1¾"	2.94	5.93		146.33
27'		0.312	0.325				25x1¾"	2.99	5.95		152.26
28'		0.344	0.320				25x1¾"	3.20	5.98		158.22
29'		0.344	0.343				25x1⅞"	3.26	6.01		164.20
30'		0.344	0.367	1½"φ		21"	25x1⅞"	3.32	6.03		170.21
31'		0.375	0.362	1¾"φ		21½"	26x1⅞"	3.55	6.06		176.25
32'	16	0.375	0.385	1¾"φ	8	21½"	26x1⅞"	3.61	6.09	25.29	182.32

ZONE 4

TOWER HGT FT.	10' SPAN (TRUSS D.L. DEFLECTION = 0.012")										
	TOWER PIPE			ANCHOR BOLTS			BASE PLATE	DESIGN LOADS			
	DIA IN.	WALL THICK IN	Δ @ ℄ TRUSS	SIZE	NO	BOLT CIRCLE DIA	SIZE W/OUT STIFF	AXIAL KIPS	SHEAR KIPS	TORSION FT. KIPS	MOMENT FT KIPS
14'	16	0.250	0.104	1¼"φ	6	20½"	24x1¼"	2.08	2.75	12.39	38.53
15'			0.119					2.13	2.76		41.23
16'			0.136					2.17	2.77		43.94
17'			0.153					2.21	2.79		46.68
18'			0.172					2.25	2.80		49.43
19'			0.191					2.29	2.81		52.20
20'			0.212					2.34	2.83		54.99
21'			0.234					2.38	2.84		57.79
22'			0.257					2.42	2.85		60.61
23'			0.280					2.46	2.87		63.45
24'			0.305					2.50	2.88		66.30
25'			0.331	1¼"φ		20½"	24x1¼"	2.55	2.89		69.16
26'			0.358	1⅜"φ		20¾"	24½x1⅜"	2.59	2.90		72.04
27'			0.386					2.63	2.92		74.93
28'			0.416					2.67	2.93		77.84
29'			0.446					2.71	2.94		80.76
30'			0.477	1⅜"φ		20¾"	24½x1⅜"	2.76	2.96		83.69
31'			0.509	1½"φ		21"	25x1½"	2.80	2.97		86.64
32'	16	0.250	0.543	1½"φ	6	21"	25x1½"	2.84	2.98	12.39	89.61

EXPLANATION OF NUMBERS IN PARENTHESES IN BASE PLATE COLUMN

(1) = Alternate Base Plate 1¾" thick with ¾" Stiffeners.
(2) = Alternate Base Plate 1⅞" thick with ¾" Stiffeners.
(3) = Alternate Base Plate 2" thick with ¾" Stiffeners.
(4) = Alternate Base Plate 2⅛" thick with ¾" Stiffeners.

Design loads listed are loads at Column Base Plate.
Truss members are all angles.
Number of High Strength Bolts required in truss connection or splice are indicated thus (3) after the member size.
Deflections shown include the design loads for Truss, Sign Panel, Lights and Walkways.

ZONE 1	TRUSS DETAILS				
SPAN	10', 15' & 20'	25'	30'	35'	40'
W×D = WIDTH × DEPTH	4.5 X 4.5	4.5 X 4.5	4.5 X 4.5	4.5 X 4.5	4.5 X 4.5
CHORD	3 X 3 X 3/16 (3)	3 X 3 X ¼ (4)	3½X3½X¼(HS50) (7)	3½X3½X5/16(HS50) (9)	3½X3½X5/16(HS50) (8)
DEAD LOAD DIAGONAL	2½ X 1½ X 3/16 (2)	2½ X 1½ X 3/16 (2)	2½ X 1½ X 3/16 (2)	2½ X 1½ X 3/16 (2)	3 X 2 X 3/16 (2)
WIND LOAD DIAGONAL	3 X 3 X 3/16 (2)	3 X 3 X 3/16 (2)	3 X 2½ X ¼ (3)	3 X 3 X ¼ (3)	3 X 3 X ¼ (3)
DEAD LOAD VERTICAL	2½ X 1½ X 3/16 (2)	2½ X 1½ X 3/16 (2)	2½ X 1½ X 3/16 (2)	2½ X 1½ X 3/16 (2)	3 X 2 X 3/16 (2)
WIND LOAD STRUT	2 X 2 X 3/16 (1)	2 X 2 X 3/16 (1)	2 X 2 X 3/16 (1)	2 X 2 X 3/16 (1)	2½ X 2½ X 3/16 (1)
TRUSS DEAD LOAD	42 #/ft	47 #/ft	53 #/ft	60 #/ft	70 #/ft
SIZE H.S. BOLTS IN CONN.	⅝"φ	⅝"φ	⅝"φ	⅝"φ	¾"φ
NO. & SIZE OF H.S. BOLTS IN CHORD ANGLE TO TOWER CONNECTION PLATE	3 ~ ⅝"φ ea	5 ~ ⅝"φ or 3 ~ ¾"φ ea.	7 ~ ⅝"φ or 5 ~ ¾"φ ea.	9 ~ ⅝"φ or 7 ~ ¾"φ ea	11 ~ ⅝"φ or 8 ~ ¾"φ ea.

ZONE 4	TRUSS DETAILS				
SPAN	10', 15' & 20'	25'	30'	35'	40'
W×D = WIDTH × DEPTH	4.0 X 4.0	4.0 X 4.0	4.0 X 4.0	4.0 X 4.0	4.0 X 4.0
CHORD	3 X 3 X 3/16 (4)	3 X 3 X 3/16 (4)	3X3X¼(HS50) (6)	3X3X5/16(HS50) (6)	3X3X5/16(HS50) (9)
DEAD LOAD DIAGONAL	2½ X 1½ X 3/16 (2)	2½ X 1½ X 3/16 (2)	2½ X 1½ X 3/16 (2)	2½ X 1½ X 3/16 (2)	2½ X 2 X 3/16 (3)
WIND LOAD DIAGONAL	2½ X 2 X 3/16 (2)	2½ X 2½ X 3/16 (2)	2½ X 2½ X 3/16 (2)	3 X 3 X 3/16 (2)	3 X 3 X 3/16 (2)
DEAD LOAD VERTICAL	2½ X 1½ X 3/16 (2)	2½ X 1½ X 3/16 (2)	2½ X 1½ X 3/16 (2)	2½ X 1½ X 3/16 (2)	2½ X 1½ X 3/16 (2)
WIND LOAD STRUT	2 X 2 X 3/16 (1)	2 X 2 X 3/16 (1)	2 X 2 X 3/16 (1)	2 X 2 X 3/16 (1)	2 X 2 X 3/16 (1)
TRUSS DEAD LOAD	37 #/ft	38 #/ft	43 #/ft	50 #/ft	56 #/ft
SIZE H.S. BOLTS IN CONN.	⅝"φ	⅝"φ	⅝"φ	⅝"φ	⅝"φ
NO. & SIZE OF H.S. BOLTS IN CHORD ANGLE TO TOWER CONNECTION PLATE	4 ~ ⅝"φ or 3 ~ ¾"φ ea	4 ~ ⅝"φ or 3 ~ ¾"φ ea	6 ~ ⅝"φ or 5 ~ ¾"φ ea.	6 ~ ⅝"φ or 5 ~ ¾"φ ea	9 ~ ⅝"φ or 7 ~ ¾"φ ea.

TABLE 3.1(b) 25 FT TRUSS LENGTH

ZONE 1

25' SPAN (TRUSS D.L. DEFLECTION = 0.154')											TOWER HGT
TOWER PIPE			ANCHOR BOLTS			BASE PLATE	DESIGN LOADS				
DIA IN	WALL THICK IN	Δ @ ℄ TRUSS	SIZE	NO	BOLT CIRCLE DIA	SIZE W/OUT STIFF	AXIAL KIPS	SHEAR KIPS	TORSION FT KIPS	MOMENT FT KIPS	FT.
24	0.310	0.165	1 3/4"φ	8	29 3/8"	33 3/4 X 1 1/2"	4.90	14.40	168.25	205.58	14'
	0.310	0.189				33 3/4 X 1 1/2"	4.98	14.44		219.64	15'
	0.310	0.215				33 3/4 X 1 5/8"	5.05	14.48		233.79	16'
	0.344	0.221				33 3/4 X 1 5/8"	5.27	14.52		248.21	17'
	0.344	0.248				33 3/4 X 1 5/8"	5.35	14.56		262.29	18'
	0.344	0.276	1 3/4"φ		29 3/8"	33 3/4 X 1 3/4"	5.43	14.60		276.65	19'
	0.344	0.306	2"φ		29 3/4"	34 1/2 X 1 3/4"	5.50	14.64		291.07	20'
	0.375	0.311				34 1/2 X 1 7/8"	5.75	14.68		305.54	21'
	0.375	0.341				34 1/2 X 1 7/8"	5.84	14.72		320.07	22'
	0.375	0.373				34 1/2 X 2"	5.93	14.76		334.66	23'
	0.406	0.376				34 1/2 X 2"	6.20	14.80		349.29	24'
	0.406	0.408				34 1/2 X 2"(1)	6.30	14.84		363.98	25'
	0.406	0.442				34 1/2 X 2"(1)	6.39	14.88		378.72	26'
	0.406	0.476				34 1/2 X 2 1/8"(1)	6.48	14.92		393.51	27'
	0.438	0.477	2"φ		29 3/4"	34 1/2 X 2 1/8"(1)	7.09	14.96		408.34	28'
	0.438	0.512	2 1/4"φ		30"	35 X 2 1/4"(1)	7.20	15.00		423.22	29'
	0.469	0.513				35 X 2 1/4"(2)	7.56	15.04		438.15	30'
	0.469	0.548				35 X 2 1/4"(2)	7.68	15.08		453.12	31'
24	0.469	0.584	2 1/4"φ	8	30"	35 X 2 1/4"(2)	7.80	15.12	168.25	468.13	32'

ZONE 4

25' SPAN (TRUSS D.L. DEFLECTION = [illegible])											TOWER HGT
TOWER PIPE			ANCHOR BOLTS			BASE PLATE	DESIGN LOADS				
DIA IN	WALL THICK IN	Δ @ ℄ TRUSS	SIZE	NO	BOLT CIRCLE DIA	SIZE W/OUT STIFF	AXIAL KIPS	SHEAR KIPS	TORSION FT KIPS	MOMENT FT KIPS	FT.
20	0.250	0.333	1 3/8"φ	8	24 3/4"	28 1/2 X 1 3/8"	4.35	7.00	82.44	107.23	14'
		0.382					4.40	7.02		113.64	15'
		0.435					4.45	7.03		120.14	16'
		0.491					4.50	7.05		126.71	17'
		0.550	1 3/8"φ		24 3/4	28 1/2 X 1 3/8"	4.56	7.07		133.34	18'
		0.613	1 1/2"φ		25"	29 X 1 1/2"	4.61	7.08		140.03	19'
		0.679					4.66	7.10		146.77	20'
	0.250	0.749					4.72	7.12		153.56	21'
	0.281	0.735				29 X 1 1/2"	4.93	7.13		160.39	22'
		0.803				29 X 1 5/8"	4.99	7.15		167.26	23'
		0.874	1 1/2"φ		25"		5.05	7.16		174.17	24'
	0.281	0.949	1 3/4"φ		25 3/8"		5.11	7.18		181.12	25'
	0.312	0.920				29 X 1 5/8"	5.33	7.20		188.02	26'
		0.992				29 3/4 X 1 3/4"	5.39	7.21		195.03	27'
		1.067				29 3/4 X 1 3/4"	5.46	7.23		202.07	28'
	0.312	1.145				29 3/4 X 1 3/4"	5.52	7.24		209.14	29'
	0.344	1.119				29 3/4 X 2"	5.81	7.26		216.23	30'
	0.344	1.194				29 3/4 X 2"	5.88	7.28		223.35	31'
20	0.344	1.273	1 3/4"φ	8	25 3/8"	29 3/4 X 2"	5.95	7.29	82.44	230.50	32'

EXPLANATION OF NUMBERS IN PARENTHESES IN BASE PLATE COLUMN

(1) = Alternate Base Plate 1 3/4" thick with 3/4" Stiffeners.
(2) = Alternate Base Plate 1 7/8" thick with 3/4" Stiffeners.
(3) = Alternate Base Plate 2" thick with 3/4" Stiffeners.
(4) = Alternate Base Plate 2 1/8" thick with 3/4" Stiffeners.

Design loads listed are loads at Column Base Plate

Truss members are all angles

Number of High Strength Bolts required in truss connection or splice are indicated thus (3) after the member size.

Deflections shown include the design loads for Truss, Sign Panel, Lights and Walkways.

ZONE 1	TRUSS DETAILS				
SPAN	10', 15' & 20'	25'	30'	35'	40'
W×D = WIDTH × DEPTH	4.5 X 4.5	4.5 X 4.5	4.5 X 4.5	4.5 X 4.5	4.5 X 4.5
CHORD	3 X 3 X 3/16 (3)	3 X 3 X 1/4 (4)	3 1/2 X 3 1/2 X 1/4 (HS50) (7)	3 1/2 X 3 1/2 X 5/16 (HS50) (9)	3 1/2 X 3 1/2 X 3/8 (HS50) (8)
DEAD LOAD DIAGONAL	2 1/2 X 1 1/2 X 3/16 (2)	2 1/2 X 1 1/2 X 3/16 (2)	2 1/2 X 1 1/2 X 3/16 (2)	2 1/2 X 1 1/2 X 3/16 (2)	3 X 2 X 3/16 (2)
WIND LOAD DIAGONAL	3 X 3 X 3/16 (2)	3 X 3 X 3/16 (2)	3 X 2 1/2 X 1/4 (3)	3 X 3 X 1/4 (3)	3 X 3 X 1/4 (3)
DEAD LOAD VERTICAL	2 1/2 X 1 1/2 X 3/16 (2)	2 1/2 X 1 1/2 X 3/16 (2)	2 1/2 X 1 1/2 X 3/16 (2)	2 1/2 X 1 1/2 X 3/16 (2)	3 X 2 X 3/16 (2)
WIND LOAD STRUT	2 X 2 X 3/16 (1)	2 X 2 X 3/16 (1)	2 X 2 X 3/16 (1)	2 X 2 X 3/16 (1)	2 1/2 X 2 1/2 X 3/16 (1)
TRUSS DEAD LOAD	42 #/ft	47 #/ft.	53 #/ft	60 #/ft.	70 #/ft.
SIZE H.S. BOLTS IN CONN.	5/8"φ	5/8"φ	5/8"φ	5/8"φ	3/4"φ
NO. & SIZE OF H.S. BOLTS IN CHORD ANGLE TO TOWER CONNECTION PLATE	3 ~ 5/8"φ ea.	5 ~ 5/8"φ or 3 ~ 3/4"φ ea.	7 ~ 5/8"φ or 5 ~ 3/4"φ ea.	9 ~ 5/8"φ or 7 ~ 3/4"φ ea.	11 ~ 5/8"φ or 8 ~ 3/4"φ ea.

ZONE 4	TRUSS DETAILS				
SPAN	10', 15' & 20'	25'	30'	35'	40'
W×D = WIDTH × DEPTH	4.0 X 4.0	4.0 X 4.0	4.0 X 4.0	4.0 X 4.0	4.0 X 4.0
CHORD	3 X 3 X 3/16 (4)	3 X 3 X 3/16 (4)	3 X 3 X 1/4 (HS50) (6)	3 X 3 X 5/16 (HS50) (6)	3 X 3 X 3/8 (HS50) (9)
DEAD LOAD DIAGONAL	2 1/2 X 1 1/2 X 3/16 (2)	2 1/2 X 1 1/2 X 3/16 (2)	2 1/2 X 1 1/2 X 3/16 (2)	2 1/2 X 1 1/2 X 3/16 (2)	2 1/2 X 2 X 3/16 (3)
WIND LOAD DIAGONAL	2 1/2 X 2 X 3/16 (2)	2 1/2 X 2 1/2 X 3/16 (2)	2 1/2 X 2 1/2 X 3/16 (2)	3 X 3 X 3/16 (2)	3 X 3 X 3/16 (2)
DEAD LOAD VERTICAL	2 1/2 X 1 1/2 X 3/16 (2)	2 1/2 X 1 1/2 X 3/16 ✓ (2)	2 1/2 X 1 1/2 X 3/16 (2)	2 1/2 X 1 1/2 X 3/16 (2)	2 1/2 X 1 1/2 X 3/16 (2)
WIND LOAD STRUT	2 X 2 X 3/16 (1)	2 X 2 X 3/16 ✓ (1)	2 X 2 X 3/16 (1)	2 X 2 X 3/16 (1)	2 X 2 X 3/16 (1)
TRUSS DEAD LOAD	37 #/ft	38 #/ft	43 #/ft	50 #/ft	56 #/ft
SIZE H.S. BOLTS IN CONN.	5/8"φ	5/8"φ	5/8"φ	5/8"φ	5/8"φ
NO. & SIZE OF H.S. BOLTS IN CHORD ANGLE TO TOWER CONNECTION PLATE	4 ~ 5/8"φ or 3 ~ 3/4"φ ea.	4 ~ 5/8"φ or 3 ~ 3/4"φ ea.	6 ~ 5/8"φ or 5 ~ 3/4"φ ea.	6 ~ 5/8"φ or 5 ~ 3/4"φ ea.	9 ~ 5/8"φ or 7 ~ 3/4"φ ea.

TABLE 3.1(c) 40 FT TRUSS LENGTH

ZONE 1

40' SPAN (TRUSS D.L. DEFLECTION = 0.582")												TOWER HGT. FT.
TOWER PIPE			ANCHOR BOLTS			BASE PLATE	DESIGN LOADS					
DIA IN	WALL THICK. IN.	Δ @ ℄ TRUSS	SIZE	NO.	BOLT CIRCLE DIA.	SIZE W/OUT STIFF.	AXIAL KIPS	SHEAR KIPS	TORSION FT KIPS	MOMENT FT KIPS		
30	0 375	0 206	2¼"φ	8	36"	41 X 1⅞"	8 78	22 89	432 38	347.21		14'
	0 410	0 219					9 07	22 94		368.40		15'
	0 410	0.249					9 20	22 99		389 82		16'
	0 410	0 282					9 33	23 04		411 46		17'
	0 410	0.316				41 X 1⅞"	9 45	23 09		433 29		18'
	0 440	0 327				41 X 2"	9.80	23 14		455 29		19'
	0 440	0 362					9 94	23 19		477 44		20'
	0 440	0 399					10 08	23 24		499 74		21'
	0 440	0 438				41 X 2"	10 22	23 29		522 16		22'
	0 470	0 531	2¼"φ		36"	41X2⅛"(2)	10 61	23 34		544 69		23'
	0 470	0 489	2½"φ		36½"	42X2⅛"(2)	10 75	23.39		567 34		24'
	0 470	0 531				42X2¼"(3)	10 90	23 44		590 10		25'
	0 500	0 540				42X2¼"(3)	11 33	23.49		612 95		26'
	0 500	0 582				42X2¼"(3)	11 49	23 54		635 89		27'
	0 500	0 626				42X2⅜"(3)	11 64	23 59		658 93		28'
	0 531	0 647				42X2⅜"(4)	12 11	23 64		682 04		29'
	0 531	0 692				42X2⅜"(4)	12 27	23 69		705 24		30'
	0 562	0 687				42X2⅜"(4)	12 77	23 73		728.52		31'
30	0.562	0 732	2½"φ	8	36½"	42X2½"(4)	12 94	23 78	432 38	751 87		32'

ZONE 4

40' SPAN (TRUSS D L DEFLECTION = 0.754")												TOWER HGT. FT.
TOWER PIPE			ANCHOR BOLTS			BASE PLATE	DESIGN LOADS					
DIA IN	WALL THICK IN	Δ @ ℄ TRUSS	SIZE	NO	BOLT CIRCLE DIA	SIZE W/OUT STIFF	AXIAL KIPS	SHEAR KIPS	TORSION FT KIPS	MOMENT FT KIPS		
30	0250	0280	1¾"φ	8	35⅜"	39¾X1½"	7 55	11 22	211 94	200 44		14'
		0322					7 63	11 24		209 33		15'
		0 366					7 71	11 27		218 45		16'
		0 413					7 79	11 29		227.79		17'
		0 463					7 87	11.32		237 32		18'
	0 250	0 516					7 95	11 34		247 01		19'
	0 281	0 510					8.25	11 37		256.86		20'
		0 562					8 34	11 39		266 86		21'
		0 617					8 43	11 41		276 98		22'
		0 675				39¾ X 1½"	8 52	11 44		287.22		23'
		0 735	1¾"φ		35⅜"	39¾ X 1⅝"	8 61	11 46		297 57		24'
		0 797	2"φ		35¾"	40½ X 1⅝"	8 70	11 49		308 01		25'
		0 862				40½ X 1⅝"	8 79	11 51		318 55		26'
		0 930				40½ X 1⅞"	8 88	11 54		329 18		27'
		1 000				40½ X 1¾"	8 96	11 56		339 89		28'
		1 073					9 05	11 58		350.68		29'
		1 148					9 14	11 61		361 53		30'
		1 226					9 23	11 63		372 46		31'
30	0 281	1 306	2"φ	8	35¾"	40½ X 1¾"	9 41	11 68	211 94	384 26		32'

EXPLANATION OF NUMBERS IN PARENTHESES
IN BASE PLATE COLUMN

(1) = Alternate Base Plate 1¾" thick with ¾" Stiffeners
(2) = Alternate Base Plate 1⅞" thick with ¾" Stiffeners
(3) = Alternate Base Plate 2" thick with ¾" Stiffeners.
(4) = Alternate Base Plate 2⅛" thick with ¾" Stiffeners

Design loads listed are loads at Column Base Plate.

Truss members are all angles.

Number of High Strength Bolts required in truss connection or splice are indicated thus (3) after the member size.

Deflections shown include the design loads for Truss, Sign Panel, Lights and Walkways.

ZONE 1	TRUSS DETAILS				
SPAN	10', 15' & 20'	25'	30'	35'	40'
W×D = WIDTH × DEPTH	4.5 X 4.5	4.5 X 4.5	4.5 X 4.5	4.5 X 4.5	4.5 X 4.5
CHORD	3 X 3 X 3/16 (3)	3 X 3 X ¼ (4)	3½X3½X¼(HS50) (7)	3½X3½X5/16(HS50) (9)	3½X3½X⅜(HS50) (8)
DEAD LOAD DIAGONAL	2½ X 1½ X 3/16 (2)	2½ X 1½ X 3/16 (2)	2½ X 1½ X 3/16 (2)	2½ X 1½ X 3/16 (2)	3 X 2 X 3/16 (2)
WIND LOAD DIAGONAL	3 X 3 X 3/16 (2)	3 X 3 X 3/16 (2)	3 X 2½ X ¼ (3)	3 X 3 X ¼ (3)	3 X 3 X ¼ (3)
DEAD LOAD VERTICAL	2½ X 1½ X 3/16 (2)	2½ X 1½ X 3/16 (2)	2½ X 1½ X 3/16 (2)	2½ X 1½ X 3/16 (2)	3 X 2 X 3/16 (2)
WIND LOAD STRUT	2 X 2 X 3/16 (1)	2 X 2 X 3/16 (1)	2 X 2 X 3/16 (1)	2 X 2 X 3/16 (1)	2½ X 2½ X 3/16 (1)
TRUSS DEAD LOAD	42 #/ft	47 #/ft	53 #/ft.	60 #/ft.	70 #/ft.
SIZE H.S. BOLTS IN CONN.	⅝"φ	⅝"φ	⅝"φ	⅝"φ	¾"φ
NO & SIZE OF H.S. BOLTS IN CHORD ANGLE TO TOWER CONNECTION PLATE	3 ~ ⅝"φ ea	5 ~ ⅝"φ or 3 ~ ¾"φ ea	7 ~ ⅝"φ or 5 ~ ¾"φ ea.	9 ~ ⅝"φ or 7 ~ ¾"φ ea.	11 ~ ⅝"φ or 8 ~ ¾"φ ea.

ZONE 4	TRUSS DETAILS				
SPAN	10', 15' & 20'	25'	30'	35'	40'
W×D = WIDTH × DEPTH	4.0 X 4.0	4.0 X 4.0	4.0 X 4.0	4.0 X 4.0	4.0 X 4.0
CHORD	3 X 3 X 3/16 (4)	3 X 3 X 3/16 (4)	3X3X¼(HS50) (6)	3X3X5/16(HS50) (6)	3X3X⅜(HS50) (9)
DEAD LOAD DIAGONAL	2½ X 1½ X 3/16 (2)	2½ X 1½ X 3/16 (2)	2½ X 1½ X 3/16 (2)	2½ X 1½ X 3/16 (2)	2½ X 2 X 3/16 (3)
WIND LOAD DIAGONAL	2½ X 2 X 3/16 (2)	2½ X 2½ X 3/16 (2)	2½ X 2½ X 3/16 (2)	3 X 3 X 3/16 (2)	3 X 3 X 3/16 (2)
DEAD LOAD VERTICAL	2½ X 1½ X 3/16 (2)	2½ X 1½ X 3/16 (2)	2½ X 1½ X 3/16 (2)	2½ X 1½ X 3/16 (2)	2½ X 1½ X 3/16 (2)
WIND LOAD STRUT	2 X 2 X 3/16 (1)	2 X 2 X 3/16 (1)	2 X 2 X 3/16 (1)	2 X 2 X 3/16 (1)	2 X 2 X 3/16 (1)
TRUSS DEAD LOAD	37 #/ft	38 #/ft	43 #/ft	50 #/ft	56 #/ft
SIZE H.S. BOLTS IN CONN.	⅝"φ	⅝"φ	⅝"φ	⅝"φ	⅝"φ
NO & SIZE OF H.S. BOLTS IN CHORD ANGLE TO TOWER CONNECTION PLATE	4 ~ ⅝"φ or 3 ~ ¾"φ ea	4 ~ ⅝"φ or 3 ~ ¾"φ ea	6 ~ ⅝"φ or 5 ~ ¾"φ ea.	6 ~ ⅝"φ or 5 ~ ¾"φ ea.	9 ~ ⅝"φ or 7 ~ ¾"φ ea.

TABLE 3.2(a) MODAL NATURAL FREQUENCIES

Truss Description					
Truss Length (ft)	Upright Height (ft)	Zone	Mode 1 (cps)	Mode 2 (cps)	Mode 3 (cps)
10	14	1	5.3753	5.4813	12.042
	23		2.7969	2.8287	8.8225
	32		1.7729	1.7855	7.8673
	14	4	5.5518	5.6419	12.568
	23		2.7865	2.8159	8.8345
	32		1.6675	1.6786	7.1536
25	14	1	4.2549	4.4705	12.638
	23		3.1834	3.2209	6.9663
	32		2.3200	2.3688	5.0923
	14	4	3.0848	3.3014	10.654
	23		2.2578	2.3405	5.7133
	32		1.7287	1.7325	4.0230
40	14	1	3.1124	3.2935	12.595
	23		2.6431	2.7782	7.3023
	32		2.2640	2.2879	4.6418
	14	4	2.7096	2.8993	12.167
	23		2.2195	2.3758	7.2142
	32		1.7934	1.8753	4.4872

TABLE 3.2(b) EIGENVECTORS FOR 10 FT TRUSS SIGN STRUCTURE

Sign Description Zone	Pole Height ft.	Mode No.	Pole End X* Translation	Pole End Y Translation	Pole End Z Translation	Truss Free End X Translation	Truss Free End Y Translation	Truss Free End Z Translation	Dominant Motion of Body
1	14	1	-48.1	-0.511	2.57	-48.2	45.1	-1.44	Rocking
		2	5.38	8.52	-43.8	5.53	8.82	-70.7	Flexural
		3	-33.7	10.6	-53.1	-40.0	20.4	52.0	Torsional
	23	1	46.7	0.593	-4.58	46.7	-26.8	-3.68	Rocking
		2	-2.17	5.85	-45.8	-2.14	8.21	-54.8	Flexural
		3	30.98	-4.73	37.3	31.2	-8.88	-68.4	Torsional
	32	1	40.8	0.535	-5.61	40.8	-16.9	-5.41	Rocking
		2	4.82	-3.86	40.7	4.82	-6.21	43.9	Flexural
		3	27.3	-2.12	24.9	27.6	-3.74	-75.5	Torsional
4	14	1	-48.4	-0.153	0.798	-48.5	47.0	-4.24	Rocking
		2	7.09	7.74	-43.7	7.27	6.11	-72.6	Flexural
		3	-31.6	10.1	-55.9	-32.1	19.8	54.4	Torsional
	23	1	48.5	0.362	-3.08	48.6	-28.6	-1.86	Rocking
		2	-0.557	5.45	-47.4	-0.521	6.90	-57.5	Flexural
		3	-29.8	4.74	-41.6	-30.1	9.11	70.5	Torsional
	32	1	46.1	0.347	-4.03	46.2	-19.7	-3.58	Rocking
		2	2.95	-3.91	45.8	2.94	-5.55	50.4	Flexural
		3	28.1	-2.70	34.1	28.3	-5.09	-75.8	Torsional

*All values times 10^{-2}

TABLE 3.2(c) EIGENVECTORS FOR 25 FT TRUSS SIGN STRUCTURE

Sign Description Zone	Pole Height ft.	Mode No.	Pole End X* Translation	Pole End Y Translation	Pole End Z Translation	Truss Free End X Translation	Truss Free End Y Translation	Truss Free End Z Translation	Dominant Motion of Body
1	14	1	5.12	1.43	-7.25	5.86	-1.54	-60.3	Torsional
		2	-17.4	-0.061	0.413	-18.0	53.7	-3.83	Rocking
		3	9.48	-10.2	50.0	10.5	-25.8	-6.75	Torsional
	23	1	5.64	2.12	-16.5	6.05	-2.56	-53.7	Torsional
		2	-23.0	0.139	-1.05	-24.2	42.6	-6.54	Rocking
		3	-8.22	5.32	-41.5	-9.04	9.52	29.2	Torsional
	32	1	25.9	0.217	-2.28	26.0	-30.2	-2.97	Rocking
		2	-0.640	2.19	-22.9	-0.473	4.77	-42.6	Flexural
		3	-7.61	2.67	-28.5	-8.83	4.47	44.3	Torsional
4	14	1	4.44	1.31	-7.37	4.98	-0.180	-62.6	Torsional
		2	-18.9	-0.110	0.683	-19.4	56.6	-2.01	Rocking
		3	9.98	-11.2	61.4	11.0	-26.1	-9.71	Torsional
		1	-3.10	-1.90	16.4	-3.38	-1.67	57.6	Torsional
		2	26.5	0.100	-0.864	26.7	-46.3	0.673	Rocking
		3	9.02	-6.12	52.9	9.70	-11.3	-28.2	Torsional
	32	1	-28.1	-0.695	8.10	-28.3	32.4	14.9	Rocking
		2	-7.45	1.93	-22.6	-7.34	12.9	-46.6	Torsional
		3	-8.32	3.35	-39.7	-8.85	5.90	41.5	Torsional

*All values times 10^{-2}

TABLE 3.2(d) EIGENVECTORS FOR 40 FT TRUSS SIGN STRUCTURE

Sign Description Zone	Pole Height ft.	Mode No.	Pole End X* Translation	Pole End Y Translation	Pole End Z Translation	Truss Free End X Translation	Truss Free End Y Translation	Truss Free End Z Translation	Dominant Motion of Body
1	14	1	-2.21	-0.382	1.93	-3.09	0.655	48.7	Torsional
		2	7.40	0.0140	-0.119	8.27	-46.0	1.41	Rocking
		3	-7.37	5.02	-23.0	-6.87	33.1	-16.0	Flexural
	23	1	-2.17	-0.652	5.06	-2.80	0.096	47.1	Torsional
		2	-12.0	-0.0081	0.118	-12.6	42.5	-1.18	Rocking
		3	3.56	-4.37	33.8	4.42	-7.47	-12.5	Torsional
	32	1	3.21	0.925	-9.69	3.68	-2.76	-43.2	Torsional
		2	-15.4	0.084	-0.832	-15.7	35.8	-4.83	Rocking
		3	3.01	-2.61	27.6	3.73	-3.59	-22.2	Torsional
4	14	1	2.08	0.349	-1.94	2.92	-0.605	-51.7	Torsional
		2	7.73	0.013	-0.132	8.58	-49.1	1.30	Rocking
		3	10.4	-4.53	22.4	9.29	-38.1	20.5	Rocking-Flexural
	23	1	2.01	0.596	-5.14	2.56	0.180	-50.2	Torsional
		2	-12.9	-0.013	0.190	-13.5	45.9	-0.705	Rocking
		3	-4.72	4.94	-42.3	-5.59	8.63	13.0	Torsional
	32	1	1.82	0.829	-9.65	2.17	0.491	-47.5	Torsional
		2	-17.5	-0.008	0.175	-17.9	40.4	-0.664	Rocking
		3	3.61	-3.28	38.4	4.27	-4.82	-20.9	Torsional

*All values times 10^{-2}

In each mode the dominant displacement direction was determined by comparing the mode shape ordinates at the free end and support end of the truss. Figure 3.1 describes the modal shapes labeled as rocking, flexural, and torsional. In Table 3.2, where more than one mode is listed, the shape was a combination of the two listed.

A definite trend can be seen in the data. For the shortest truss lengths, the rocking motion has the lowest natural frequency. The lower the natural frequency, the more flexible the structure is in the direction of motion relative to the other displacement modes. The second mode is flexural and the third torsional. This trend is independent of the pole height for the 10 ft truss.

The first mode of the 25 ft truss shows a transition in which the first mode shifts from the rocking to a torsionally dominated mode. For the longest support pole, the decreased flexural stiffness is more significant than the torsional effects from a long truss. The flexural displacement mode is only found in one case of the 25 ft truss length.

Torsional motion completely dominates the first mode of the 40 ft truss length group. The second and third modes are rocking and torsional or flexural, respectively.

As a truck passes underneath the sign face, the displaced air imposes an upward load on the lighting case while loading the sign face horizontally in the direction of traffic flow. Because the area of the sign face is much larger than that of the lighting case area, horizontal motion dominates, as observed in the field tests.

This dominant horizontal force is very important in the study of the magnitude and direction of sign response. Actual sign response is a complex summation of modal responses, the lower modes

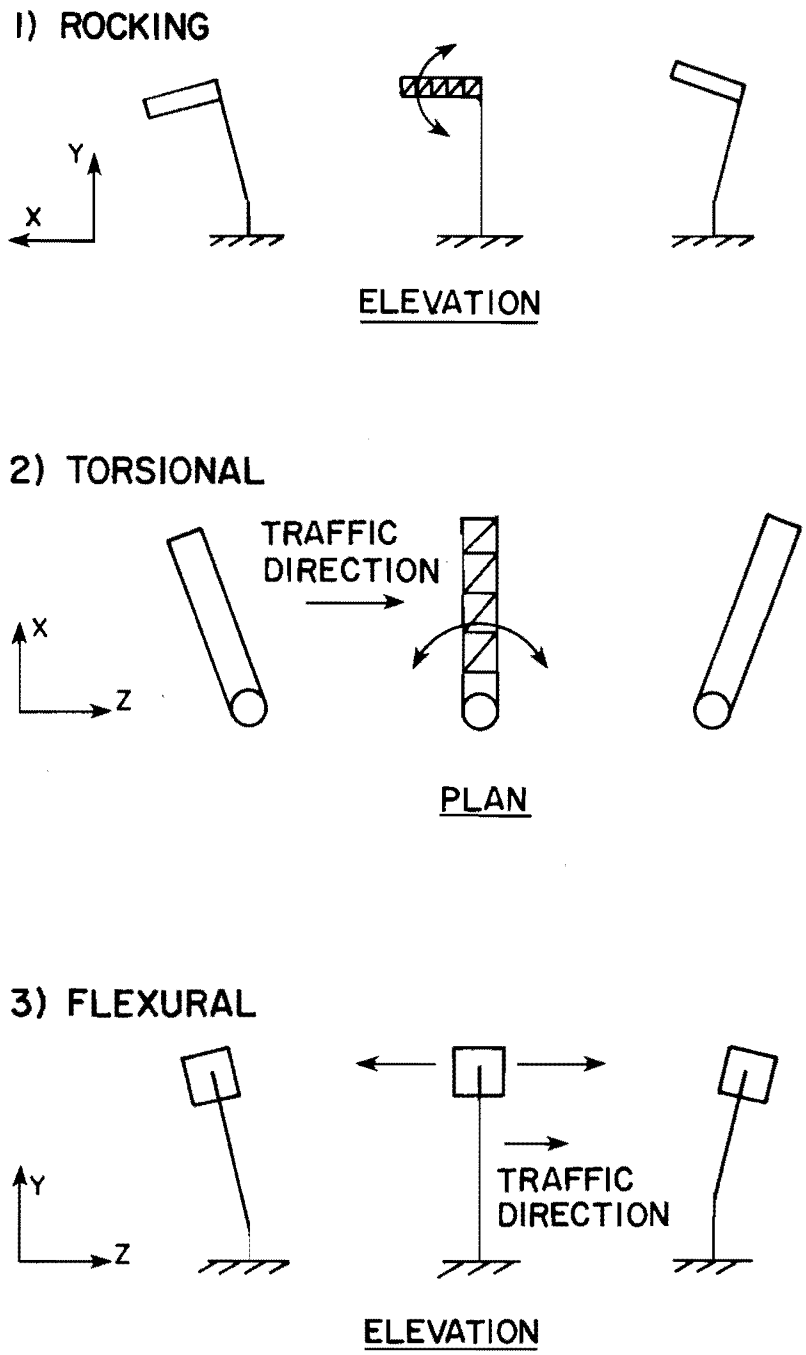

Fig. 3.1 Shape definitions

generally being more significant than higher modes in producing forces at the base of the sign.

The sign will respond in those modes that are excited by the applied loads. The torsional and flexural modes are characterized by horizontal displacements of the sign and truss. They would correspondingly be excited by the dominant horizontal wind force. The structural response of the sign structure will be examined by examining the relationship of sign response to the torsional and flexural modes.

3.3 The Dynamic Load Factor

The dynamic load factor (DLF) is defined as the maximum dynamic response to the loading function, divided by the maximum force resulting from a static application of the loading function at its peak value. Dynamic load factors for torsion moment and flexural shear at the support base were calculated from SAP4 outputs.

3.3.1 The Dynamic Load Factor for Base Shear. The DLF for base shear was obtained using the static and dynamic base forces parallel to the direction of traffic (z-direction), as calculated by SAP4. Shear forces in the traffic direction are caused by flexural displacements of the upright, corresponding to the flexural mode shape. Table 3.3 gives the static and dynamic shear forces, the flexural natural frequency with mode number, and the torsional natural frequency with mode number for each sign. The dominant mode will have the lowest natural frequency and, in many cases, the flexural mode did not dominate. Figure 3.2 shows graphically the relationship between the flexural frequency and the shear DLF. Figure 3.3 shows the shear DLF plotted against the dominant (lowest) torsional or flexural natural frequency.

The reason for considering the dominant natural frequency is the lack of definition of the modes. In a torsionally

TABLE 3.3 SAP4 SHEAR DLF

Sign Description: Zone	Sign Description: Upright Height (ft)	Flexural: Frequency (cps)	Flexural: Mode	Torsional: Frequency (cps)	Torsional: Mode	Static Base Shear Z-Direction (lbs)	Dynamic Base Shear Z-Direction (lbs)	Base Shear DLF
10 ft. Truss								
1	14	5.4813	2	12.042	3	41.200	58.304	1.42
	23	2.8287	2	8.8225	3	41.200	66.522	1.61
	32	1.7855	2	7.8673	3	41.200	62.629	1.52
4	14	5.6419	2	12.568	3	41.200	57.868	1.40
	23	2.8159	2	8.8345	3	41.200	66.500	1.61
	32	1.6786	2	7.1536	3	41.200	60.838	1.48
25 ft. Truss								
1	14	-	-	4.2549	1	92.200	130.29	1.41
	23	-	-	3.1834	1	92.200	168.62	1.83
	32	2.3688	2	5.0923	3	92.200	182.88	1.98
4	14	-	-	3.0848	1	92.300	148.79	1.61
	23	-	-	2.2578	1	92.300	163.26	1.77
	32	-	-	1.7325	2	92.300	168.61	1.83
40 ft. Truss								
1	14	12.595	3	3.1124	1	92.200	163.68	1.78
	23	-	-	2.6431	1	92.200	165.01	1.79
	32	-	-	2.2640	1	92.200	196.68	2.13
4	14	12.167	3	2.7096	1	92.300	153.93	1.67
	23	-	-	2.2195	1	92.300	159.03	1.72
	32	-	-	1.7934	1	92.300	178.24	1.93

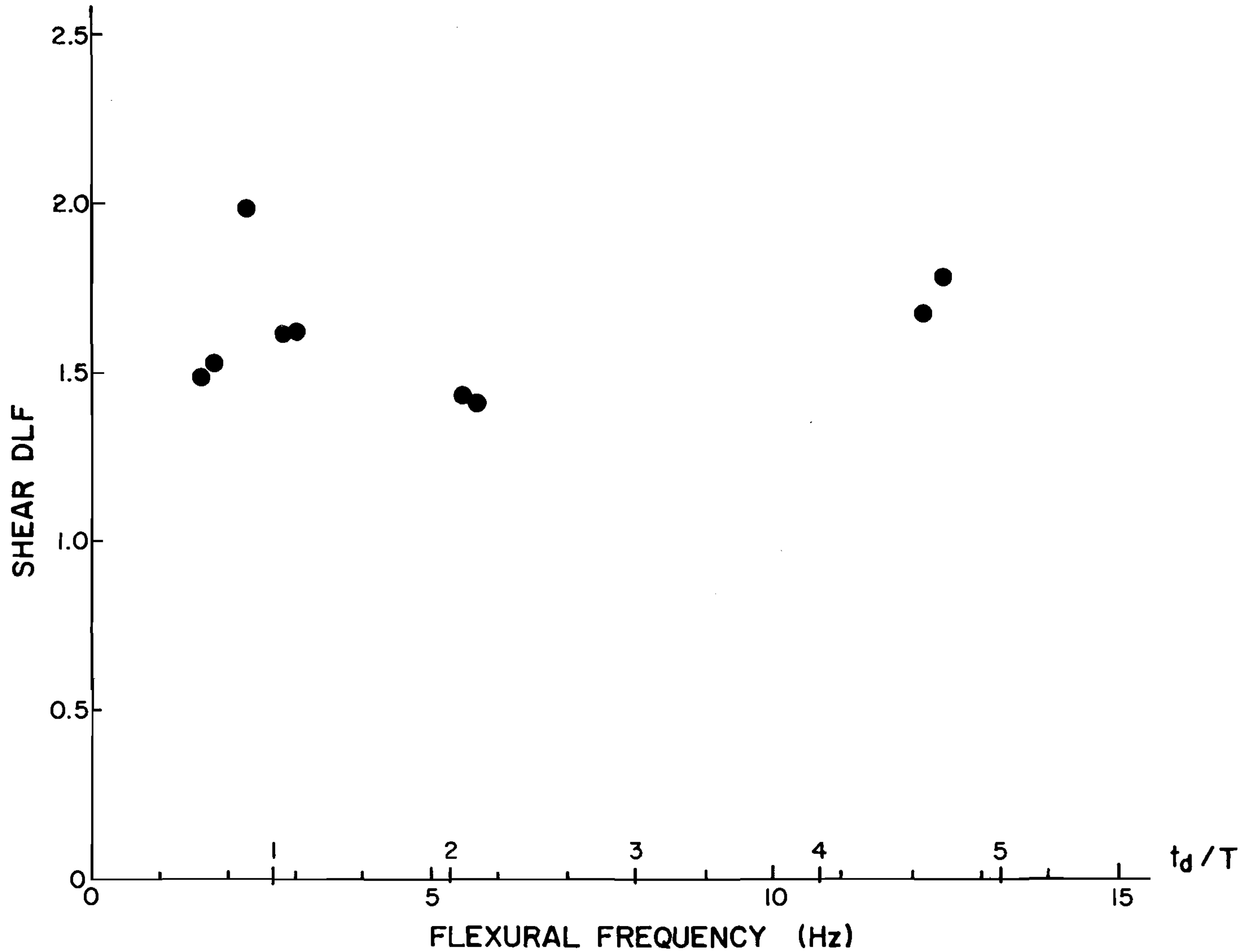

Fig. 3.2 Shear DLF vs SAP4 flexural frequency

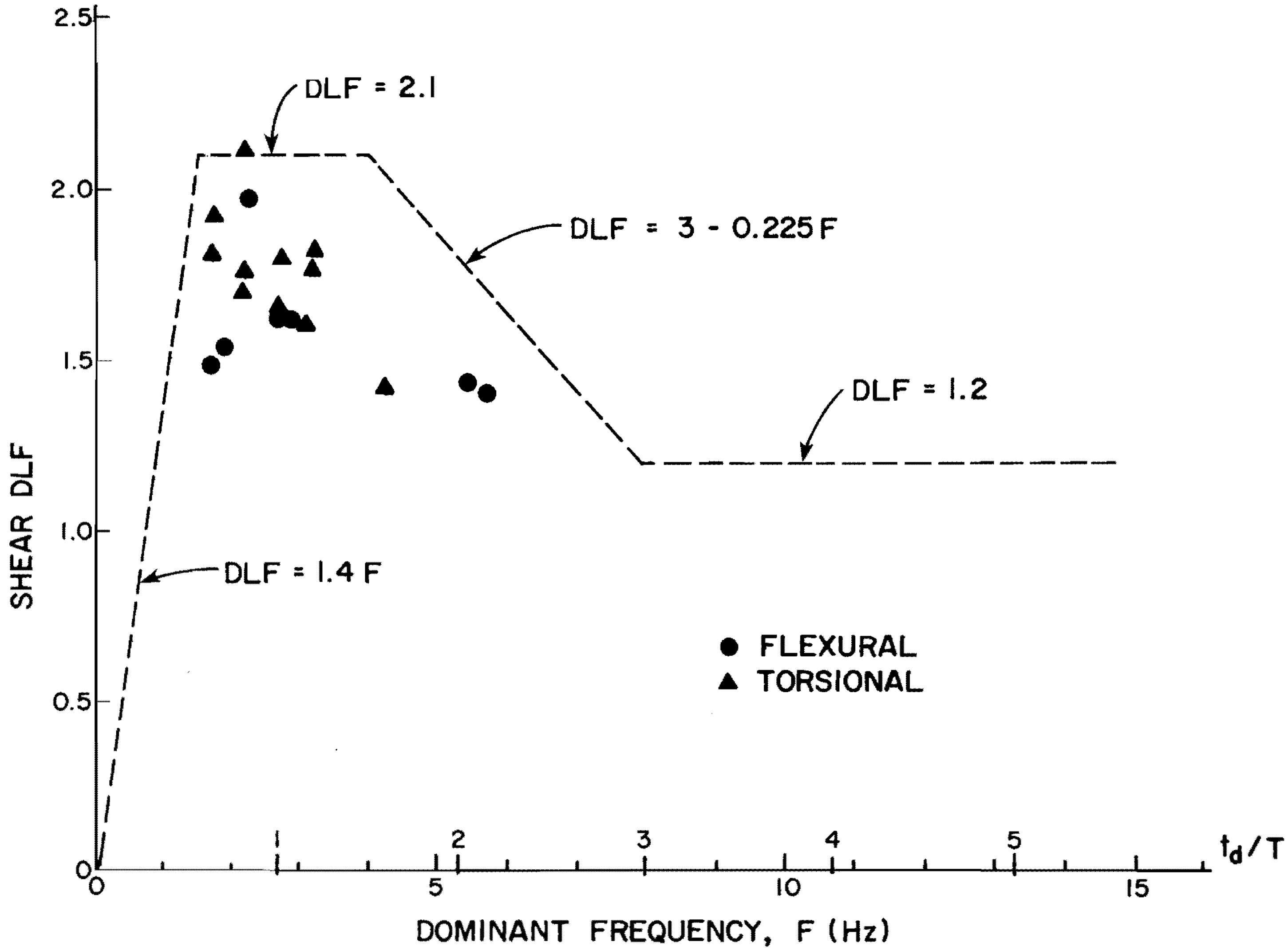

Fig. 3.3 Dominant frequency vs shear DLF

dominated mode, some degree of flexural motion is always present, and vice versa. The amount of flexure present in the torsional modes based on the nodal displacements ranged from 4 to 48 percent.

The small number of points plotted in Fig. 3.2 does not allow a general curve to be drawn. The points do show a grouping between flexural frequency values of 2.4 and 3.0 cps. This high response area is analogous to the curve peak in Fig. 1.7. The greatest response occurs when the duration of the triangular pulse, t_d, approximates the sign's natural period, T, of vibration. The maximum amount of load energy is transferred to the sign during this phasing. The period of the assumed loading function, t_d, is 0.375 seconds, the inverse being 2.67 cycles per second. The maximum DLF is seen to occur in the region of t_d/T equal to 1, as would be expected.

The high response condition is shown more clearly in Fig. 3.3, which has more points plotted. All of the points fall between natural frequency values of 1.5 and 6.0 cps. The majority of the points fall in a narrow band between 1.67 and 3.33 cps. The higher DLF then shown in Fig. 1.7 and the scatter in results is felt to be due to a lack of a clearly defined simple mode shape of many of the signs.

3.3.2 Torsional Dynamic Load Factor. The values of the static and dynamic torsional moments, the lowest torsional mode natural frequencies, and the torsional DLF are listed in Table 3.4.

The results are plotted in Fig. 3.4. The behavior corresponds to the DLF curve for the triangular pulse load shown in Fig. 1.7 with the maximum DLF occurring at $t_d/T = 1$. Two of the points fall below a load factor of 1.0. These points can be explained by examining the eigenvalues and eigenvectors for the 10 ft truss/32 ft support signs. Each of these signs has extremely strong flexural domination of the second mode, caused by a

TABLE 3.4 TORSIONAL DLF

Sign Description: Zone	Sign Description: Upright Height (ft)	Lowest Torsional Frequency (cps)	Static Torque (in.-lbs)	Dynamic Torque (in.-lbs)	DLF
10 ft. Truss					
1	14	12.042	2958	3848	1.30
	23	8.8225	2958	3352	1.13
	32	7.8673	2958	2441	0.83
4	14	12.568	2970	3829	1.29
	23	8.8345	2970	3452	1.16
	32	7.1536	2970	2754	0.93
25 ft. Truss					
1	14	4.2549	20466	28100	1.37
	23	3.1834	20466	29531	1.44
	32	5.0923	20466	24154	1.18
4	14	3.0848	20496	31727	1.55
	23	2.2578	20496	28821	1.41
	32	1.7325	20496	22525	1.10
40 ft. Truss					
1	14	3.1124	37062	58254	1.57
	23	2.6431	37062	55425	1.50
	32	2.2640	37062	50157	1.35
4	14	2.7096	37110	55756	1.50
	23	2.2195	37110	55609	1.50
	32	1.7934	37110	48008	1.29

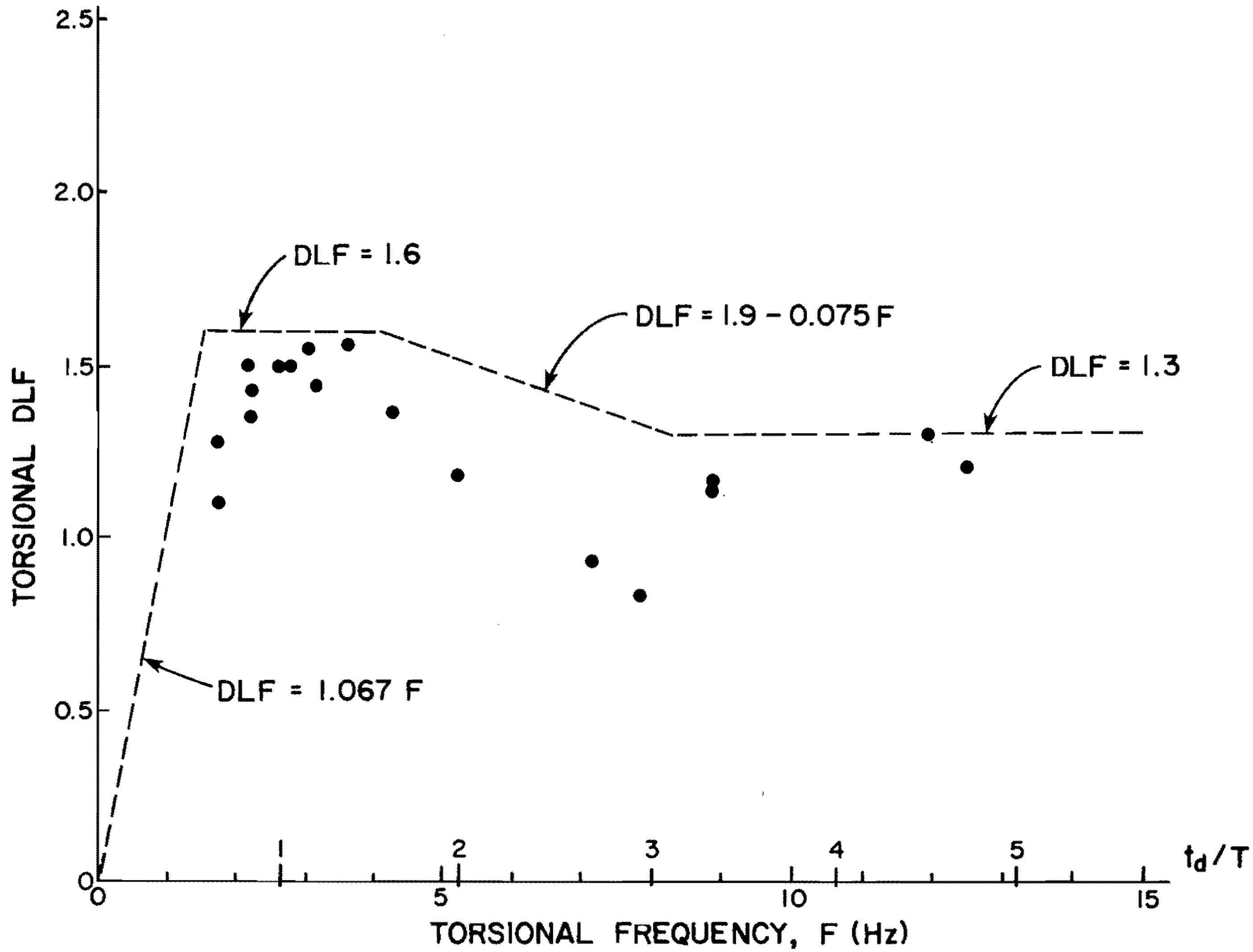

Fig. 3.4 Torsional frequency vs torsional DLF

combination of short truss and long flexible pole. These two signs are the most flexible (lowest first mode frequency values) of all the signs studied. Because of the great flexural flexibility and the short duration of load application, the signs do not have time to develop significant torsional response. These signs constitute a special case and it would not be realistic from a design standpoint to utilize DLF values of magnitude less than one.

3.3.3 Dynamic Load Factor Design Curves. Sign response is directly related to t_d/T, the ratio between the pulse duration and each period of vibration of the sign. Those signs with natural periods close to the duration of the applied pulse will have the largest dynamic load factors. The exact position of the high response area found in the DLF graphs is a function of the assumed pulse duration. The duration of the loading function roughly corresponds to a 30 ft long vehicle travelling at 50 mph. If the vehicle is travelling at a different speed, both the loading intensity and duration will change. As the duration changes, the frequency at which the peak DLF occurs will also change. This fact makes it difficult to draw a curve through the points in either Fig. 3.3 or Fig. 3.4 that will be representative for the range of vehicle speeds expected in actual traffic. Some inaccuracy in the natural frequencies from SAP4 can also be expected.

A blocking or banding approach using the curve shown in Fig. 1.7 as a model was used to account for the variation in vehicle speeds. The dashed lines in Figs. 3.3 and 3.4 show the recommended values of DLF for specified ranges of sign natural frequency. A constant DLF of 2.1 for base shear and 1.6 for torsional base moment was used for frequencies of 1.5 to 4 Hz. This corresponds to a range of t_d/T of 0.56 to 1.50. A linear variation of DLF with frequency was used between 0 and 1.5 Hz and between 4 and 8 Hz for both forces. The DLF equations for these regions are given in Figs. 3.3 and 3.4. These functions were selected to give the necessary DLF of zero for t_d/T equal to zero and match a constant DLF for t_d/T greater than 3 similar to Fig. 1.7. The DLF for both forces is constant for t_d/T greater than 3 or 8 Hz. The torsional DLF is 1.3 for this region. The shear DLF is a constant 1.2. The actual DLF would be expected to vary between a value of 1 and these constant values. This cyclic variation of DLF with frequency was neglected in this region.

3.4 Estimating the Natural Frequency

In the previous sections the DLF was related to values of model natural frequency. The natural frequencies were computed by SAP4. It is not convenient to use a computer program for most design situations. Consequently, simpler closed form means were developed to estimate a sign's natural frequency.

The simplest means of estimating natural frequency is by a single degree of freedom (SDOF)model. A SDOF model assumes displacements are possible in only one direction. Actual sign response is a complex combination of displacements in many directions, but the three motions shown in Fig. 3.1 dominate. Simple procedures for estimating the frequency of each motion will now be discussed.

3.4.1 Torsional Natural Frequency Estimate. Figure 3.5 was used in the derivation of the torsion model. The truss was assumed rigid with rigid body rotations occurring about the pole centerline. Equation 3.1 gives the relationship between torque and rotation for a prismatic circular section.

$$\theta = \frac{T\ L}{J\ G} \tag{3.1}$$

where θ = total rotation in radians

T = torque of twisting moment

L = member length

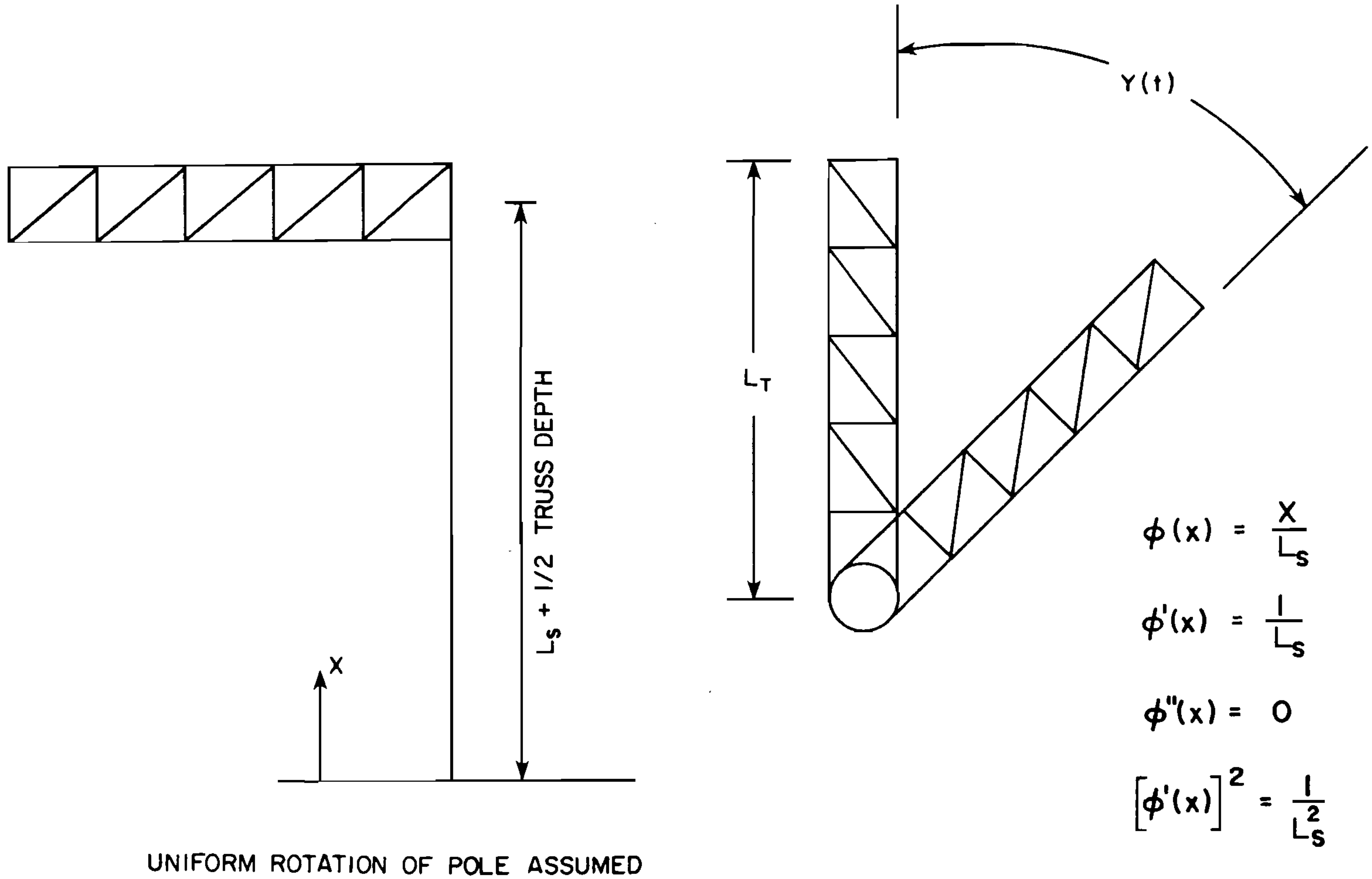

Fig. 3.5 Torsional frequency model

J = polar moment of inertia of gross section

G = shear modulus of elasticity

The stiffness JG is defined as the moment required for a unit rotation per unit length.

The generalized spring stiffness is defined as: [1]

$$K^* = GJ \int_{\ell} [\phi'(x)]^2 \, dx \tag{3.2}$$

where K^* = system generalized stiffness

$\phi(x)$ = shape function of the assumed displacements

$\phi'(x)$ = the first derivative of the shape function

Since we have assumed uniform rotation and a rigid truss, the following shape function can be used:

$$\phi(x) = \frac{x}{L_s} \tag{3.3}$$

$$\phi'(x) = \frac{1}{L_s}$$

where x = vertical distance from pole base

L_s = support height to truss centerline

Substituting into Eq. (3.2), we get expression 3.4 for the generalized stiffness.

$$K^* = GJ \int_{o}^{L_s} \frac{1}{L_s^2} \, dx = \frac{GJ}{L_s} \tag{3.4}$$

The generalized mass of the system is given by expression 3.5, neglecting any torsional inertia effects of the pole mass.

$$M^* = I_o [\phi(x)]^2 \tag{3.5}$$

where M^* = generalized system mass

I_o = mass moment of inertia about the upright = $\frac{m_T L_T^3}{3}$

m_T = distributed truss mass

L_T = truss length

This expression reduces to expression 3.6 upon substitution of the assumed unit rotation at the top of the pole.

$$M^* = \frac{m_T L_T}{3} \tag{3.6}$$

The undamped torsional natural frequency can now be obtained by substituting into Eq. (3.7)

$$\omega = \sqrt{\frac{K^*}{M^*}} = \sqrt{\frac{3GJ}{m_T L_s L_T^3}} \quad \text{(rad/sec)} \tag{3.7}$$

$$f = \frac{\omega}{2\pi} \quad \text{Hz} \tag{3.8}$$

Table 3.5 gives a comparison of the estimated SDOF model frequencies corrected as given below and the torsional frequencies from SAP4. The estimated frequencies from Eq. (3.8) divided by the SAP4 results have been plotted in Fig. 3.6. The ratio of truss length to support height is plotted on the abscissa in the figure. The two curves fitted to the data points suggest a correction coefficient for estimating the natural frequency of the model. The point where a vertical line from the abscissa intersects the curve is used to determine the correction coefficient plotted on the ordinate. The corrected SDOF model frequency is obtained dividing by the ordinate ratio. Corrected torsional frequency values are compared to the actual values in Table 3.5. The maximum error is seen to be less than 6 percent.

The discontinuity in the curve in the region of L_T/L_s equalling 0.8 is caused by the shifting of the dominant natural frequency from a flexural mode to a torsional mode.

3.4.2 Flexural Natural Frequency Estimate. The assumed sign displacements for the derivation of the flexural model frequency are shown in Fig. 3.7. The truss is assumed to be made up

TABLE 3.5 TORSIONAL FREQUENCY PREDICTION ACCURACY

Sign Description: Zone	Sign Description: Upright Height (ft)	Ratio L_T/L_S	Torsional f_T Correction Coeffecient	Corrected Torsional Model f_T (cps)	SAP4 Torsional Frequency (cps)	Percent Error in Frequency	Actual DLF	DLF Predicted	Percent Error in Frequency
10 ft. Truss									
1	14	0.714	0.666	12.012	12.042	-0.2	1.30	1.09*	-16.15
	23	0.435	0.735	8.789	8.8225	-0.4	1.13	1.00*	-11.50
	32	0.313	0.760	7.776	7.8673	-1.2	0.83	1.00*	+20.50
4	14	0.714	0.666	12.447	12.568	-1.0	1.29	1.15	-10.85
	23	0.435	0.735	8.803	8.8345	-0.4	1.16	1.00*	-13.80
	32	0.313	0.760	7.211	7.1536	+0.8	0.93	1.00*	+7.50
25 ft. Truss									
1	14	1.786	1.149	3.994	4.2549	-6.1	1.37	1.38	+0.73
	23	1.087	1.265	3.003	3.1834	-5.7	1.44	1.61	+11.81
	32	0.781	0.647/1.462**	5.301/2.346	5.0923/--	+4.1	1.18	1.15/1.53	-2.54/+29.66
4	14	1.786	1.149	3.046	3.0848	-1.3	1.55	1.60	+3.23
	23	1.087	1.265	2.252	2.2578	-0.3	1.41	1.52	+7.8
	32	0.781	0.647/1.462	3.988/1.765	--/1.7325	+1.9	1.10	1.39/1.31	+26.36/+19.09
40 ft. Truss									
1	14	2.857	1.150	2.991	3.1124	-3.9	1.57	1.63	+3.82
	23	1.739	1.147	2.520	2.6431	-4.7	1.50	1.58	+5.33
	32	1.250	1.203	2.144	2.2640	-5.3	1.35	1.49	+10.37
4	14	2.857	1.150	2.791	2.7096	+3.0	1.50	1.61	+7.33
	23	1.739	1.147	2.276	2.2195	+2.5	1.50	1.52	+1.33
	32	1.250	1.203	1.837	1.7934	+2.4	1.29	1.37	+6.20

*Minimum DLF used.

**Two values indicate in the zone of both equations.

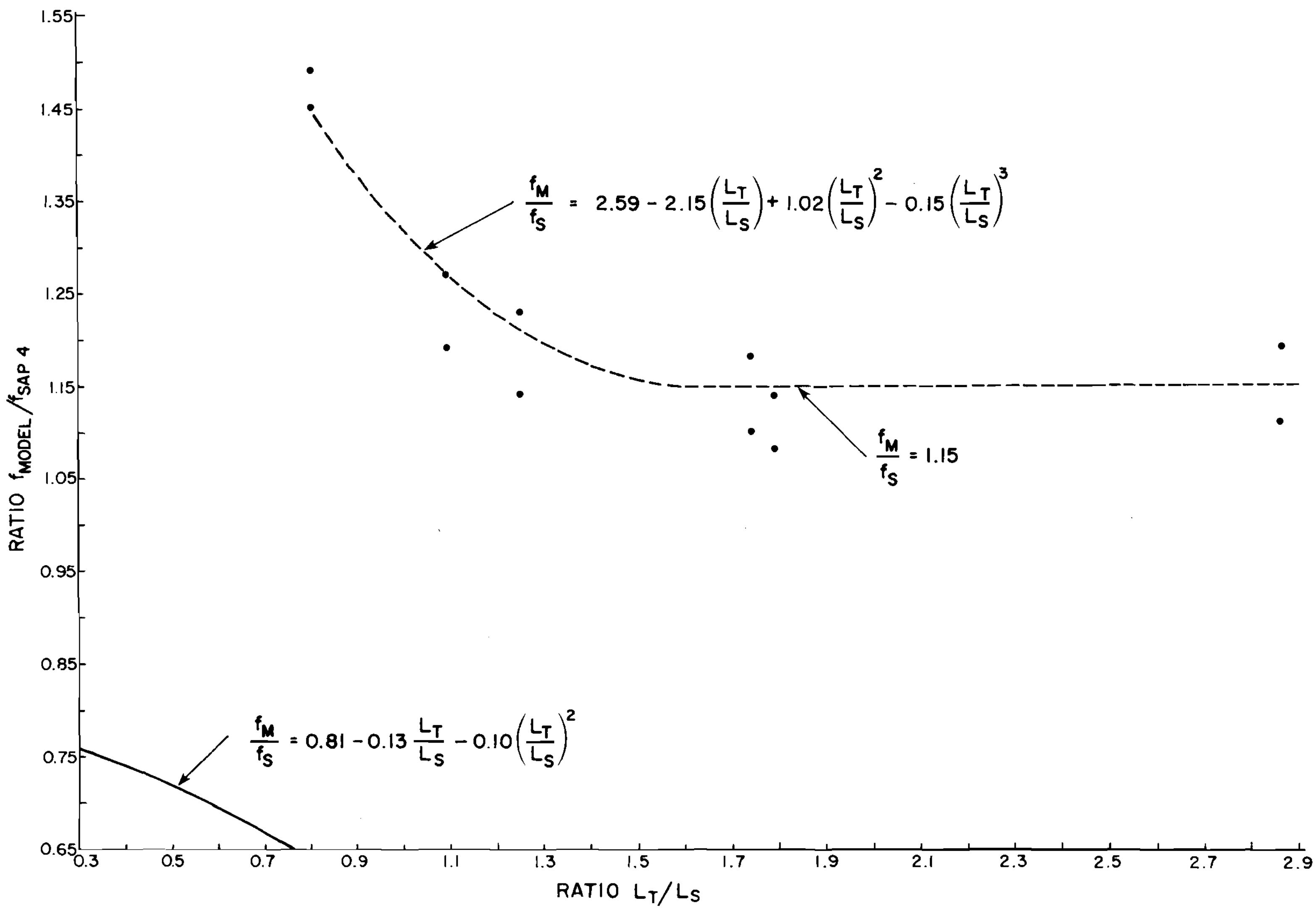

Fig. 3.6 Torsional frequency correction curves

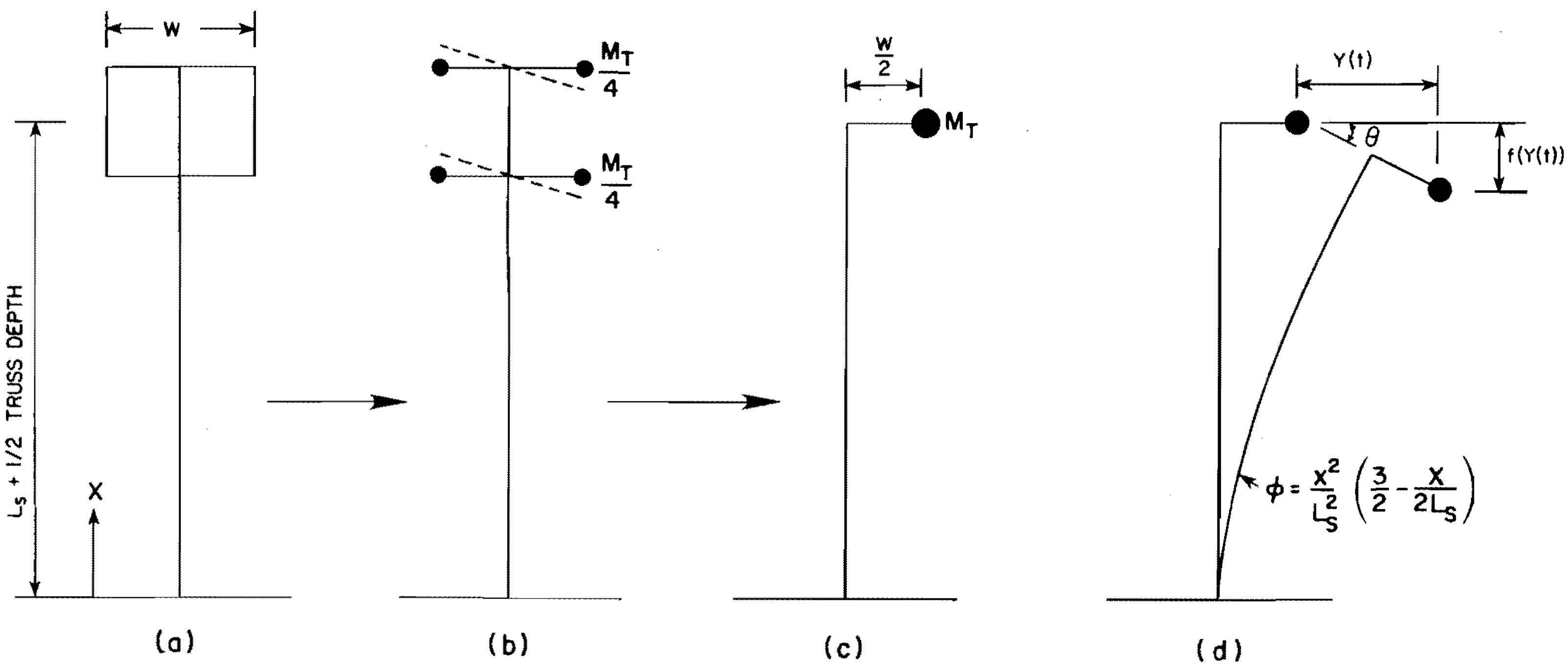

Fig. 3.7 Flexural frequency model

of four equal masses lumped at the corners of the truss, as shown in Fig. 3.7(b). Any flexural displacements of the pole will cause equal movement in the truss masses; the movement is proportional to the distance from the pole centerline to the mass. Figure 3.7(c) is equivalent to the Fig. 3.7(b) and is easier to interpret. The assumed shape function for displacements along the pole length is given by Eq. (3.9) [1].

$$\phi(x) = \frac{x^2}{L_s^2}\left(\frac{3}{2} - \frac{x}{2L_s}\right) \tag{3.9}$$

The displacement angle theta of the horizontal arm is given by Eq. (3.10)

$$\theta = \phi'(L_s) = \frac{3}{4}\,\frac{\text{[illegible]}}{L_s} \tag{3.10}$$

For small displacements, the angle in radians is approximately equal to its sine and tangent. The generalized stiffness is given in expression 3.11 which includes a term for the decreased stiffness due to axial load.

$$\begin{aligned} K^* &= \int_L EI[\phi''(x)]^2\,dx - \int_L N[\phi'(x)]^2\,dx \\ &= K_1^* - K_2^* \end{aligned} \tag{3.11}$$

where E = modulus of elasticity

I = the pole flexural moment of inertia

N = axial load

$\phi''(x)$ = second derivative of the shape function

Substituting the shape function leads to the expressions:

$$K_1^* = EI \int_o^{L_s} \left[\frac{9}{L_s^4} - \frac{18x}{L_s^5} \right] + \frac{9x^2}{L_s^6} \quad dx$$

$$K_2^* = -N \int_o^{L_s} \left[\frac{9x^2}{L_s^4} - \frac{18x^3}{2L_s^5} + \frac{9x^4}{4L_s^6} \right] dx$$

$$= - 5.25 \frac{N}{L_s}$$

$$K^* = \frac{3EI}{L_s^3} - 5.25 \frac{N}{L_s} \qquad (3.12)$$

The expression for the generalized mass is given by Eq. (3.13), for the support and truss mass contributions.

$$M^* = M_s^4 + M_T^4$$

$$= \int_o^{L_s} m_s [\phi(x)]^2 \; dx$$

$$+ \int_o^{L_s} [m_T L_T (\phi(x))^2 + m_T L_T (\theta)^2] \; dx \qquad (3.13)$$

In the second integral term of Eq. (3.13) the generalized mass term for the truss is shown to come from horizontal and vertical displacement components.

Substitution of the variables leads to:

$$M^* = 0.236 \; m_s L_s + m_T L_T \left[1 + \left(\frac{3}{4} \; \frac{\omega}{L_s} \right)^2 \right] \qquad (3.14)$$

The natural circular frequency is then:

$$\omega = \sqrt{\frac{3EI/L_s^3 - 5.25 \; N/L_s}{0.236 \; m_s L_s + m_T L_T \left[1 + \left(\frac{3}{4} \frac{\omega}{L_s} \right)^2 \right]}} \quad \text{rad/sec} \qquad (3.15)$$

The natural frequency values from Eq. (3.15) are listed along with the SAP4 values in Table 3.6. The values are plotted to obtain the flexural correction factor in Fig. 3.8. Flexure is the dominant natural frequency only for the shorter truss lengths.

For ratios of truss length-to-support length greater than 0.9, the flexural natural frequency was not one of the first three modes. In all cases, the correction factors apply only to the range of natural frequencies shown in the curves.

3.4.3 Rocking Natural Frequency Estimate. The derivation of the rocking natural frequency is similar to that of the flexural natural frequency. Figure 3.9 shows the geometrical assumptions made for the rocking model.

The expression for the generalized stiffness is identical to that from the flexural model.

$$K^* = \frac{3EI}{L^3} - 5.25\frac{N}{L_s}$$

The shape function for upright displacements used in the flexural model derivation was used for the generalized mass expression. The two terms shown correspond to support and truss contributions.

$$M^* = M_s^* + M_T^*$$

$$M_s^* = \int_o^{L_s} m_s[\phi(x)]^2\,dx$$

$$= m_s\int_o^{L_s}\left[\frac{9x^4}{4L_s^{\,4}} - \frac{3x^5}{2L_s^{\,5}} + \frac{x^6}{4L_s^{\,6}}\right]dx \tag{3.16}$$

$$= 0.236\ m_s L_s$$

$$M_T^* = M_{T1}^* + M_{T2}^*$$

TABLE 3.6 FLEXURAL FREQUENCY CORRELATION

Sign Description: Zone	Sign Description: Upright Height (ft)	Flexural Model f (cps)	Frequency Correction Coefficient	Corrected Flexural Frequency (cps)	SAP4 Flexural Frequency (cps)	% Error
10 ft. Truss						
1	14	6.22	1.147	5.245	5.4813	-1.0
	23	2.97	1.061	2.800	2.8287	-1.0
	32	1.87	1.052	1.778	1.7855	-0.4
4	14	6.44	1.147	5.617	5.6419	-0.4
	23	2.98	1.061	2.809	2.8159	-0.2
	32	1.75	1.052	1.664	1.6786	-0.9
25 ft. Truss						
1	14	--	--	--	--	--
	23	--	--	--	--	--
	32	2.75	1.181	2.329	2.3688	-1.7
4	14	--	--	--	--	--
	23	--	--	--	--	--
	32	--	--	--	--	--
40 ft. Truss						
1	14	10.79	Not Valid	10.79	12.595	-14.3
	23	--	--	--	--	--
	32	--	--	--	--	--
4	14	10.11	Not Valid	10.11	12.167	-16.9
	23	--	--	--	--	--
	32	--	--	--	--	--

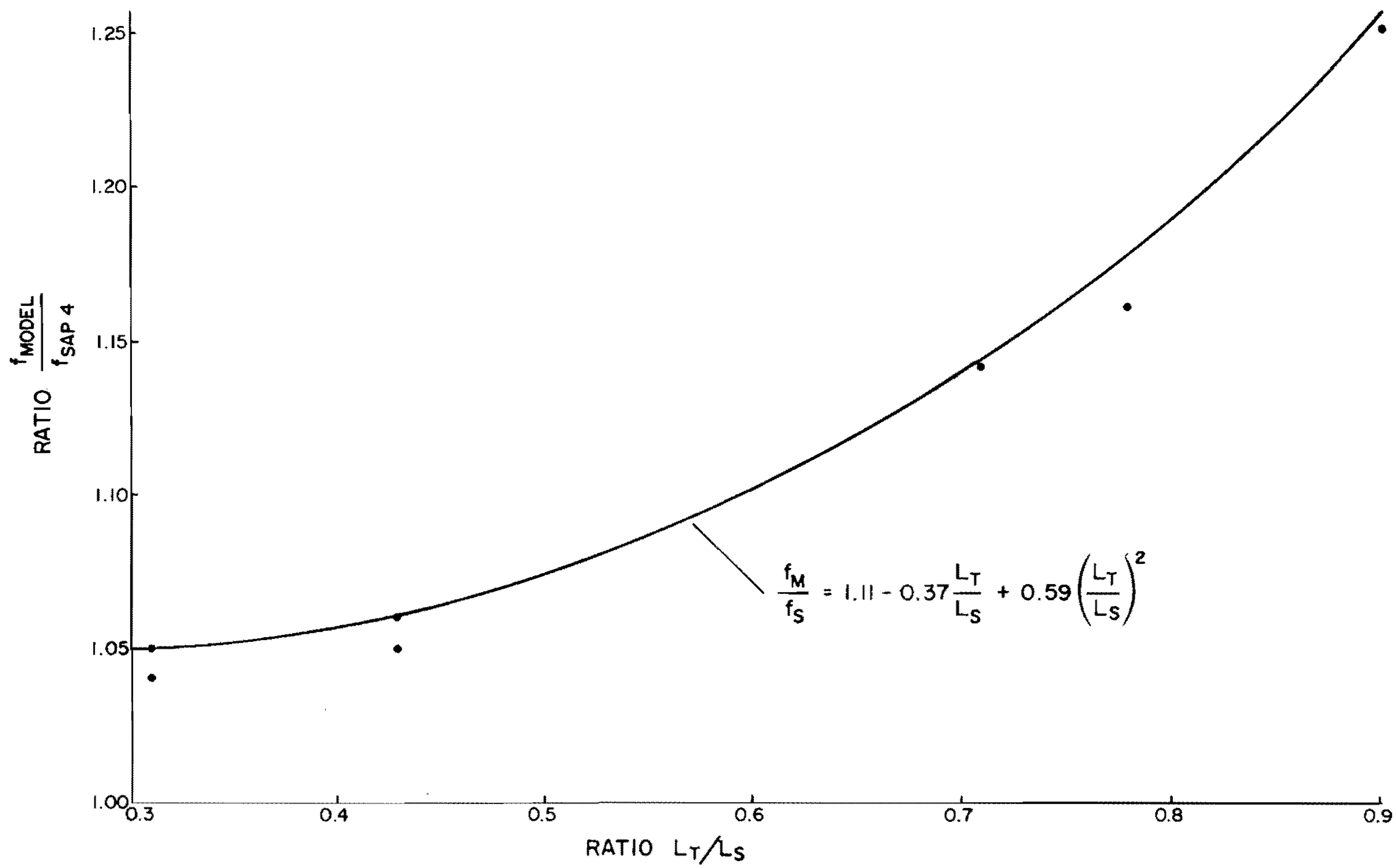

Fig. 3.8 Flexural frequency correction factors

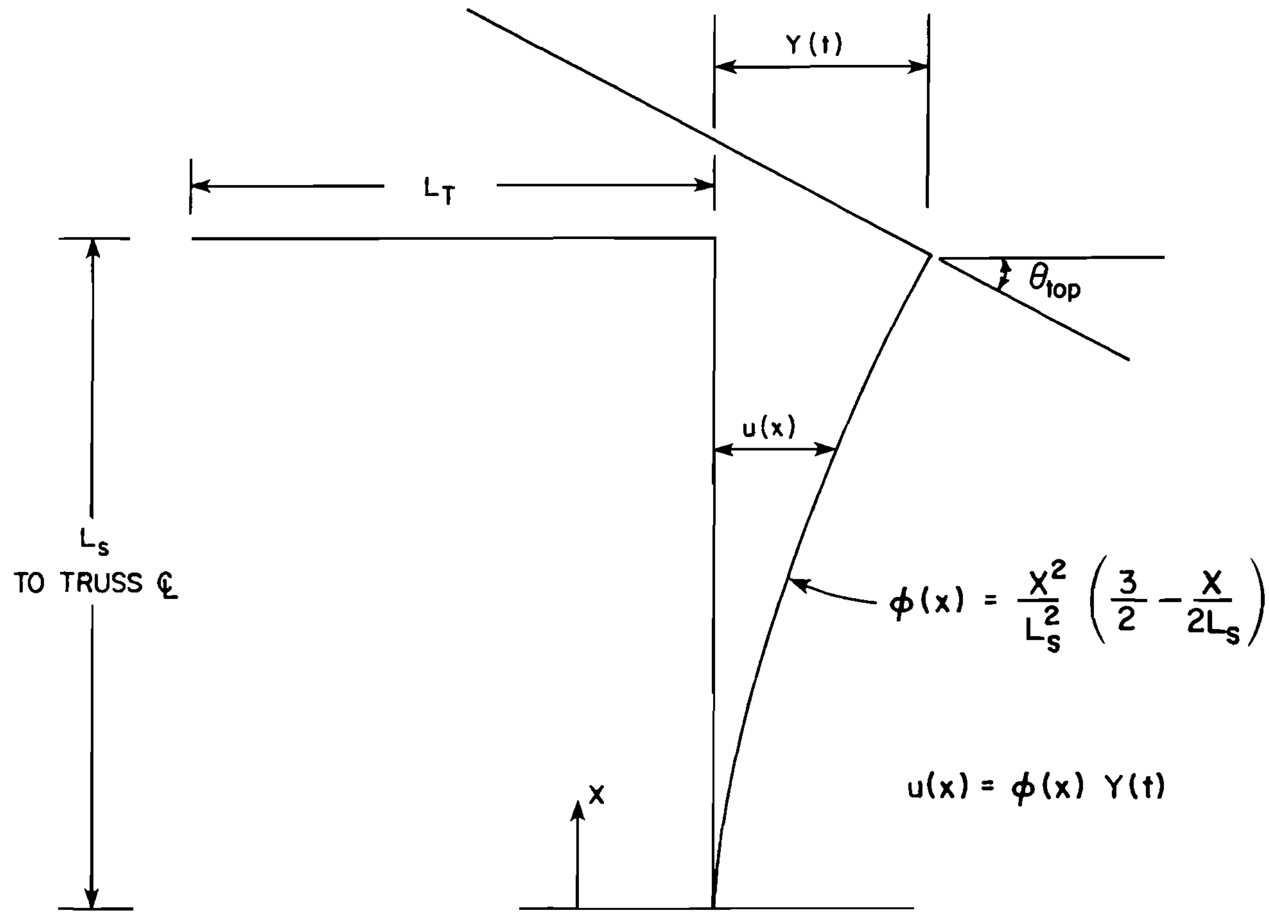

Fig. 3.9 Rocking frequency model

$$M^*_{T1} = m_T L_T = \text{total truss and sign mass}$$

$$M^*_{T2} = I_o(\theta_{top})^2 \qquad (I_o \text{ about end})$$

$$I_o = \frac{ML^2}{3} = m_T L_T{}^3/3$$

$$\theta_{top} = \phi'(x) \text{ evaluated at } x = L_s$$

$$= \frac{3}{L_s} - \frac{3}{2L_s} = \frac{3}{2L_s}$$

$$M^*_{T2} = \frac{m_T L_T{}^3}{3}\left(\frac{3}{2L_s}\right)^2 = \frac{m_T L_T{}^3}{L_s{}^2}$$

$$M^*_T = m_T L_T \left[1 + \frac{3}{4}\frac{L_T{}^2}{L_s{}^2}\right] \tag{3.17}$$

$$M^* = 0.236\ m_s L_s + m_T L_T \left[1 + \frac{3}{4}\frac{L_T{}^2}{L_s{}^2}\right] \tag{3.18}$$

The generalized stiffness and mass yield the natural frequency:

$$\omega = \sqrt{\frac{3EI/L_s{}^3 - 5.25\ N/L_s}{0.236\ m_s L_s + m_T L_T \left[1 + \frac{3}{4}\frac{L_T{}^2}{L_s{}^2}\right]}} \quad \text{(rad/sec)} \tag{3.19}$$

Correction factors for the rocking model frequencies are plotted in Fig. 3.10. The points were plotted from the values in Table 3.7. The table also compares the corrected rocking natural frequencies to the actual values.

Because of the small amount of force present to excite rocking motion, the rocking frequency does not contribute significantly to the response of cantilever signs to vehicle-induced gust

TABLE 3.7 CORRELATION OF THE ROCKING MODEL NATURAL FREQUENCIES

Sign Description Zone	Upright Height (ft)	Rocking Model Frequency (cps)	Frequency Correction Coefficient	Corrected Rocking Frequency (cps)	SAP4 Rocking Frequency (cps)	% Error
10 ft. Truss						
1	14	5.38	1.00	5.38	5.3753	+0.1
	23	2.80	1.00	2.80	2.7969	+0.1
	32	1.81	1.00	1.81	1.7729	+2.1
4	14	5.56	1.00	5.56	5.5518	-0.1
	23	2.81	1.00	2.81	2.7865	+0.8
	32	1.70	1.00	1.70	1.6675	+1.9
25 ft. Truss						
1	14	5.02	1.148	4.372	4.4705	-2.2
	23	3.30	1.032	3.199	3.2209	-0.7
	32	2.35	1.00	2.35	2.3200	+1.3
4	14	3.82	1.148	3.327	3.3014	+0.8
	23	2.48	1.032	2.404	2.3405	+2.7
	32	1.78	1.00	1.78	1.7325	+2.7
40 ft. Truss						
1	14	4.18	1.327	3.150	3.2935	-4.4
	23	3.10	1.140	2.718	2.7782	-2.2
	32	2.37	1.059	2.238	2.2879	-2.2
4	14	3.89	1.327	2.931	2.8993	+1.1
	23	2.81	1.140	2.464	2.3758	+3.7
	32	2.06	1.059	1.946	1.8753	+3.7

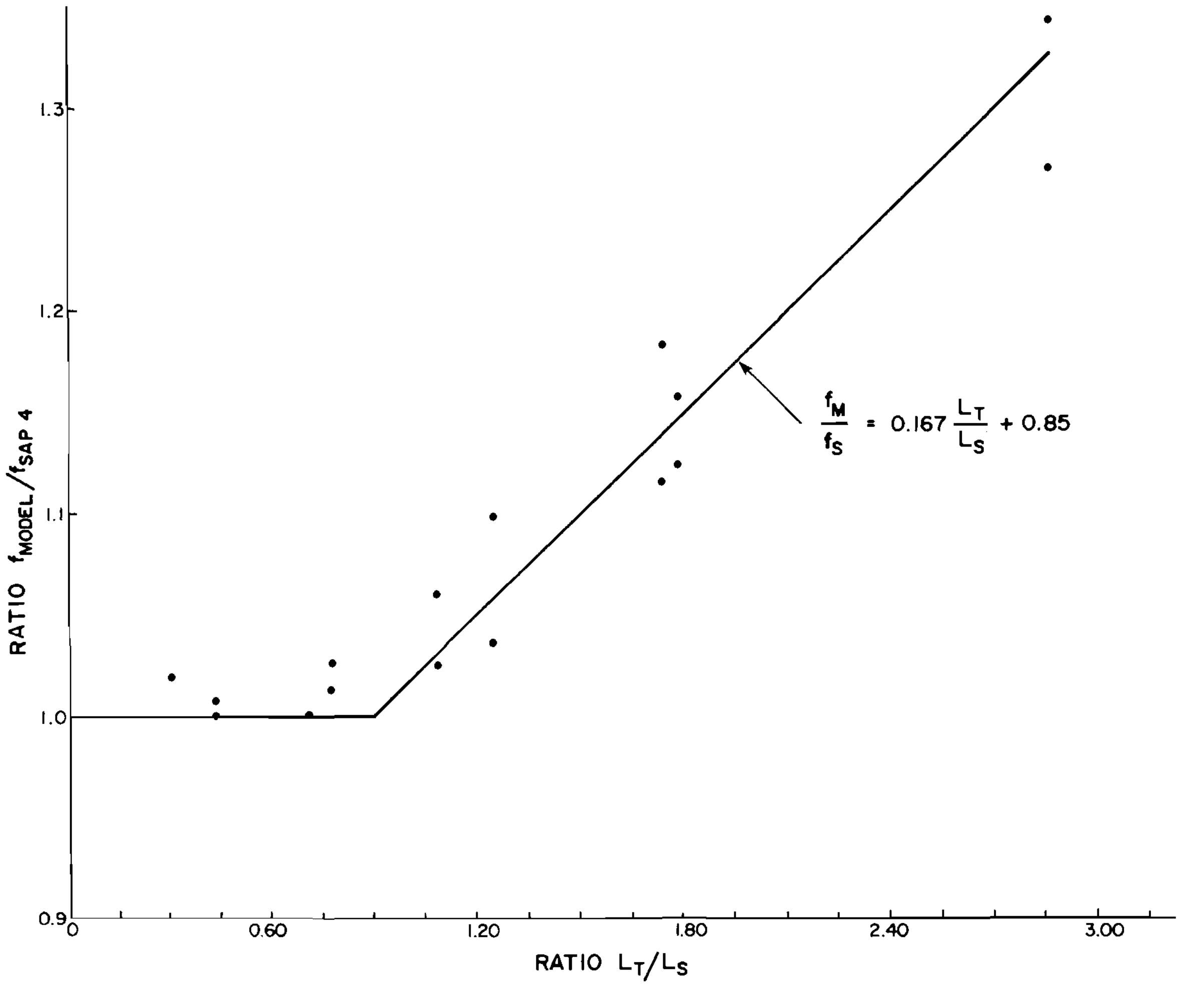

Fig. 3.10 Rocking frequency correction factor

loads. However, the derivation of the SDOF model rocking natural frequency was included for completeness.

3.5 Sign Geometries at Mode Shifting

In the previous sections, three dominant modes were discussed. The lowest mode of vibration will be either torsional, flexural, or rocking depending on the truss length and support height. From the previous information it was seen that the torsional mode frequency decreased as the truss length increased, while the flexural frequency increased with increasing truss length.

The relationship between truss length and support height that causes the mode with the lowest natural frequency to change can be approximated by the SDOF model expressions for natural frequency. The general expressions for the modal frequencies are alternatively set equal to each other and either the truss length or support height solved for. Equations 3.20, 3.21 and 3.22 correspond to torsional equaling flexural, flexural equaling rocking, and torsional equaling rocking, respectively.

(Torsional equaling flexural)

$$L_s = \left[\frac{1.3\ m_T L_T^{\ 3} - 0.563\ w^2}{0.236\ m_s L_s + m_T L_T}\right]^{\frac{1}{2}} \qquad (3.20)$$

(Flexural equaling rocking)

$$L_T = \left[\frac{3w^2}{4m_T L_T}\right]^{\frac{1}{2}} \qquad (3.21)$$

(Torsional equaling rocking)

$$L_s = \left[\frac{0.55\ m_T L_T^{\ 3}}{0.236\ m_s L_s + m_T L_T}\right] \qquad (3.22)$$

where m_T = distributed truss mass

m_s = distributed support mass

L_T = truss length

L_s = support height to the truss centerline

w = truss width

The torsional and flexural modes are most significant in sign response and will be examined to determine critical dimensions. Table 3.8 shows the critical values of support height calculated for each of the signs in the parametric study using Eq. (3.20).

The mode changes when the truss length and the support height are approximately equal. If the truss length is less than the support height, the flexural mode will govern. In cases where the truss length is greater, torsion is the governing mode. This approximation is confirmed by an examination of the eigenvectors for the signs in the parametric study.

TABLE 3.8 TORSIONAL-FLEXURAL MODE SHIFT SIGN GEOMETRIES

Sign Description Zone	Upright Height (ft)	Shift Value, L_S (T - f) (ft)
10 ft. Truss		
1	14	10.9
	23	10.6
	32	10.2
4	14	10.9
	23	10.6
	32	10.3
25 ft. Truss		
1	14	27.6
	23	26.8
	32	25.8
4	14	27.7
	23	27.1
	32	26.3
40 ft. Truss		
1	14	44.3
	23	43.0
	32	41.6
4	14	44.4
	23	43.4
	32	42.6

CHAPTER 4

DESIGN OF ANCHOR BOLTS FOR FATIGUE

4.1 Static Design Load

The parametric study of cantilever highway signs presented in the previous chapter was made using a loading function developed in Ref. 2. The loading function reproduced analytically the response of Sign No. 1 to its largest recorded vehicle loading. A means of estimating natural modal frequencies. Torsional and shear dynamic load factors were also developed. The dynamic load factors were calculated from static and dynamic application of the loading function.

A peak pressure of 1.23 psf was applied to the sign face in the parametric study. This value will be examined to see how it compares to response magnitudes measured in the field.

A histogram of the frequency of occurrence of the ratio of experimental chord 4 forces to the analytical chord 4 force was made using 76 events recorded at Signs No. 1 and 3. The histogram is shown in Fig. 4.1. The majority of the experimental events produced forces less than 50 percent of the force produced analytically using the loading function. The very small responses, ratios less than 0.1, were not included in the 76 events studied.

Using the statistics for a Gaussian distribution, one-sided tolerance limits were calculated for various combinations of exceedence and confidence levels. It was found that there is a 99 percent probability that 99 percent of the loading events produce ratios less than 0.85. Only three measured events exceeded this level. A peak pressure of 1.23 psf is, consequently, a conservative

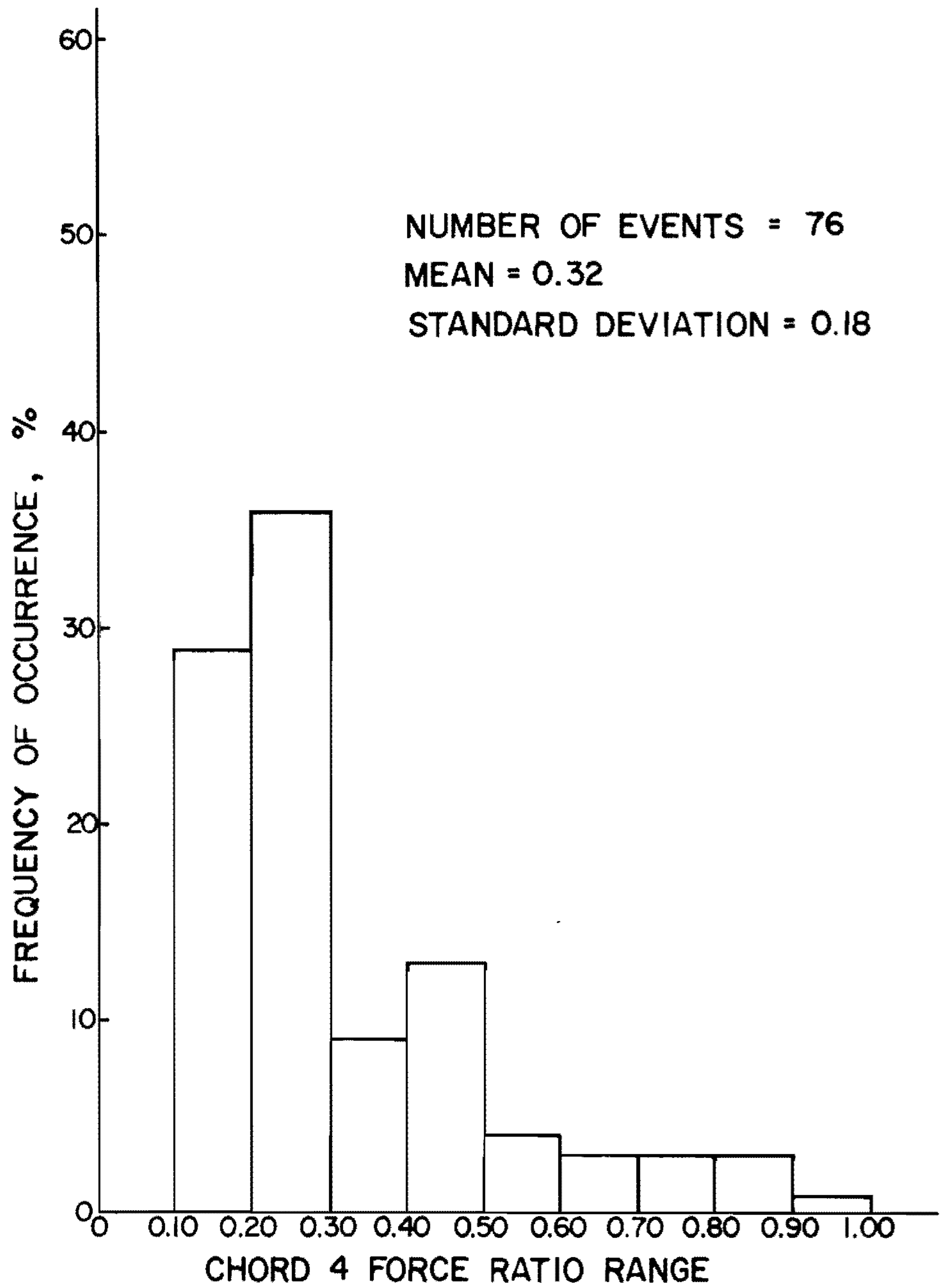

Fig. 4.1 Experimental-analytical chord 4 force load frequency histogram

value. The frequency and magnitude of very large loading events were difficult to determine for Sign No. 3 because of the short recording time. It is unlikely that a longer observation period would change the overall distribution of the loading.

In the design procedure, a pressure will be statically applied to the sign face and base forces calculated. The pressure of 1.23 psf was statistically shown to be a reasonably conservative value. For convenience, a design pressure of 1.25 psf is recommended.

4.2 Fatigue Stress Cycles for Design

The fatigue life is a function of the stress range and number of loading cycles over the design life. The higher the applied stress range the lower the number of cycles that will cause failure. Fatigue damage occurs when the stress range is above a crack growth threshold. The greater the stress is above this threshold, the greater the damage. No damage is believed to be caused by stresses below the crack threshold. Miner's theory suggests that damage is accumulated in a linear fashion, as verified by tests [6]. Failure occurs when the accumulated damage reaches the critical point for the member in question.

The number of response cycles from a given loading event is a function of the load magnitude and the damping of the structure. The damping ratios measured for cantilever highway sign structures were very low, on the order of 0.7 percent of critical damping. A large load may produce many stress cycles above the threshold value for damping this low.

The larger number of stress cycles produced by a single truck as a function of damping can be examined using Eq. (4.1).

$$v_n / v_o = (e^{2\pi\xi})^{-n} \tag{4.1}$$

where v_o = amplitude of first cycle (DLF x Static Value)

v_n = amplitude after n cycles

ξ = percent of critical damping

Table 4.1 shows numerically the effect of damping on the theoretical number of response cycles for four different damping ratios. The system does not return to rest until 282 oscillations have occurred in a system with 0.3 percent critical camping. A loading event causing a stress range of twice the threshold value would have at least 16 damaging stress cycles for a damping ratio of 0.7, which is in the range measured in the field studies.

If we now assume that between 500 to 1000 trucks can produce this same response on a busy interstate highway each day, between 2.9 and 5.8 million damaging stress ranges occur in one year. Over a 40 year design life, this means 234 million significant stress cycles are possible. A structure could not resist this exceedingly large number of cycles if the stresses produced exceeded the threshold stress range.

TABLE 4.1 EFFECT OF DAMPING ON FREE VIBRATION RESPONSE OF AN UNDERDAMPED SYSTEM

Percent of Critical Damping	Number of positive peaks (cycles) to:			
	$v_n/v_o = 0.75$	$v_n/v_o = 0.50$	$v_n/v_o = 0.25$	$v_n/v_o = 0$
0.90	5	12	25	95
0.70	7	16	32	121
0.50	9	23	44	169
0.30	15	37	74	282

4.3 Allowable Flexural Bending Stress

Bolts are subjected to repeated variations and reversals of stress and should be designed so that the maximum stress range does not exceed the basic allowable stress as defined in the AASHTO fatigue specifications. Studies have shown that only the live load need be considered in fatigue calculations. Live load on highway signs results mainly from vehicle and ambient gusts.

Studies in Ref. 7 have shown that tightened double-nutted connections, such as sign anchor bolts, may be considered as a Category C detail in the AASHTO Specifications. The anchor bolt can also be considered as a redundant load path structure, since a single bolt fracture will not lead to collapse in most structures [6]. AASHTO fatigue specifications prescribe a maximum allowable stress range of 10 ksi for all Category C details expecting greater than two million load cycles. The 10 ksi value is the threshold below which stress cycles produce no fatigue damage. By limiting the live load anchor bolt flexural stresses to less than the threshold, the structure would have an infinite fatigue life. The combination of using an allowable fatigue stress range equal to the threshold and a static design load that provides an upper bound to the measured values will provide a design which should not be susceptible to fatigue, regardless of the number of loading cycles.

4.4 Design Example

The sign structure analyzed in this example is shown in Fig. 4.2. The sign structure corresponds to Texas standard 40 ft. truss Zone 4 design. The example is presented as a check for fatigue on a sign structure previously designed for static loads. A fatigue design load distributed linearly from a value of 1.25 psf at the bottom to zero at the top of the sign is used to simulate the truck-induced gust load. The pressure is applied to the total sign face in the example. This produces a loading which corresponds

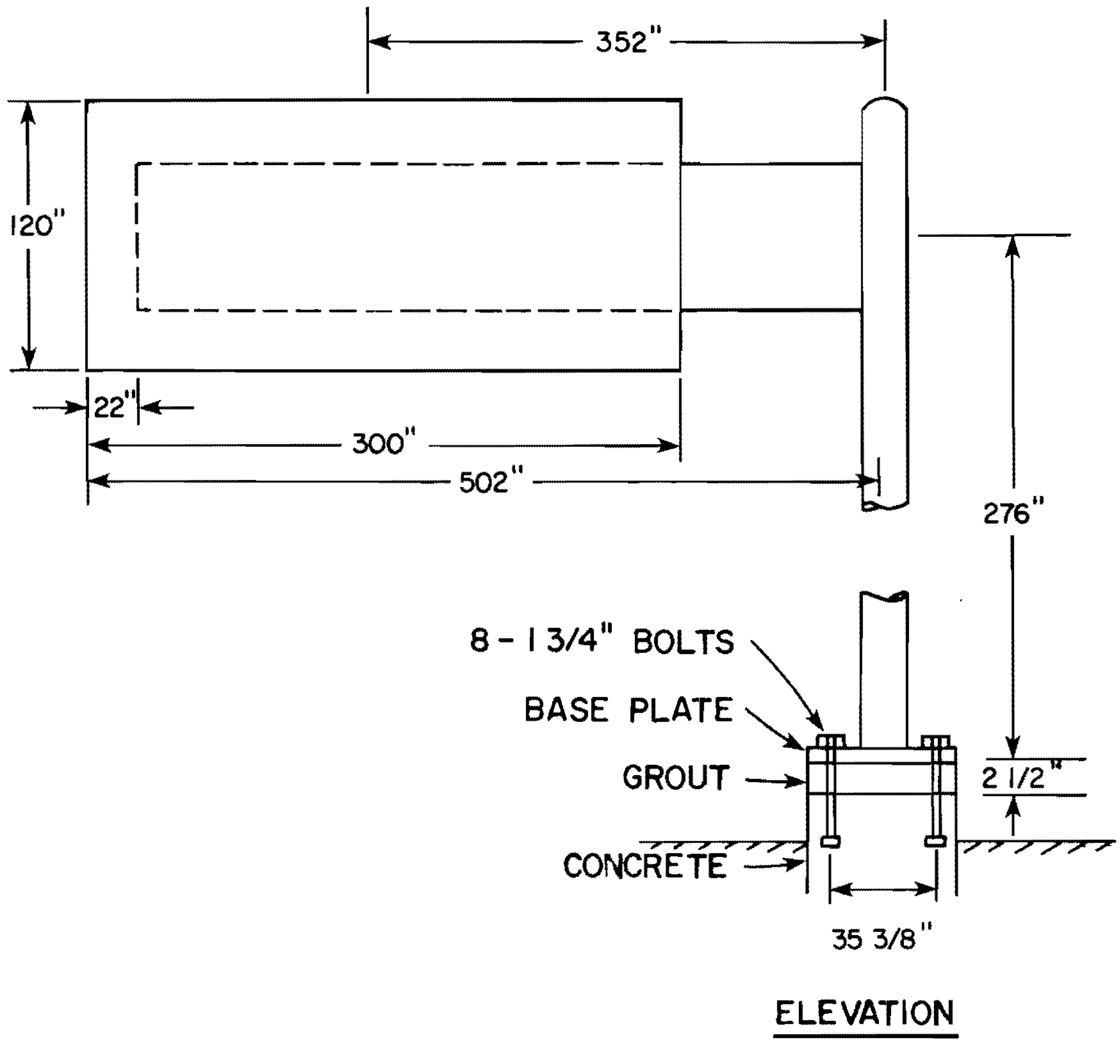

Fig. 4.2 Design example

to two adjacent trucks passing under the sign. The static forces produced by this loading are then multiplied by the approximate dynamic load factors estimated using the relationships developed in Chapter 3. The anchor bolts of the sign are then analyzed for fatigue using the amplified force resultant. Only the shearing components of bolt force are considered in the check for fatigue. The axial stress variation due to wind loading has been found to be negligible.

1. <u>Resolve Static Forces</u>:

$$\text{Total Horizontal Force} = \frac{1}{2}\left(\frac{120}{12}\right)\left(\frac{300}{12}\right)(1.25) = 156.25 \text{ lb.}$$

$$\text{Torsion Moment} = 352\,(156.25) = 55{,}000 \text{ in.-lb.}$$
$$= 55 \text{ in.-kips}$$

$$\text{Horizontal Shear} = 156.25 \text{ lb.}$$
$$= 0.156 \text{ kips}$$

2. <u>Estimate Natural Frequencies</u>

A. Torsional Frequency

$$K^* = GJ/L_s \quad \text{(Eq. 3.4)}$$

$$G = \frac{30{,}000{,}000}{2(1 + 0.3)} \text{ psi}$$

$$J = 2\pi r^3 t = 2\pi(14.86)^3\,(0.281) = 5793.5 \text{ in.}^4$$

$$L_s = \text{Support Height} = 276 \text{ in.}$$

$$K^* = \frac{\frac{30{,}000{,}000}{2(1 + 0.3)}\,(5703.5)}{276} = 2.42203 \times 10^8$$

Calculate Total Truss Mass

<u>Truss Members</u>

Chords: $4(480 \text{ in.})(2.11 \text{ in.}^2) = 4051.2 \text{ in.}^3$

D.L. Diag.: $16(76.8 \text{ in.})(0.809 \text{ in.}^2) = 994.6 \text{ in.}^3$

W.L. Diag.: $16(76.8 \text{ in.})(1.09 \text{ in.}^2) = 1340.1 \text{ in.}^3$

W.L. Strut: $16(48\text{ in.})(0.715\text{ in.}^2) = 549.1\text{ in.}^3$

D.L. Vert.: $18(48\text{ in.})(0.715\text{ in.}^3) = 617.8\text{ in.}^3$

Cross Brace: $8(67.9\text{ in.})(0.621\text{ in.}^3) = \underline{337.2\text{ in.}^3}$

7890.0 in.^3

$$\text{wt.} = 0.286\text{ lb/in.}^3\ (7890\text{ in.}^3) = 2256.5\text{ lb.}$$

$$g = 32.2\text{ ft/sec}^2 = 386.4\text{ in./sec}^2$$

$$\text{Truss Member Mass} = \frac{2256.5}{386.4} = 5.84\ \frac{\text{lb-sec}^2}{\text{in.}}$$

<u>Sign, Lights, Walkway, Mounting Bracket</u>

Walkway = (300/12 ft)(50 lb/ft) = 1250 lb

Lights = (300/12 ft)(20 lb/ft) = 500 lb

Sign Face = $(120/12\text{ ft})(300/12\text{ ft})(3\text{ lb/ft}^2) = 750\text{ lb}$

Bracket = $3[\frac{1}{12}(48'' + 11'' + 36'')\text{ft}](7.7\text{ lb/ft}) = \underline{183\text{ lb}}$

2683 lb

$$\text{Signing Structure Mass} = \frac{2683\text{ lb}}{3864\ \frac{\text{in.}}{\text{sec}^2}} = 694\text{ lb-sec}^2\text{/in.}$$

<u>Pole Mass between Trusses (48")</u>

$$A = 26.24\text{ in.}^2$$

$$\text{Vol} = (26.24\text{ in.}^2)(48\text{ in.}) = 1259.5\text{ in.}^3$$

$$\text{wt} = (0.286\text{ lb/in.}^3)(1259.5\text{ in.}^3) = 360.2\text{ lb}$$

$$\text{Pole Mass} = \frac{360.2\text{ lb}}{386.4\text{ in./sec}^2} = 0.93\text{ lb-sec}^2\text{/in.}$$

$$\text{Total Mass} = 5.84 + 6.94 + 0.93 = 12.7\text{ lb-sec}^2\text{/in.}$$

$$M^* = \frac{M\,L_T^2}{3} = \frac{13.7(480)^2}{3} = 1052160.0 \qquad \text{(Eq. 3.6)}$$

$$\omega = \sqrt{\frac{K^*}{M^*}} = \sqrt{\frac{3GJ}{M\,L_s L_T^2}} = \sqrt{\frac{2.42203 \times 10^8}{1052160}} = 15.2\text{ rad/sec} \qquad \text{(Eq. 3.7)}$$

$$f = \frac{\omega}{2\pi} = \frac{15.2}{2\pi} = \underline{\underline{2.41 \text{ cps}}} \qquad \text{(Eq. 3.8)}$$

Correction Factor = L_T/L_s = 40 ft/23 ft = 1.74

From Fig. 3.6

$$\frac{f_{model}}{f_{SAP4}} = 1.15$$

$$f_{corrected} = 2.41/1.15 = \underline{\underline{2.10 \text{ cps}}}$$

B. Flexural Natural Frequency

Find Total Mass

Truss Members

The total mass = 5.84 lb-sec^2/in. is the same as for the torsional frequency calculations.

Sign, Lights, Walkway, Mounting Bracket

The total mass = 6.94 lb-sec^2/in. is again the same as for the torsional frequency calculations.

One-half the Pole between Trusses (24")

$$\text{Vol} = 24 \text{ in.}(26.24 \text{ in.}^2) = 629.8 \text{ in.}^3$$

$$\text{Wt} = 629.8 \text{ in.}^3(0.286 \text{ lb/in.}^3) = 180.1 \text{ lb}$$

$$\text{Mass} = \frac{180.1 \text{ lb}}{386.4 \text{ in./sec}^2} = 0.47 \text{ lb-sec}^2\text{/in.}$$

$$M_T = \text{Total Truss Mass} = 5.84 + 6.94 + 0.47 = \underline{\underline{13.25 \text{ lb-sec}^2\text{/in.}}}$$

Support Mass (pole)

$$\text{Vol} = 276 \text{ in.}(26.24 \text{ in.}^2) = 7242.2 \text{ in.}^3$$

$$\text{Wt} = (7242.2 \text{ in.}^3)(0.286 \text{ lb/in.}^3) = 2071.3 \text{ lb}$$

$$\text{Mass} = M_s = \frac{2071.3 \text{ lb}}{386.4 \text{ in./sec}^2} = \underline{\underline{5.36 \text{ lb-sec}^2\text{/in.}}}$$

Calculate the vertical weight supported by pole

$$\text{Mass} = M_T + \frac{1}{2} M_s = 13.25 + \frac{1}{2}(5.36) = 15.93 \text{ lb-sec}^2/\text{in.}$$

$$N = 15.93 \frac{\text{lb-sec}^2}{\text{in.}} (386.4 \text{ in./sec}^2) = 6155 \text{ lb}$$

Calculated Generalized Stiffness

$$I = \pi r^3 t = 2896.8 \text{ in.}^4$$

$$K^* = \frac{3EI}{L_s^3} - 5.25 \frac{N}{L_s} \qquad \text{(Eq. 3.12)}$$

$$K^* = \frac{3(30000000)(2896.8)}{(276)^3} - 5.25 \frac{(6155)}{276}$$

$$K^* = 12400.35 - 117.1 = \underline{12283.3}$$

Calculate Generalized Mass

$$M^* = 0.236 M_s + M_T(1 + (\frac{3}{4} \frac{w}{L_2})^2) \qquad \text{(Eq. 3.14)}$$

w = width of truss cross section = 48 in.

$$M^* = 0.236(5.36) + 13.25(1 + (\frac{3}{4} - \frac{48}{276})^2)$$

$$M^* = 1.26 + 13.25(1.02) = \underline{14.74}$$

$$\omega = \sqrt{\frac{K^*}{M^*}} = \sqrt{\frac{12283.3}{14.74}} = 28.9 \text{ rad/sec} \qquad \text{(Eq. 3.15)}$$

$$f = \frac{\omega}{2\pi} = \frac{28.9}{2\pi} = \underline{\underline{4.59 \text{ cps}}}$$

Frequency Correction Factor from Fig. 3.8

$$L_T/L_s = 40/23 = 1.74 > 0.9$$

Because L_T/L_s is greater than 0.9, the flexural natural frequency is not the dominant mode. A flexural frequency correction factor need not be determined, since the DLF factors will be estimated using the dominant torsional natural frequency.

3. Dynamic Load Factors

The torsional dynamic load factor can either be read or calculated from Fig. 3.4. Because the torsional frequency of 2.21 cps is between 1.5 and 4.0 Hz, the constant DLF of 1.6 is used. The shear DLF must be calculated using the torsional natural frequency from Fig. 3.3. The corresponding shear DLF is 2.2.

4. Amplify Base Forces

Fatigue Design Torque = 1.6(55) = 88.0 in.-kips

Fatigue Design Shear = 2.1(0.156) = 0.328 kips

5. Calculate Bolt Forces

The horizontal shear force will be distributed equally between the bolts (Fig. 4.3).

$$F_s = \frac{0.328}{8} = 0.04 \text{ kips}$$

Because all bolts are the same distance from the bolt group center, and of the same cross-sectional area, the torsional shear force in each bolt will be equal.

$$F_T = \frac{\text{Torque}}{8r} = \frac{88.0}{8(17.69)} = 0.62 \text{ kips}$$

The maximum vector sum of the torsional and shear forces occurs in bolt number 7 and equals 0.66 kips. This value represents the maximum dynamic force in the bolt. The bolt force range is twice this value.

6. Flexural Moment

The distance between the steel base plate bottom and the concrete foundation top is normally infilled with grout. The grout is assumed to have no shear resistance. Studies have estimated that

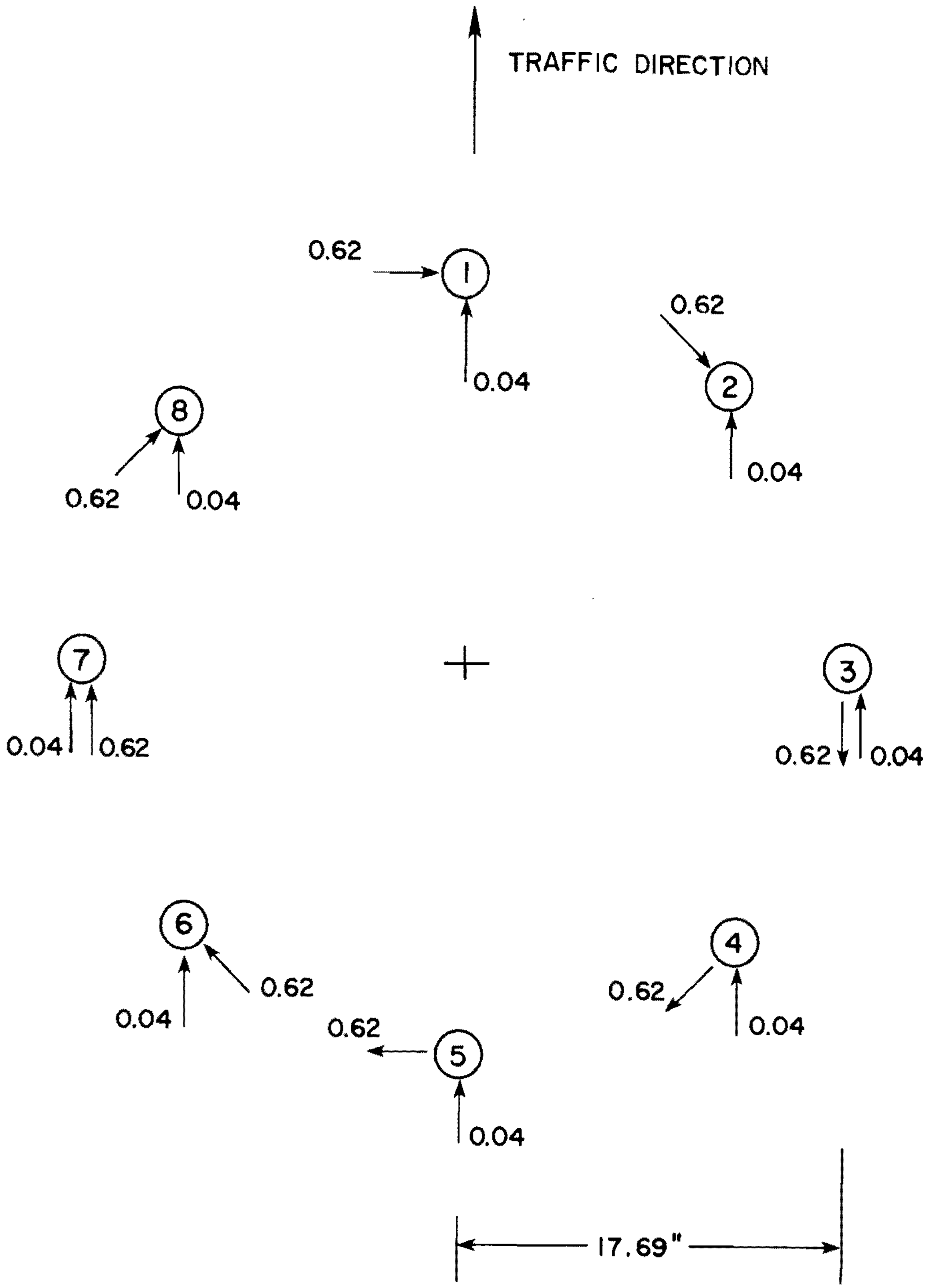

Fig. 4.3 Applied live load forces on anchor bolt group

the shear forces produce moment equal to the shear times 0.7 of the grout distance [7]. The actual length through which the shear acts is a function of the degree of bolt fixity. The seven-tenths value is an approximation. The estimated moment range in the bolt is:

$$\text{Moment} = 2[0.66(0.7)(2.5)] = 3.32 \text{ in.-kips}$$

7. Effective Bolt Area

The tensile stress area of a threaded bolt is given by Eq. (4.2) from the AISC Steel Manual.

$$A = \frac{\pi}{4}(D - 0.9743/n)^2 \qquad (4.2)$$

where A = tensile stress area
D = basic major diameter
n = number of threads per inch

where the quantity (D - 0.9743/n) can be taken as the effective diameter, D_{eff}, in calculating the section modulus of the bolt. The bolts in the example are 1.75 in. in diameter. The design will be checked for the standard coarse thread of four threads per inch and the more efficient constant thread pitch series of eight threads per inch.

$$A_4 = 1.78 \text{ in.}^2$$
$$D_{eff} = 1.51 \text{ in.}$$
$$S_4 = \pi D_{eff}^3/32 = 0.34 \text{ in.}^3$$

$$A_8 = 2.08 \text{ in.}^2$$
$$D_{eff} = 1.63 \text{ in.}$$
$$S_8 = 0.43 \text{ in.}^3$$

8. Flexural Fatigue Stresses

The resulting flexural stresses in the bolt are given by

$$F_b = \frac{M}{S}$$

where M represents the moment range.

$$F_b = \frac{3.32}{0.34} = 6.79 \text{ ksi} < 10 \text{ ksi}$$

for eight threads per inch

$$F_b = \frac{3.32}{0.43} = 5.40 \text{ ksi} < 10 \text{ ksi}$$

Since both bolts have stresses less than the allowable fatigue threshold of 10 ksi, the fatigue capacity is satisfactory. The difference in the flexural stresses for the two thread series points out the benefit of using a higher number of threads per inch. The finer threaded bolts are also easier to install.

The design procedure outlined can be considerably shortened if the designer uses the maximum DLF factors of 2.1 for shear and 1.6 for torsion. These values are conservative for all signs. If these values are used, the designer does not have to calculate the modal frequencies.

The axial fatigue stress range in the bolts in this example is 1.58 ksi and 1.14 ksi, respectively, for the four and eight thread series bolts. These stress ranges can easily be calculated from the base moment which is equal to the fatigue design shear times the distance from the sign pressure resultant to the base plate. It has been found that these axial stresses are negligible for the signs considered. The bolts with maximum axial stresses, bolts 1 and 5, are also not subjected to the highest shear. Consequently, the axial stress range in the bolts can be neglected in most designs.

CHAPTER 5

CONCLUSIONS

The dynamic respone of three cantilever highway signs was measured experimentally. The experimental data were used in the analytical development of a simulated gust-loading function. A parametric study using SAP4 and the simulated loading function was performed on a variety of possible sign configurations. Simplified models for estimating natural modal frequencies of vibration and dynamic load factors were developed from the parametric study information. The models apply to a wide range of sign geometries. The magnitude of the gust-induced base forces can be estimated. An anchor bolt design procedure was outlined to check for adequate fatigue resistance. The study conclusions are outlined below:

(1) Vehicle-induced gusts can produce significant sign response and a large number of stress fluctuations. Box-type trailer trucks produced greatest number forces.

(2) The load energy dissipation capacities for the signs, as measured by damping ratios, were all very low.

(3) A single loading event produces a number of stress cycles approximately equal to the initial stress magnitude.

(4) Stresses measured in the superstructure members were low and do not present a fatigue problem.

(5) Good agreement was found between the experimental and analytical forces in the truss chord members.

(6) The maximum anchor bolt stresses were the result of torsional shear forces in the tubular upright support.

(7) A static sign face pressure of 1.25 psf with appropriate dynamic load factor modification was found to conservatively estimate the truck-induced gust forces. A triangular loading pulse was found to adequately simulate the response of the signs measured in the field.

The effect of changes in the distance from the road surface to the sign face on the assumed gust pressure distribution was neglected. Truck height also affects the pressure distribution shape. The State Department of Highways and Public Transportation signing specifications prescribe a minimum sign clearance height. The majority of signs are at approximately the same clearance height. The effects of gust forces for a variety of truck heights were measured in the experimental program. The assumed loading function was based on the largest recorded loading event in the field tests.

APPENDICES

A P P E N D I X A

SIGN GEOMETRIES

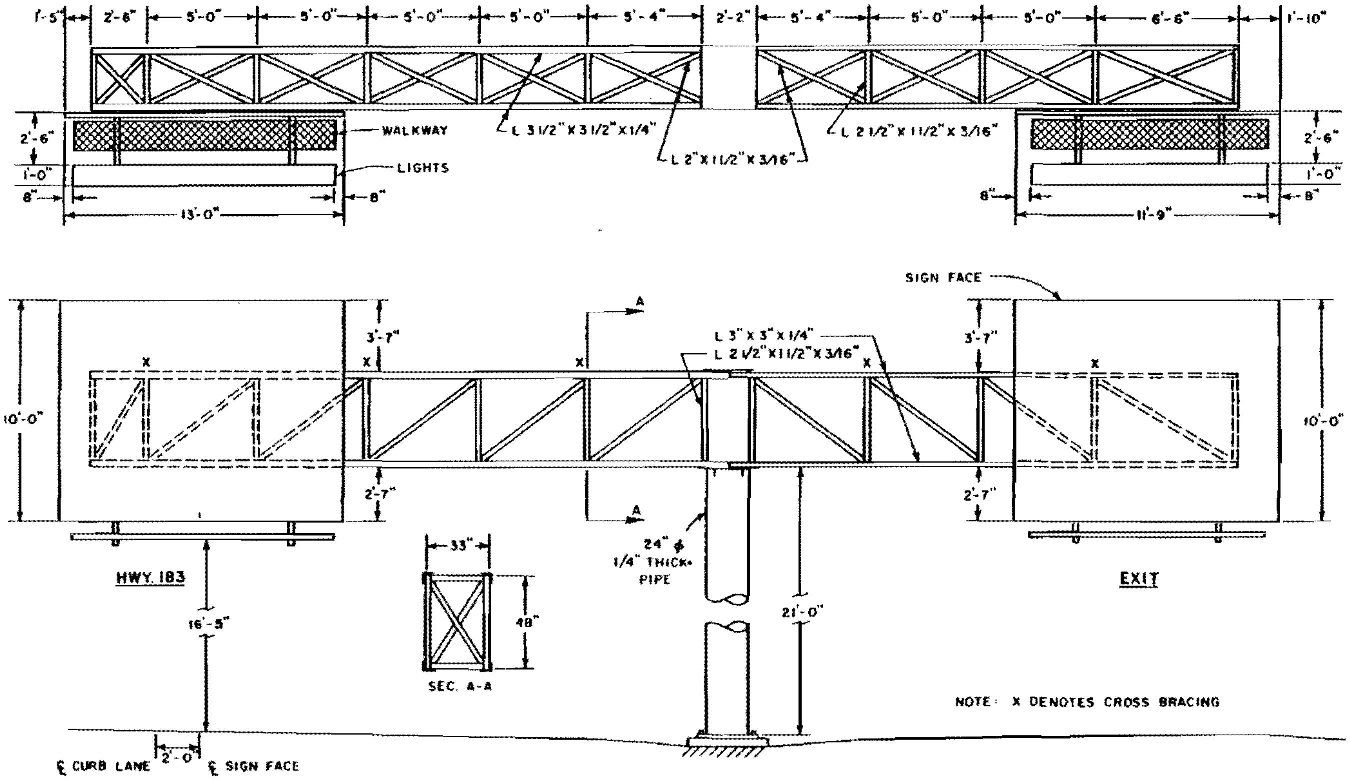

Fig. A.1 Dimensions of double cantilever sign --Sign No. 1

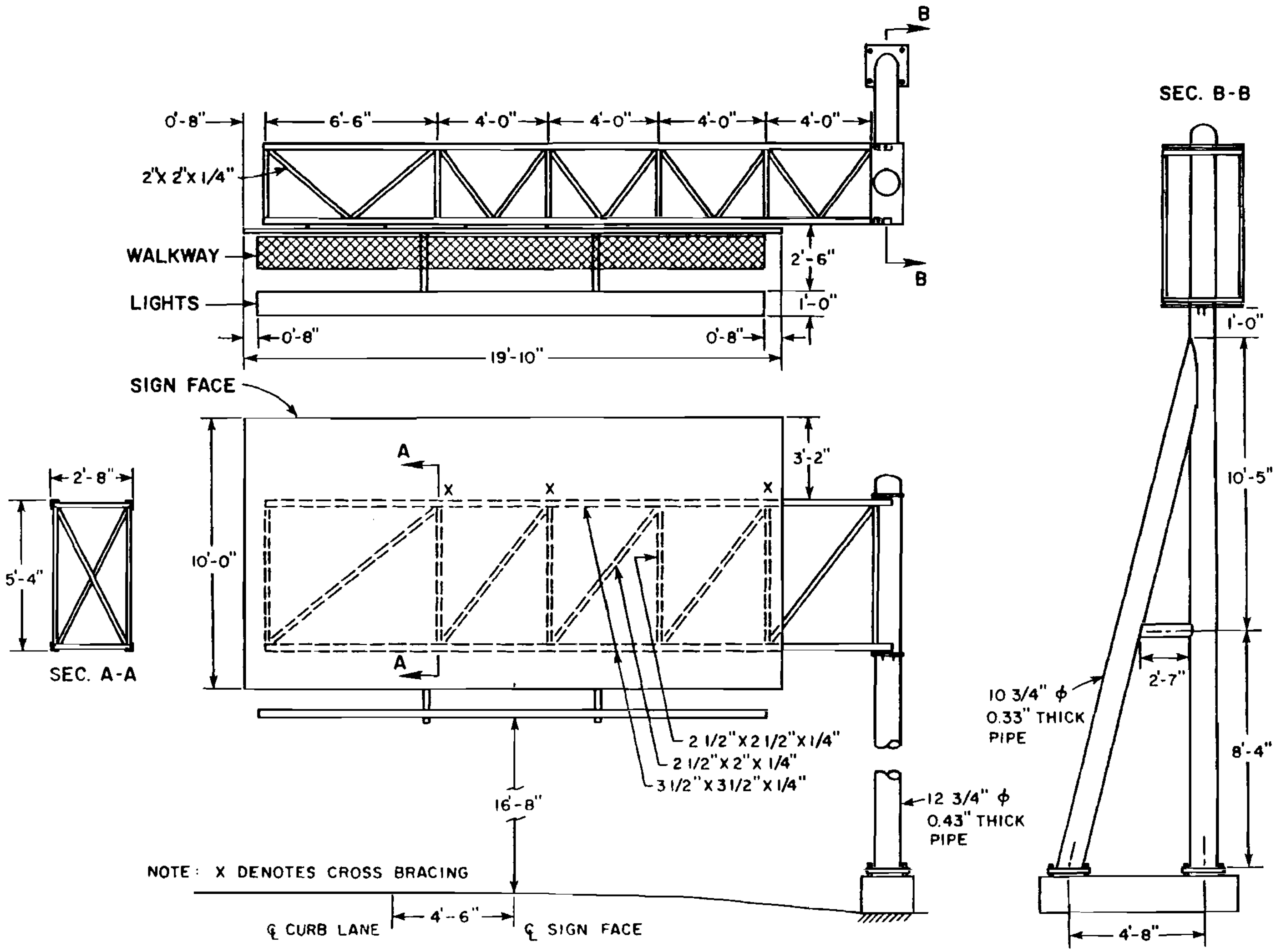

Fig. A.2 Dimensions of single cantilever sign --Sign No. 2

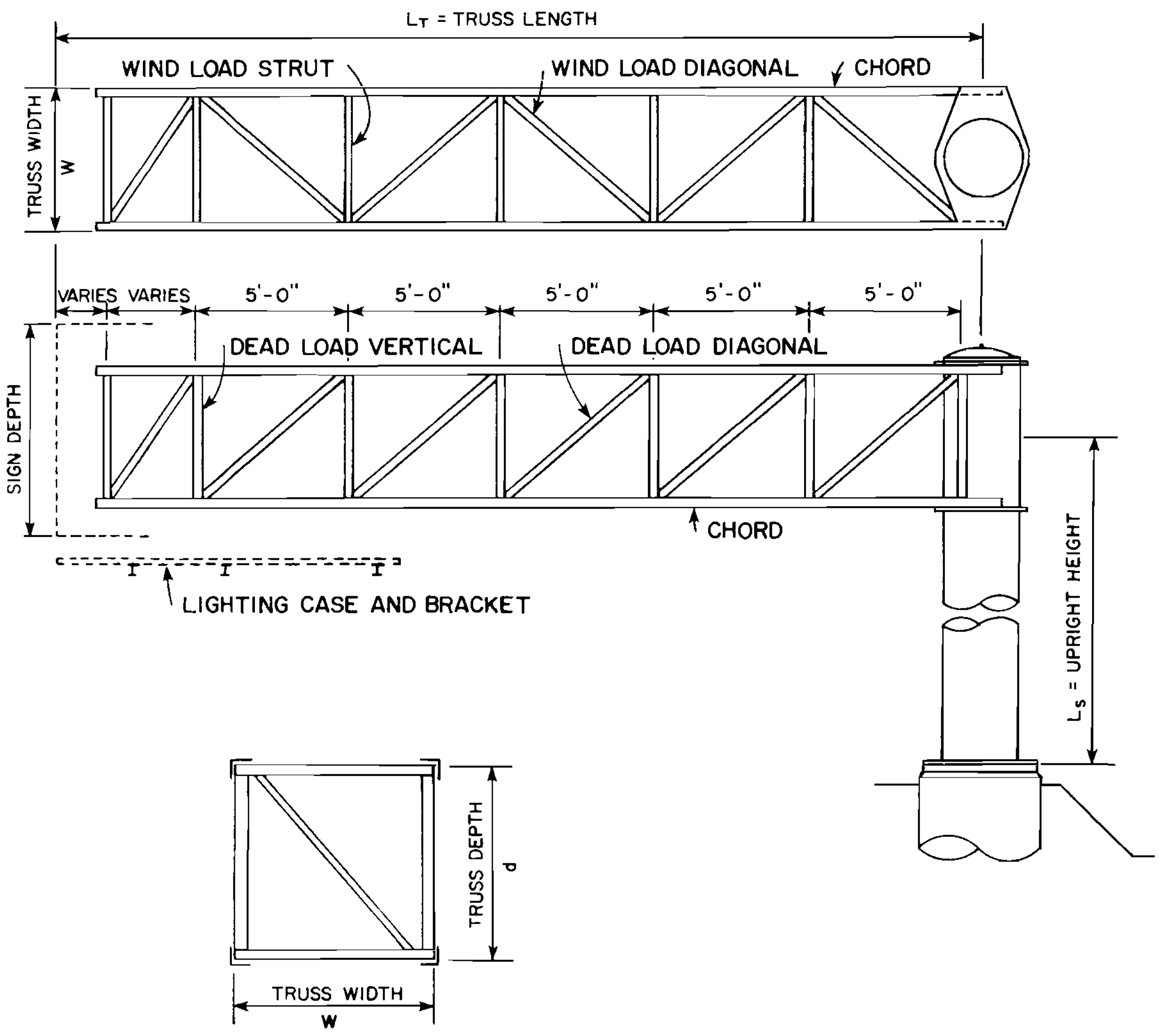

Fig. A.3 Tidwell Exit sign, Sign No. 3, and standard SDHPT design structure

A P P E N D I X B

DISTRIBUTION OF SIGN PRESSURE TO NODAL POINTS

The beam analogy approach used in the analytical study of cantilever highway signs is outlined in the steps below. A simplified approach, discussed in Chapter 4, will be used in the design procedure.

(1) Determine the horizontal sign face distribution factors by examining only the sign and light bracket. The beam reactions correspond to the loads distributed from the sign face to the supporting bracket; for a simple beam with cantilevered ends, the reactions are: (see Fig. B.1)

$$R_L = \frac{X_5}{X_2} \text{ x (applied load)}$$

$$R_R = \frac{X_4}{X_2} \text{ x (applied load)}$$

$$X_{c1} = \tfrac{1}{2}(X_1 + X_2 + X_3)$$

$$X = 2(X_{c1})$$

The horizontal force on the sign face is the volume of the assumed triangular pressure distribution: (see Fig. B.2)

$$\text{Horizontal Resultant} = \tfrac{1}{2}(Y)\ (X)\ (p)$$

where p = maximum value of pressure
Y = total sign face height
X = total sign face length

(2) Horizontal and vertical force distribution factors are found from the geometry of the lighting bracket to truss connection (see Fig. B.3). The horizontal forces are:

$$Y' = \frac{1}{3}\,(Y) - Y_3$$

$$R_{TH} = \frac{Y'}{Y_2}\,(R_L \text{ or } R_R)$$

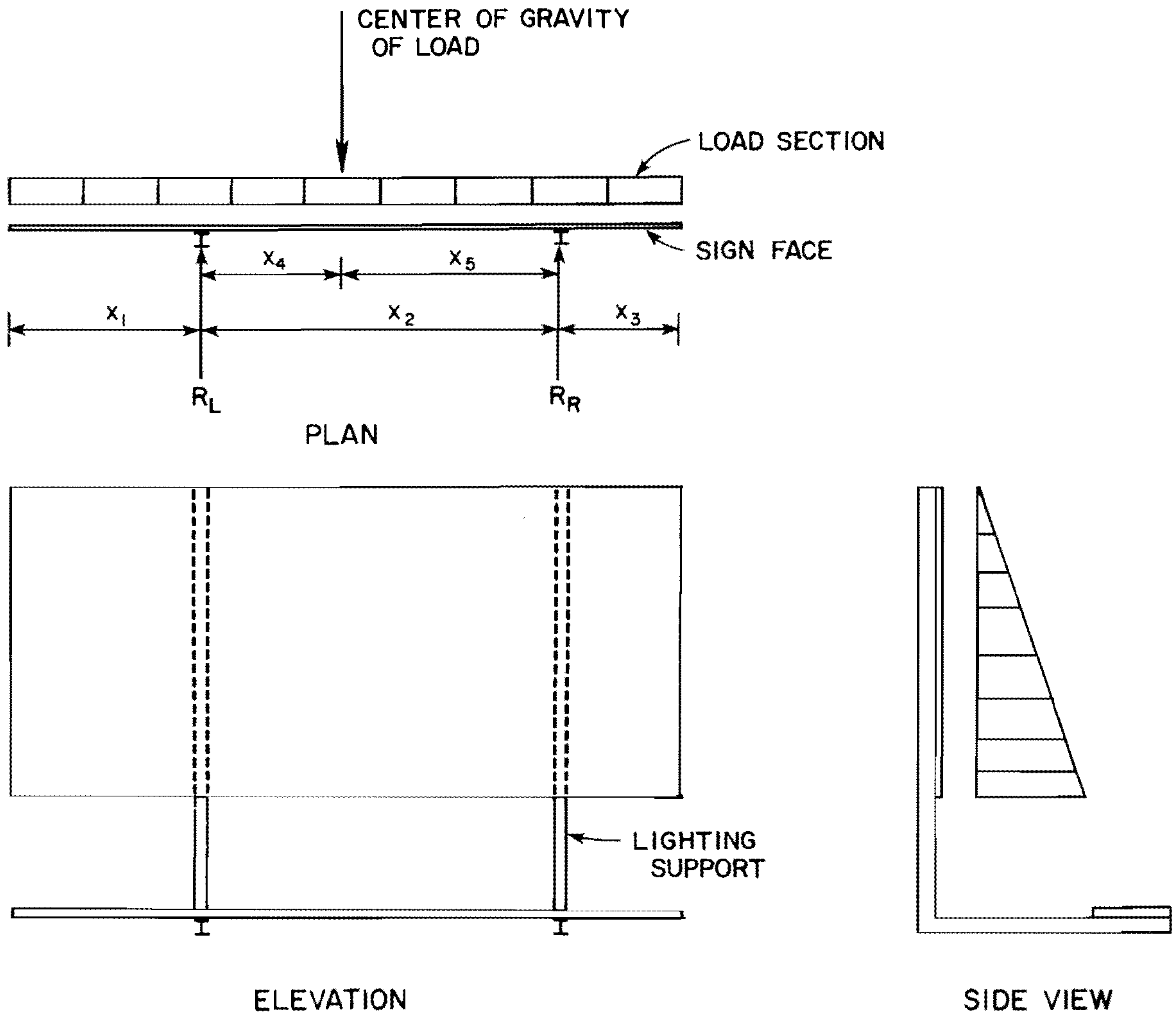

Fig. B.1 Horizontal distribution of sign force to support brackets

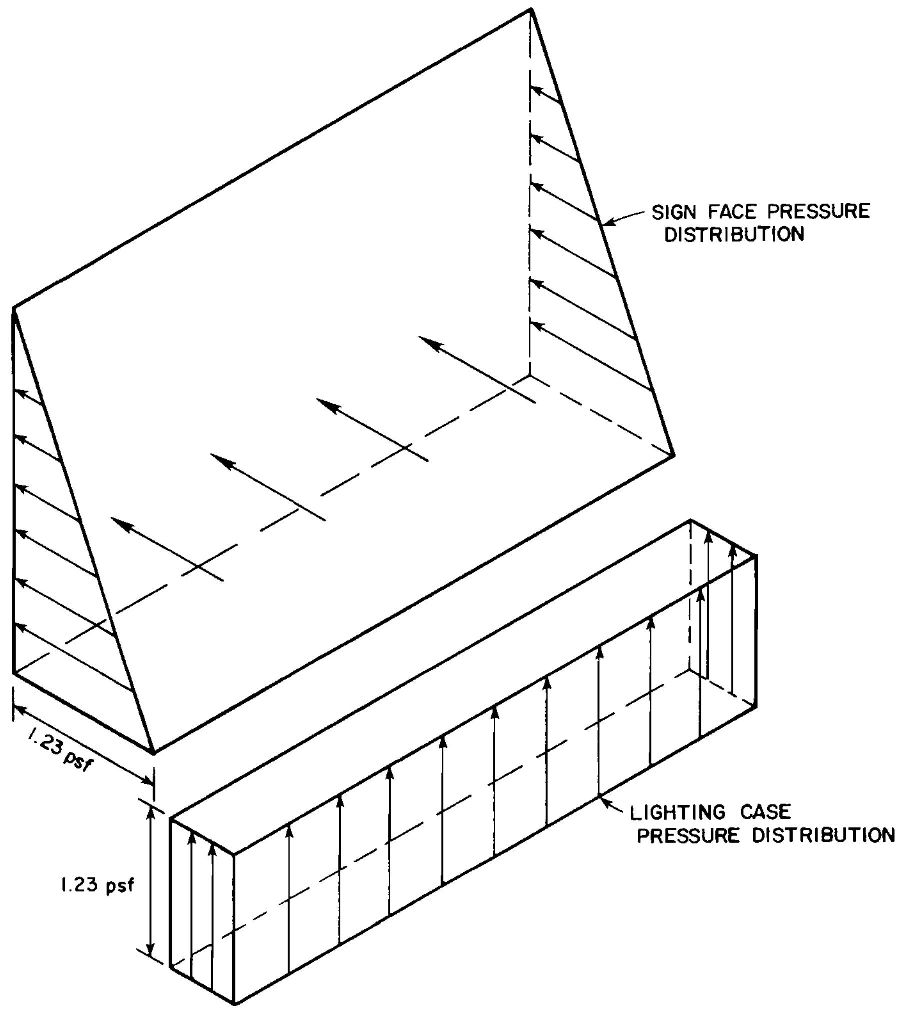

Fig. B.2 Distribution of pressure on sign and lighting case

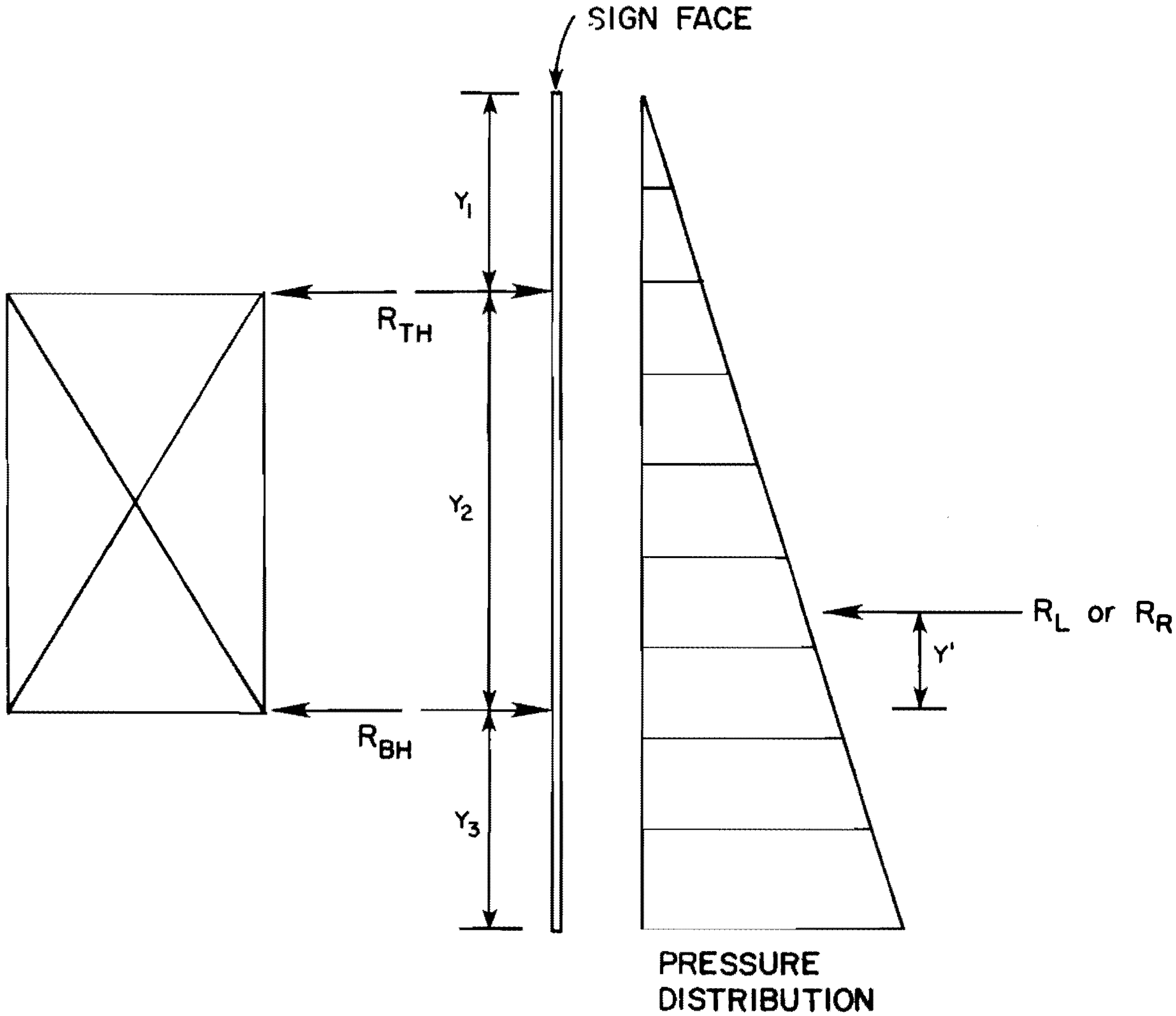

Fig. B.3 Vertical distribution of sign force to truss chords

$$R_{BH} = \frac{Y_2 - Y'}{Y_2} (R_L \text{ or } R_R)$$

The vertical pressure force on the lights causes a vertical shear force and a horizontal couple which must be resisted by the truss. The force carried in each lighting bracket is a function of the horizontal sign face distribution factors when the lights and sign are of equal length. The magnitude of the vertical resultant is given below. The vertical bracket forces are defined using the coefficients in Step 1.

$$\text{Vertical Resultant} = (1)\ (X)\ (p)$$

Vertical shears on the truss were assumed equal at the top and bottom of each lighting bracket. The horizontal overturning forces are a function of truss depth and distance from the truss to the lights. Summation of moments and equilibrium of horizontal forces in Fig. B.4 yield:

$$R_{TOL} = \frac{R_{LV}\ (Z)}{Y_2}$$

$$R_{BOL} = -R_{TOL}$$

$$R_{TOR} = \frac{R_{RV}\ (Z)}{Y_2}$$

$$R_{BOR} = -R_{TOR}$$

(3) The following estimates of self-weights are used by the State Department of Highways and Public Transportation:

Sign = 3.0 lb/ft^2

Light fixture = 20.0 lb/ft

Walkway = 50.0 lb/ft

Mounting bracket = 7.7 lb/ft

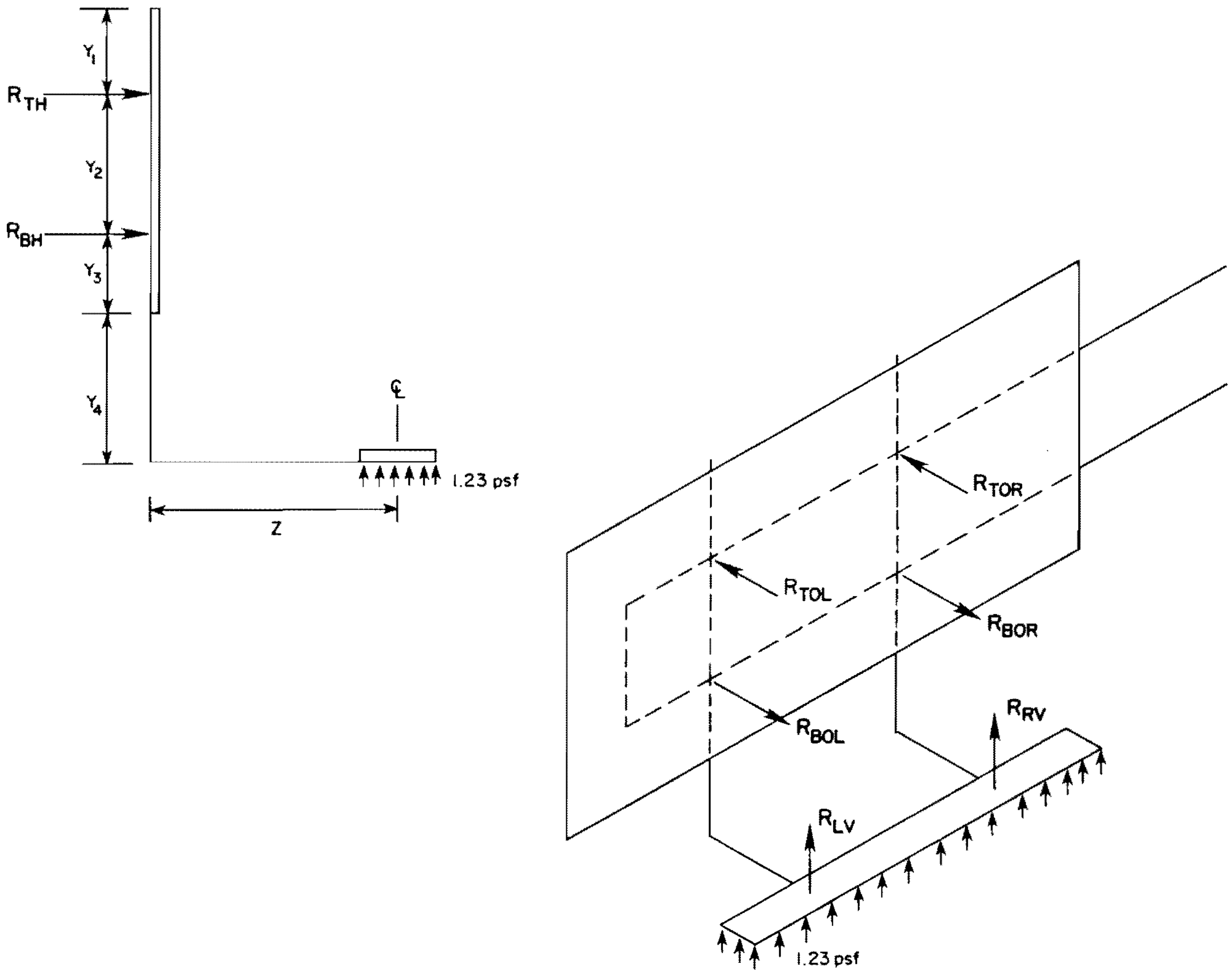

Fig. B.4 Distribution of vertical forces to truss

Using the horizontal distribution factors, we obtain:

$$R_{LVW} = \frac{X_5}{X_2} \text{ (total vertical weight)}$$

$$+ \text{ (support bracket weight)}$$

$$R_{RVW} = \frac{X_4}{X_2} \text{ (total vertical weight)}$$

$$+ \text{ (support bracket weight)}$$

(4) The component forces can now be summed, as shown in Fig. B.5 with appropriate direction. One final distribution is required to move the connection forces to the nodal points. The forces were distributed in proportion to their distance between nodal points.

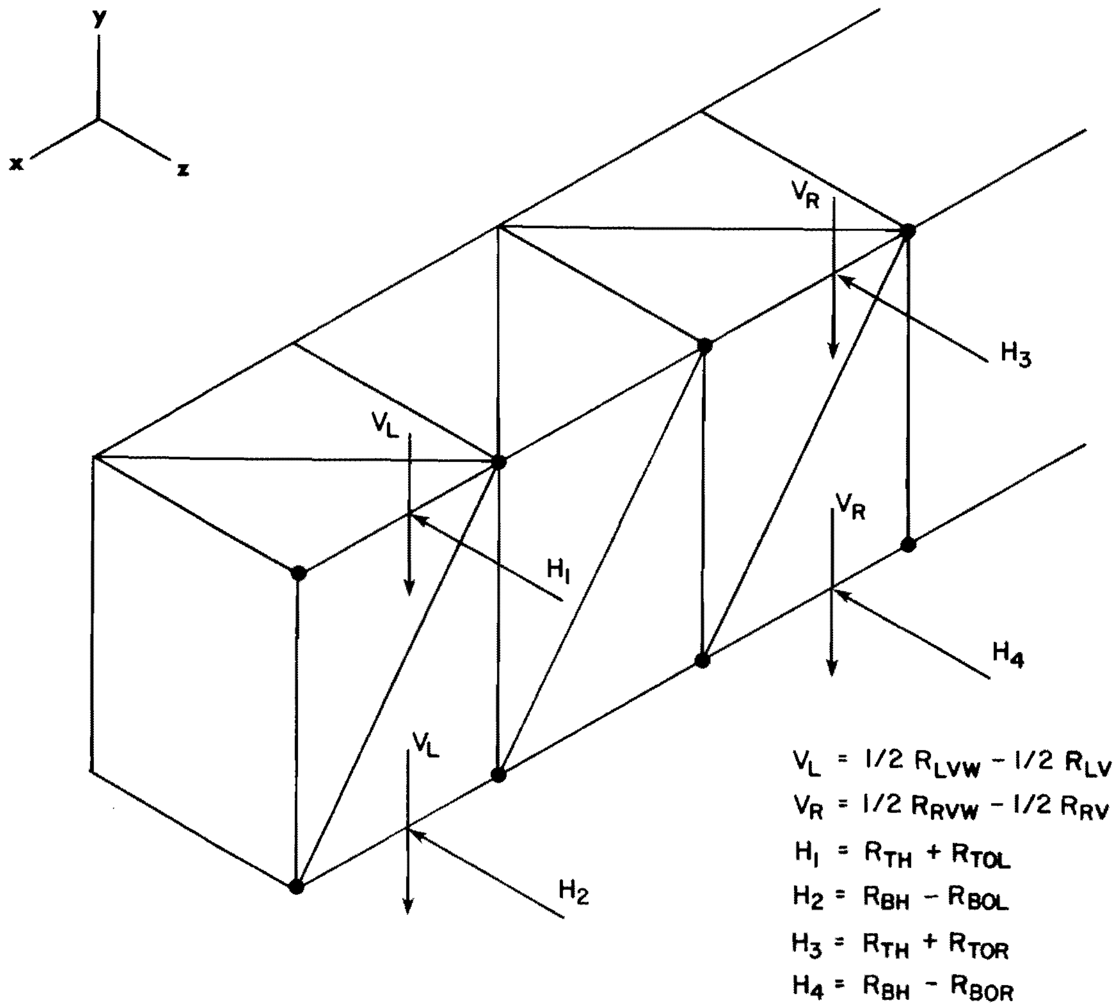

Fig. B.5 Resultant forces on truss

REFERENCES

1. Clough, Ray W., and Penzien, Joseph, Dynamics of Structures, McGraw-Hill Book Company, Inc., New York, 1975.

2. Cocavessis, Nicolas S., "Dynamic Response of Cantilever Highway Sign Structures Subjected to Gust Loadings," unpublished MS thesis, The University of Texas at Austin, May 1978.

3. Bathe, Klaus-Jurgen, Wilson, Edward, and Peterson, Fred, "SAP 4 Structural Analysis Program," University of California at Berkeley, April 1974.

4. Kyropoulos, Peter, "Truck Aerodynamics," SAE Transactions, 1962, p. 307.

5. Texas Department of Highways and Public Transportation, "Interstate Signing Standards," 1978 Revision.

6. Fisher, John W., Bridge Fatigue Guide Design and Details, American Institute of Steel Construction, 1977.

7. James, Billy D., Oral conversation concerning M.S. thesis in progress at The University of Texas at Austin, November 1977.

8. Natrella, M. G., Experimental Statistics, NBS Handbook 91, National Bureau of Standards, U.S. Department of Commerce, August 1963.

9. American Institute of Steel Construction, Manual of Steel Construction, Seventh Edition, 1973.